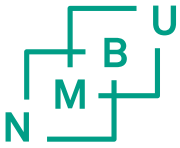
U
B
M
N

For the degree in Master of Biotechnology (60 credits)

Characterization of signalling networks in ovarian cancer cells

Author

Lise-Lotte Flage-Larsen

Main Supervisor

Kjetil Taskén

Co-Supervisor

Lena Eroukhmanoff

Main Supervisor (NMBU)

Tor Erling Lea

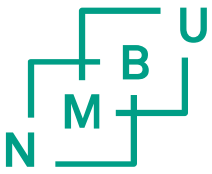

Norwegian University
of Life Sciences

1 ACKNOWLEDGEMENT

First, I would like to thank my head supervisor Kjetil Taskén for giving me this opportunity to be a part of this great project and his group of outstanding scientists, and for the support and guidance throughout this master thesis.

I would like to extend a huge gratitude to my Co-supervisor Lena Eroukhmanoff, for her enormous support, guidance and enthusiastic spirit in the lab throughout the past year. Thank you for always being there and for never letting me feel bad, you are great scientist, colleague and friend.

Then I would like to thank my internal head supervisor at NMBU, Tor Erling Lea for your inputs and guidance throughout these last months.

Thanks to everyone at The Biotechnology centre and especially thanks to everyone in the Taskén group for their help and support.

I would also like to thank my family, for their support and complete understanding throughout this year, especially the last few months.

Finally yet importantly, I would like to thank my boyfriend for his understanding, love and never-ending support throughout this year, you “rocks my world”!

2 ABSTRACT (ENGLISH)

Ovarian cancer is one of the most lethal gynaecological diseases worldwide, and in Norway approximately 500 women die from this disease every year. Women with ovarian cancer often experience vague symptoms that can be mistaken for much less severe diseases. This leads to late stage diagnosis of many patients, which is the main reason for why the overall five year survival rate is only around 40%. Accumulation of malignant ascites is frequently observed in ovarian cancer patients that have reached stage III and IV, and it is known to support tumour progression, by creating a tumour friendly microenvironment. Our understanding of malignant ascites and its effect on the intracellular signalling networks in ovarian cancer cells is still unclear. In this thesis we have tried to characterize intracellular phosphorylation pattern in ovarian cancer cell lines treated with ascites. We put particular focus on key proteins that are known to be involved in cell proliferation, cell survival and protein synthesis.

Our result show that several ovarian cancer cell lines; OVCAR-3, OVCAR-5, OVCAR-8, NCI/ADR-RES and SKOV-3, are suitable for the protocol that is established for these experiments.

Further experiments show that multiple intracellular proteins were phosphorylated upon treatment with ascites. Ovarian cancer cells that were treated with ascites from patient panel displayed with a different phosphorylation patterns, both between cell lines and patient samples. S-6 ribosomal protein exhibited a strong phosphorylation after SKOV-3 and OVCAR-8 cells were treated with ascites from most of the patients.

Ascites from any patient induced a distinct increase in phosphorylation between 3 and 20 minutes in both SKOV-3- and OVCAR-8 cells. STAT-3 phosphorylation seemed to be independent because of a low correlation with the phosphorylation of the other proteins. A strong phosphorylation was seen in STAT-3 after treatment with ascites from all the patient samples.

By using an IL-6R blocking antibody we showed that IL-6 was dominant when it comes to activation of JAK/STAT pathway and STAT-3 phosphorylation. There was no significant change in phosphorylation of other proteins when IL-6R was blocked and cells were treated with ascites. Though, -the overall phosphorylation response amongst the other proteins were weak.

We also observed that STAT-1 displayed a moderate to strong phosphorylation in SKOV-3 cells when treated with some of the patient samples. Other proteins that were investigated, like AKT, MAPKAPK-2 and MEK-1, displayed moderate phosphorylation after treatment with ascites from multiple patients in both OVCAR-8- and SKOV-3 cells.

3 ABSTRACT (NORWEGIAN)

Kreft i eggstokkene er en av de mest dødelige gynekologiske sykdommene i verden, og hvert år dør rundt 500 kvinner i Norge av denne sykdommen. Kvinner med eggstokkreft opplever ofte vage symptomer som ofte kan bli oversett til å være mindre alvorlige sykdommer. Dette fører ofte til en sein diagnose for mange pasienter. Dette er hovedårsaken til den den generelt lave overlevningsraten på bare 40%. Akkumulering av ondartet ascites er ofte observert i pasienter med eggstokkreft som er diagnostisert med stadium III eller IV, og er kjent for å støtte progresjonen av svulst, ved å skape ett vennlig mikromiljø. Vår forståelse av ondartet ascites og dens effekt på det intracellulære signalnettverket i eggstokkreft celler er fremdeles noe uklart. I denne oppgaven har vi prøvd å karakterisere det intracellulære fosforylerings mønsteret i eggstokkreft celler som har blitt utsatt for ascites. Vi har spesielt fokusert på nøkkel proteiner som er kjent for å være involvert i forøkning og overlevelse av celler samt protein syntese.

Resultatene våre viste at flere cellelinjer var passende å bruke; OVCAR-3, OVCAR-5, OVCAR-8, NCI/ADR-RES and SKOV-3, med tanke på protokollen som er etablert for disse eksperimentene.

Eksperimentene viste at flere intracellulære proteiner ble fosforylert etter at de hadde blitt utsatt for ascites. Eggstokkreft celler som ble usatt for ascites fra pasient panelet viste forskjellige fosforyleringsmønstere, både mellom celle linjene og pasient prøvene. S-6 ribosomal protein viste en sterk fosforylering etter at SKOV-3- og OVCAR-8 celler ble utsatt for ascites fra mesteparten av pasientene.

Ascites fra enhver pasient induserte en bestemt økning i fosforyleringen på mellom 3 og 20 minutter i både SKOV-3- og OVCAR-8 celler. Fosforylering av STAT-3 viste seg å være uavhengig grunnet en lav korrelasjon med fosforyleringen til de andre proteinene som ble undersøkt. En sterk fosforylering av STAT-3 ble sett etter at celler ble utsatt for ascites fra alle pasientene.

Ved å bruke ett antistoff som blokkerte IL-6R kunne vi vise at IL-6 var dominant når det kom til å aktivere JAK/STAT og dermed STAT-3 fosforylering. Det var ingen signifikant endring i fosforyleringen av andre proteiner når IL-6R ble blokkert og cellene ble utsatt for ascites, men fosforyleringsnivået var generelt svakt blant proteinene som ble undersøkt.

Vi observerte også at STAT-1 viste moderat til sterk fosforylering i SKOV-3 celler etter de ble utsatt for ascites fra noen av pasientene. Andre proteiner som ble undersøkt, som for eksempel AKT, MAPKAPK-2 and MEK-1, viste moderat fosforylering etter at SKOV-3 og OVCAR-8 celler ble usatt for ascites fra flere av pasientene.

4 ABBREVIATIONS

ACJJ	American Joint Committee on Cancer
AKT/PKD	Protein kinase B
ARID1A	AT rich interactive domain
ATX	Autotaxin
BLC-2	B-cell lymphoma 2 gene
BRCA 1	Breast cancer 1 and 2
BRCA 2	Breast cancer 1 and 2
BRAF	V-raf murine sarcoma viral oncogene homolog B
BSA	Bovine serum albumin
CA-125	Cancer antigen 125
c-MYC	V-myc avian myelocytomatosis viral oncogene
Cl^-	Chloride
CT	Computed tomography
CTNNB1	Beta-catenin
DMSO	Dimethyl sulfoxide
DNA	DeoxyriboNucleic Acid
EGF	Epidermal growth factor
EGFR	Epidermal growth factor Receptor
ERK	Extracellular-signal-regulated kinases
GEF	Guanine exchange factor
FAB	Fragment antigen binding
FAK	Focal adhesion kinase
FC	Fragment crystallisable
FCS	Fetal bovine serum
FSC	Forward side scatter
FIGO	International Federation of Gynaecology and Obstetrics
FITC	Fluorescein isothiocyanate
GDP	Guanosine diphospha
GRB2	Growth factor receptor-bound protein 2

GTP	Guanosine triphosphate
H3 protein	Histone 3 protein
HER1-4	V-erb-b2 avian erythroblastic leukemia viral oncogene homolog 1,2,3 and 4
HGSC	High grade serous carcinoma
HNF1	Homeobox A and B
HNPCC	Hereditary nonpolyposis colorectal cancer (Lynch syndrome)
IL-6	Interleukin 6
IL-8	Interleukin 8
IL-10	interleukin 10
IRS-1	insulin like growth factor 1
JAK	Janus kinase
KRAS	Kirsten rat sarcoma viral oncogene homolog
LPA	Lysophospatidic acid
LGSC	Low grade serous carcinoma
MLL2	Histone-lysine N-methyltransferase 2
MLL3	Histone-lysine N-methyltransferase 3
MRI	Magnetic Resonance Imaging
NCI-60	National Cancer Institute (human cancer panel 60)
OPG	Osteoprotegerin
PARP	Poly(ADP-Ribose)polymerase
PBS	Phosphate-buffered saline
PerCP	Peridinin chlorophyll protein
PH	Pleckstrin Homology domain
PI3K	Phosphoinositide 3-kinase
PIP2	Phosphatidylinositol 4,5-bisphosphate
PIP3	Phosphatidylinositol (3,4,5)-trisphosphate
PKD1	Phosphoinsositide dependent kinase 1
PKD2	Phosphoinsositide dependent kinase 2
PLA 1/2	Phospholipase A 1 and 2
PMT	Photomultiplier tube
PS	Penicillin-Streptomycin

PTEN	Phosphatase and tensin homolog
SH2	Src (Schmidt-Ruppin A-2) homolog 2
SH3	Src (Schmidt-Ruppin A-2) homolog 3
SOS	Son of Sevenless
RANKL	Receptor activator of nuclear factor kappa-B ligand
RANK	Receptor activator of nuclear factor kappa-B
RAS	Rat sarcoma protein
RPMI	Roswell Park Memorial Institute
SSC	Side scatter
STAT	Signal Transducer and Activator of Transcription
TNFR	Tumour necrosis factor receptor
TRAIL	TNF-related apoptosis-inducing ligand
TP53	Tumour protein 53
VEGF	Vascular endothelial growth factor
UPA	Urokinase plasminogen activator

TABLE OF CONTENTS

5 INTRODUCTION

5.1 OVARIAN CANCER

Cancer of the ovaries is the fourth leading cause of cancer deaths among women worldwide. Every year 500 new cases of ovarian cancer are reported in Norway and the 5 year overall survival rate is approximately 40 % [2]. As shown in figure 1 the five year relative survival rate for women diagnosed with ovarian cancer is dependent on the spread of the disease at diagnosis. Women diagnosed at an early stage (localized) usually have a good prognosis. However, approximately 70 % of the patients are diagnosed when the cancer has metastasized to distant areas, within and beyond the abdominal cavity, and their prognosis is poor [2]. The low overall survival rate is mainly due to the high number of women that are diagnosed with advanced cancer.

With improved understanding of tumour, we can find new and better diagnostic tools that can help to detect ovarian cancer earlier, and thereby lead to better patient prognosis.

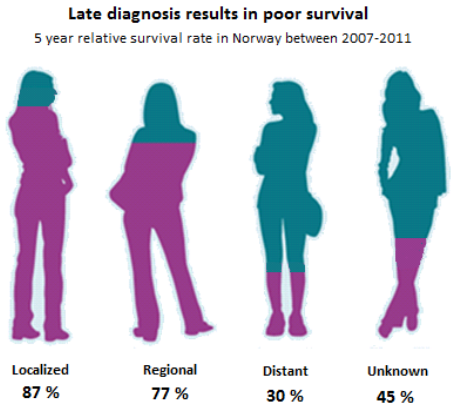

Figure 1 Five year relative survival rate dependent on the spread of the disease at diagnosis [3].

The main reason for the late diagnosis is the vague symptoms, making it difficult to detect cancer at an early stage. Some of the symptoms that women with ovarian cancer can suffer from are pelvic pain, abdominal bloating, vaginal bleeding and weight gain or loss. These symptoms can often be mistaken for much less severe diseases, thereby prolonging time to diagnosis. The exact causes of cancer in the ovaries are still unknown, but there are known risk factors associated with ovarian cancer. Some of them are; not given birth, not using oral contraceptives, obesity, increasing age and breast cancer due to the BRCA1 and BRCA2 mutations.

Prognosis and progression is dependent on where the tumour cells originate from. Ovarian cancer types can be divided in three main groups based on their morphological and biological behaviour [4] (Figure 2A and B):

1) Surface epithelial carcinoma
2) Germ cell carcinoma
3) Stromal cell carcinomas

Approximately 90 % of ovarian cancer cases are classified as epithelial ovarian cancers, meaning that the tumour arises from the outer epithelial layer [4] (Figure 2B).

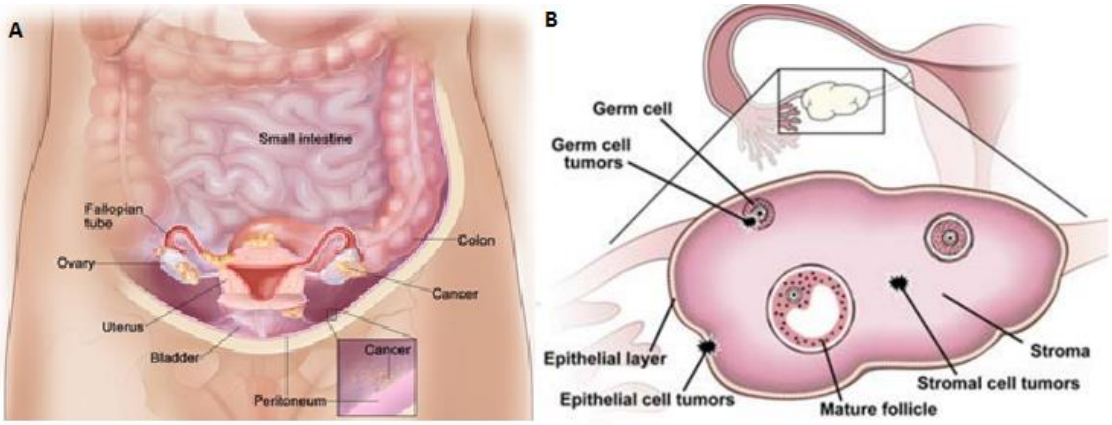

Figure 2 Abdominal cavity with focus on female reproductive organs (A) and locations for ovarian cancer origins (B), from [5]

5.1.1 Epithelial ovarian cancer

Epithelial ovarian cancer can be sub-divided into four main histological groups listed below [4, 6]:

1. Serous tumours

   These types of tumours account for approximately 75% of all epithelial ovarian carcinomas worldwide [4]. There are two sub-groups within serous neoplasms due to their differences in molecular genetics; low grade serous carcinoma (LGSC) and high grade serous carcinoma (HGSC).

   Low grade serous carcinoma is related to serous borderline tumours (benign tumours that develop into malignant tumours) and is frequently seen with mutations in BRAF (v-raf murine sarcoma viral oncogene homolog B) [6, 7]. Chemotherapy response and prognosis for patients diagnosed with LGSC are usually intermediate.

Unlike LGSC, HGSC is usually presented with mutations in TP53 (tumour protein 53) and BRCA (breast cancer 1 and 2) [6, 7]. This type of tumour is usually sensitive to chemotherapy, but patients with this diagnosis have a high probability for disease relapse and their prognoses are generally poor.

2. Mucinous tumours

   This type of tumour is frequently confined to the ovaries and only appears in approximately 3-4% of ovarian cancer cases [4]. Patients have an elevated frequency of mutations in KRAS (kirsten rat sarcoma viral oncogene homolog) and HER2 (v-erb-b2 avian erythroblastic leukemia viral oncogene homolog 2) [6], and usually have a low sensitivity to chemotherapy treatment, but the prognosis is good due to surgery.

3. Endometrioid tumours

   These tumours account for approximately 10 % of ovarian cancer cases [4]. One known risk factor for this tumour type is HNPCC (hereditary nonpolyposis colorectal cancer, also known as Lynch syndrome) and patients have an elevated frequency of mutations in PTEN (phosphatase and tensin homolog), beta-catenin (CTNNB1) and ARID1A (AT rich interactive domain) [6]. Patients are usually diagnosed at early stages and respond well to chemotherapy.

4. Clear cell tumours

   Around 10 % of ovarian cancer cases are clear cell tumours [4]. Like endometrioid carcinoma, clear cell tumours are also associated with endometriosis. Patients usually have a favourable prognosis and mutations are frequently observed in HNF1 (HNF1 homeobox A and B) and ARID1A [6].

The different mutations that are found in each of the above described tumour types indicates that they are really different diseases which calls for individual treatment.

5.1.2 Diagnosis

FIGO (International Federation of Gynaecology and Obstetrics) and ACJJ (American Joint Committee on Cancer) are two similar staging systems for ovarian cancer that are used worldwide. These staging systems divide patient populations into groups depending on how the tumours have spread, and can reveal further progression, prognosis and treatment options (Table 1). FIGO and ACJJ both divide the ovarian cancer cases into four main groups followed by a number of subgroups and tumour grades.

The main four ovarian cancer staging groups are:

Table 1 FIGO ovarian cancer main staging groups [4].

Stage I Cancer cells are found in one or both ovaries	**Stage II** Tumour involves one or both ovaries with pelvic extension or primary peritoneal cancer
Stage III Tumour involves one or both ovaries with confirmed spread to the peritoneum outside the pelvis and/or metastasised to retroperitoneal lymph nodes	**Stage IV** Distant metastasis excluding peritoneal metastasis

Diagnosis is usually set after the patient has gone through a physical examination followed by vaginal ultrasound, CT and MRI. Patients are also tested for elevated levels of CA-125 (cancer antigen 125) in serum. CA-125 is a tumour antigen that is found elevated in approximately 90 % of advanced stage epithelial ovarian carcinomas, but is only elevated in 50 % of early stage epithelial ovarian cancer patients [8]. There are also other cancers and benign conditions that can give elevated CA-125 levels so this marker alone cannot confirm diagnosis [9]. One of the main focus areas within ovarian cancer research is to find biomarkers that can detect cancer at an early stage with high specificity and sensitivity, making it possible to screen high risk patients or populations. Therefore it is important to continue studying tumour biology and its microenvironment so that one day it will be possible to improve patient prognosis and quality of life.

5.1.3 Treatment

As mentioned earlier the standard treatment for ovarian cancer is debulking surgery followed by chemotherapy (platinum- and taxane-based). There have been improvements when it comes to surgical techniques and chemotherapeutical regimes in the last decade, but the results have been modest when it comes to clinical outcome [10]. For patients that are diagnosed at advanced stages the probability of relapse is almost inevitable, and the development of chemoresistance is a significant problem when it comes to further treatment and clinical outcome [10].

However, the development of new analytical equipment with high throughput properties has given a better understanding of tumour biology. This is promising for new biologically targeted therapies that can give patients a more personalized treatment with a higher sensitivity, specificity and less side effects than traditional chemotherapy. The most promising targeted agents that already have passed randomized trials for ovarian cancer are anti-angiogenesis- (for example VEGF inhibition) and PARP inhibition agents (Inhibits PARP1 which is involved in DNA repair mechanism) [10, 11].

5.1.4 Ascites accumulation – how and why

Ascites is a term that is used when there is an accumulation of fluid in the peritoneal cavity. The reason for this accumulation can be a number of conditions, for example liver failure, tuberculosis and cancer [12]. The term malignant ascites is generally used when the peritoneal fluid tests positive for malignant cells and has an elevated level of lactate dehydrogenase (involved in tumour initiation and metabolism) [12, 13].

Malignant ascites is a complex mixture of soluble components (cytokines, chemokines and growth factors) and different cell types (free tumour cells, spheroids, mesothelial cells, fibroblasts, macrophages, white and red blood cells). Together they create a microenvironment that is crucial for further cancer progression, development of chemoresistance and recurrence of disease [12].

In a healthy human, the peritoneal cavity contains some fluid that works as a lubricant. The amount of this fluid is strictly regulated by secretion of small molecules from capillaries through the peritoneal membrane and reabsorption through lymphatic channels [12]. The main purpose of this fluid is to support organ mobility and easy transfer of solutes between adjacent organs and the peritoneum (Figure 3 A).

When tumour spreads to the abdominal cavity, there will be an elevated production of peritoneal fluid due to the disruption of the epithelial lining, increased leakiness of the tumour microvasculature, secretion from the tumour and obstruction of the lymphatic vessels [12](Figure 3 A and B).

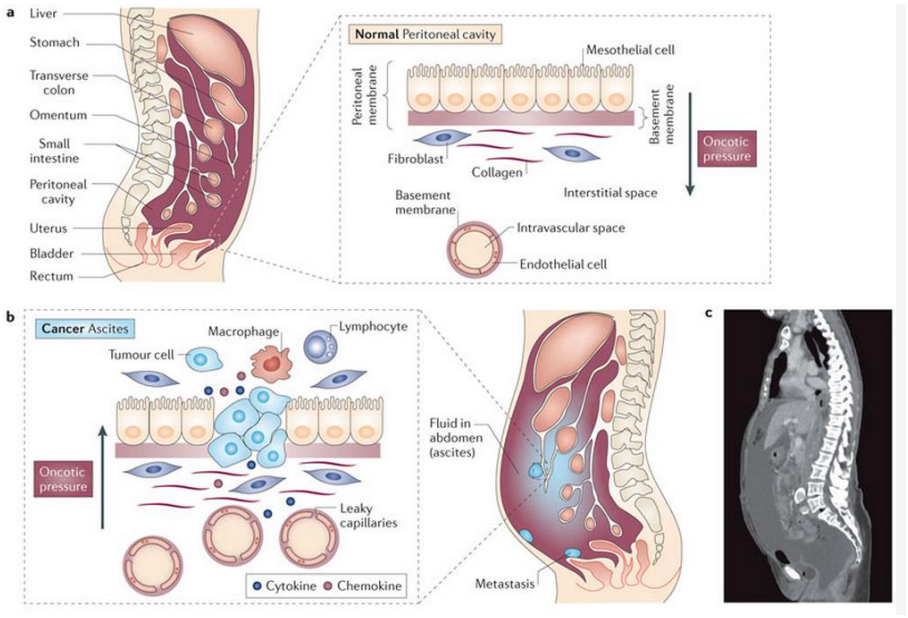

Figure 3 Normal peritoneal cavity (A), tumour metastases and ascites accumulation (B), modified from [12]

Most tumour cells grow rapidly and need an efficient supply of blood/oxygen (VEGF and other growth factors are involved in tumour angiogenesis). The newly formed blood vessels have a different architecture that supports further tumour progression. One of the main alterations is increased permeability so that cytokines, chemokines and free tumour cells can migrate into surrounding tissue and influence the microenvironment. Also tumour cells, associated stromal and immune cells secrete proteins at an elevated rate which leads to an increased volume of peritoneal fluid. In many cases the lymphatic channels that normally absorb the fluid from the peritoneal cavity and into the lymphatic circulation system can be blocked by tumour cells, restricting the reabsorption [12].

In this master thesis I have studied the effects of soluble components in malignant ascites, therefore cellular components will not be discussed further.

5.2 KEY SIGNALLING PATHWAYS IN OVARIAN CANCER

Cell growth is normally tightly controlled, but oncogenic (can cause or give rise malignant carcinoma) driver mutations in mitogenic signalling pathways combined with mutations in cellular DNA repair and/or cell cycle control mechanisms can lead to malignant transformation (cells obtains the properties of cancer). Mutations in different tumour-suppressor genes (genes that protect cells from developing cancer) and proto-oncogenes (can become an oncogene if mutated) can cause abnormal activation of signalling pathways leading to the loss of control when it comes to cell division. It is the effect of the downstream signalling events which decides tumour progression. Components found in malignant ascites can lead to the activation or deactivation of multiple signalling pathways in ovarian cancer cells. The three main signalling pathways are the PI3K (Phosphoinositide 3-kinase)-AKT/PKD (Protein kinase B), RAS-ERK (extracellular-signal-regulated kinases) and JAK (Janus kinase)/STAT (Signal Transducer and Activator of Transcription) pathways.

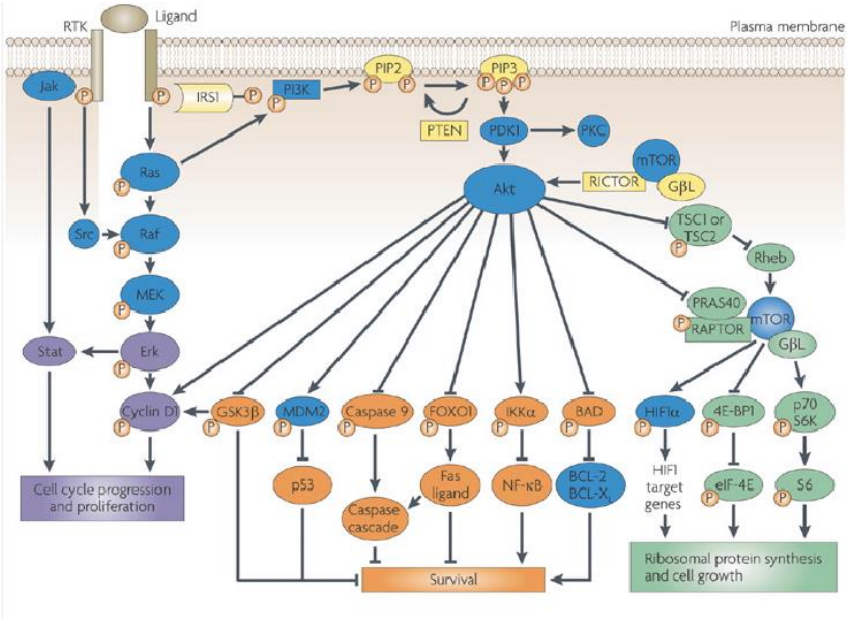

Figure 4 Key signalling pathways in ovarian cancer [14]

Activation of the RAS-ERK pathway

RAS-ERK pathway can be activated when a ligand binds to its cognate receptor which causes a conformational change that activates tyrosine kinases, leading to the phosphorylation of specific tyrosine residues in cytosolic domains. The adaptor protein GRB2 (growth factor receptor-bound protein 2) binds to the phosphorylated tyrosine residues. The SH3 (Src (Schmidt-Ruppin A-2) homolog 3) domain on GRB2 binds to SOS (Son of Sevenless) which exhibits GEF (guanine exchange

factor) activity [15]. SOS binds to the inactive RAS protein (small GTPase that function as a molecular switch. Can be activated and deactivated) and promotes dissociation from GDP (guanosine diphosphate) bound to RAS. This leads to the binding of GTP (guanosine triphosphate) to RAS and the dissociation of SOS [15]. RAS is now in its active form which leads to a phosphorylation cascade, starting with Raf. Activation of the RAS-ERK pathway supports cell cycle progression and proliferation, but it can also activate the AKT pathway [14] (Figure 4).

Activation of the AKT pathway

AKT can be activated via RAS, for example by ligand binding to insulin receptors or insulin like growth factor 1 (IRS-1) receptors. When a ligand binds to the receptor, a conformational change occurs which leads to the recruitment of IRS-1(insulin receptor substrate 1) that binds to Src homolog 2 (SH2) domains on the receptor. Specific tyrosine residues on IRS-1 are phosphorylated which results in downstream signalling transduction by further phosphorylation of PI3K. PI3K is now activated and can generate PIP3 (Phosphatidylinositol (3,4,5)-trisphosphate) from PIP2 (Phosphatidylinositol 4,5-bisphosphate) [14].

AKT exhibits kinase activity, and when PH domain (Pleckstrin Homology domain) in AKT binds to PIP3, PDK1 (phosphoinsositide dependent kinase 1) and PDK2 (phosphoinsositide dependent kinase 2) are activated in two steps and AKT is phosphorylated [14]. This results in a fully activated AKT, which leads to a cascade of intracellular signalling. The major effects of the activation of AKT pathways in ovarian cancer are seen in figure 4.

Activation of the JAK/STAT pathway

When ligand binds to its respective receptor, a conformational change occurs, leading to the recruitment of JAK1/2. Trans-phosphorylation of JAKs (tyrosine residues in the cytosolic domains) results in the phosphorylation of recruited STATs [16]. Once STATs are phosphorylated they dimerise and translocate to the nucleus were they initiate transcription of multiple genes that promote cell survival/growth and differentiation.

5.3 COMPONENTS IN ASCITES

Malignant ascites seems to play an essential role in tumour progression by creating a "tumour friendly" microenvironment [12, 17]. This fluid contains soluble components like cytokines, chemokines and growth factors, some of which are known to be overexpressed in ovarian cancer [12]. These components can affect key signalling pathways in ovarian cancer cells, by supporting and promoting cell cycle progression, cell proliferation, cell survival, protein synthesis and cell growth (Figure 4).

5.3.1 LPA (Lysophosphatidic acid)

LPA is one of the most known extracellular phospholipids that can induce a diversity of cellular responses, and are generated by autotaxin (ATX) and phospholipase A1/A2 (PLA1/2). The biological functions of LPA are mediated by G-coupled receptors (G_q, G_i and $G_{12/13}$) leading to the activation of multiple signalling pathways (Figure 5). Activation of the PI3K-AKT and the RAS-ERK pathways by LPA leads to cell survival by supressing apoptosis and cell proliferation.

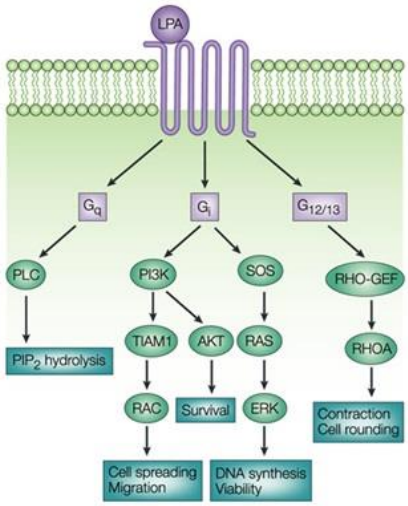

Figure 5 LPA activation of down-stream signalling pathways [18]

LPA triggers cellular responses that effect transcriptional regulation of multiple growth factors, like VEGF, UPA (urokinase plasminogen activator), IL-6 and IL-8 [12, 18]. This response can lead to increased endothelial permeability and inhibition of gap junction communication between adjacent cells [18], and thus support production and accumulation of ascites fluid. In ovarian cancer patients LPA levels are elevated in both serum and ascites, which correlates to a poor prognosis [12].

5.3.2 Cytokines

Cytokines are small polypeptides produced by cells, that individually or through cross talk with other cytokines or growth factors affect cancer progression through different mechanisms [16, 17]. Recent studies profiling malignant ascites have revealed elevated levels of multiple cytokines, including IL-6, IL-8 and IL-10 [12, 17] in ovarian cancer patients. IL-6 is regarded as a major contributor in tumourigenesis and leads to the activation of STAT3 which is known to initiate transcription of VEGF, BCL-2, c-MYC and Cyclin D1, and more. Cytokine activation of signalling pathways can promote cell survival, proliferation, migration/invasion angiogenesis and in some cases the development of chemoresistance [12, 17].

5.3.3 EGF (Epidermal growth factor) and its signalling pathway

Epidermal growth factor is a mitogenic stimulus for many cancer types. As seen in figure 6, EGF activation of its receptor leads to the phosphorylation of multiple intracellular proteins, for example AKT and STAT3. The EGFR (epithelial growth factor receptor) family consists of several receptors, HER2 (human epithelial receptor 2) , HER3 (human epithelial receptor3) and HER4 (human epithelial receptor 4), in addition to EGFR (human epithelial receptor 1) [19].

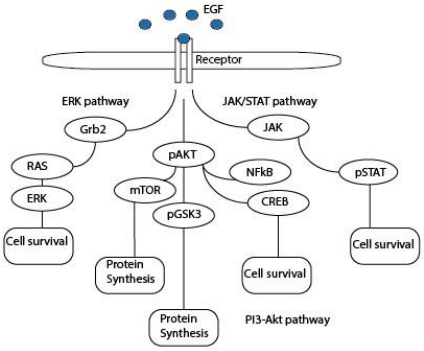

Figure 6 EGF signalling pathways

One of the known ligands that can bind and activate these receptors is EGF. However, HER2 and HER3 are thought to be co-receptors, because they do not bind ligands. EGFR is overexpressed in many cancers, due to mutations in genes coding for EGFR or in proteins that support EGFR activation and/or deactivation. Constant activation of EGFR results in uncontrolled cell division, and thereby supports tumourigenesis.

5.3.4 OPG (Osteoprotegerin)

OPG is a secreted member of the TNFR (tumour necrosis factor receptor) superfamily and it is known to regulate the homeostasis of bone re-modelling by preventing RANKL (Receptor activator of nuclear factor kappa-B ligand) binding to its receptor RANK (Receptor activator of nuclear factor kappa-B) (Figure 7).

Recent studies have revealed that OPG phosphorylates FAK (focal adhesion kinase) which results in AKT activation, supports proliferation and inhibits TRAIL-induced apoptosis in ovarian cancer cells [20, 21]. It has also been suggested that OPG works as a decoy receptor by binding to TRAIL with low affinity and inhibit TRAIL-induced apoptosis in other types of cancers, thus evading cell death (Figure 6). Recent research has shown that elevated levels of OPG are associated with a shorter progression-free survival [20]

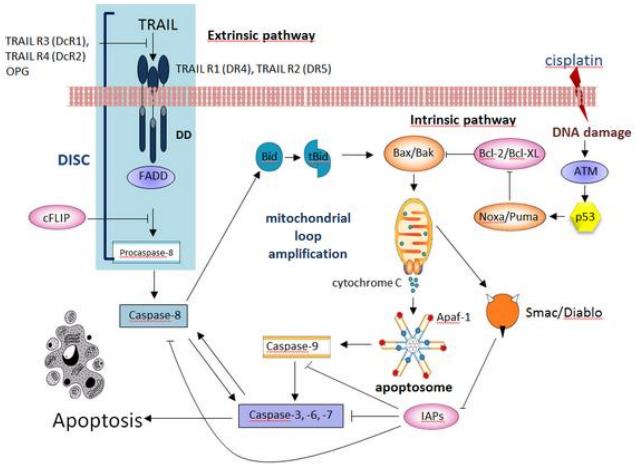

Figure 7 OPG inhibitions of RANKL and TRAIL [21].

5.3.5 VEGF (Vascular endothelial growth factor)

VEGF is a known growth factor and its expression is associated with the advanced stages of ovarian cancer [12]. There are multiple members in the VEGF family, including VEGF-A, VEGF-B, VEGF- C, VEGF-D and VEGF-E that all derive from the same gene (VEGF) by alternative splicing. Signalling transduction is mediated by tyrosine kinase receptors, VEGFR-1, VEGFR-2 and VEGFR-3 (Figure 8). Activation of VEGF pathways is known to increase angiogenesis, vasculogenesis (formation of new blood vessels, no pre-existing blood vessels) and lymphogiogenesis (formation of lymphatic vessels from pre-existing lymphatic vessels), thereby supporting tumourigenesis [22].

Overexpression of these receptors has been associated with the development of malignant ascites and poorer prognosis of ovarian cancer patients [12].

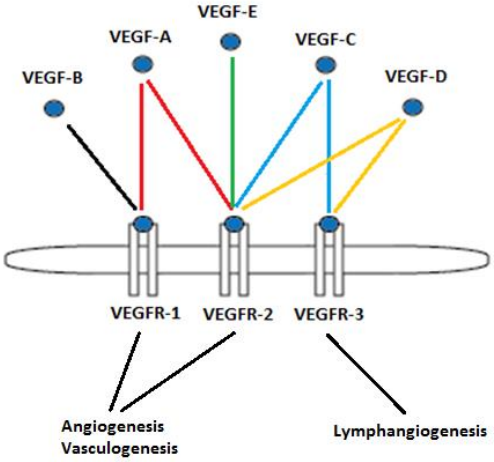

Figure 8 VEGF-A, B, C, D and E binding to its respective receptor which results in promotion of cell growth.

One of the mechanisms of VEGF activation is the down-regulation of the tight junction protein claudin 5 that increases the permeability of the peritoneal membrane by inducing angiogenesis. This leads to formation of new blood vessels with increased permeability [23]. Tight junctions are important to regulate the flow of solutes and water between epithelial and endothelial cell sheets.

5.4 OVARIAN CANCER CELL LINES

Cell lines are obtained from tumour cells in patients diagnosed with ovarian cancer. These cell lines have been characterized extensively to ensure that results can be reproduced and compared between research communities.

The NCI-60 (National Cancer Institute) human cancer cell line panel is one of the most studied panels worldwide and it has been intensely investigated so that research data can be compared between laboratories around the world [24, 25]. There are seven ovarian cancer cell lines in this panel, all with specific mutation signatures. Each of the cell lines represents individual tumours from which they were originally derived and will therefore exhibit somewhat different intracellular phosphorylation patterns when cells are treated.

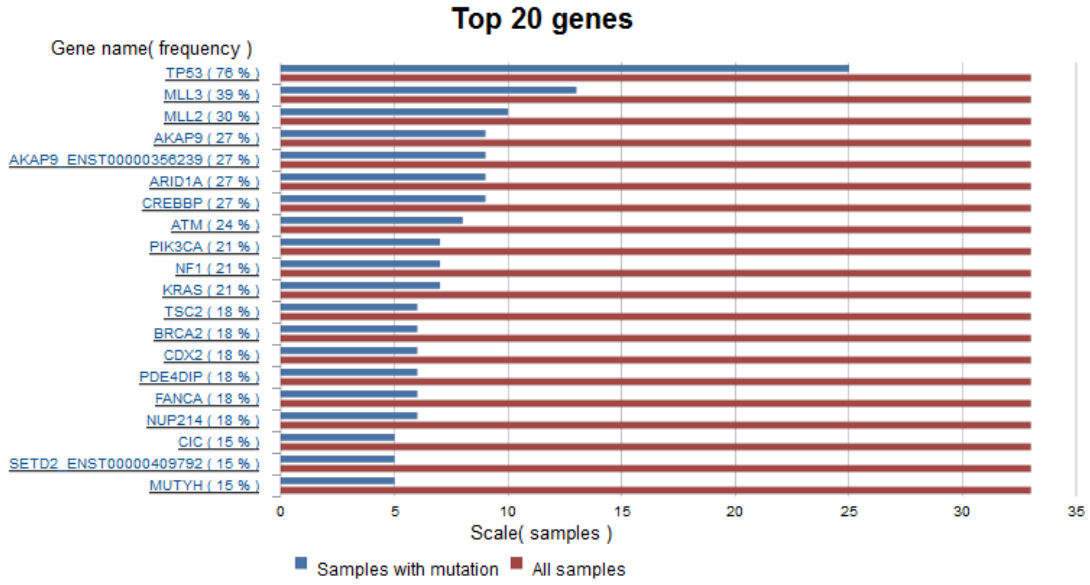

Figure 9 The 20 most frequently mutated genes found in ovarian cancer cell lines [26].

The most frequently observed mutation in ovarian cancer is TP53 which is an important tumour suppressor gene that normally contributes to the cellular and genetic stability of the cell [27] (Figure 9). A mutation in this gene might lead to loss of control in the cell division machinery, and tumours or other diseases may arise. Two other genes that are frequently mutated in ovarian cancer are MLL2 (Histone-lysine N-methyltransferase 2) and MLL3 (Histone-lysine N-methyltransferase 3) and these genes code for proteins involved with the methylation of the H3 protein (Histone 3). Mutations in H3 can lead to increased transcription of mitogenic genes [23, 24]. KRAS is another gene that is found mutated in multiple ovarian cancer cases and is an important protein when it comes to cell signalling [28]. These mutational differences are one of the reasons for why ovarian cancer is a very complex and heterogeneous disease. The ovarian cancer cell lines used in our experiments are listed in table 2.

Table 2 List of some known mutations in census genes in the different ovarian cancer cell lines from the NCI-60 panel, information is obtained from the cosmic - cell line project [26]

IGROV-1	SKOV-3	NCI/ADR-RES	OVCAR-3	OVCAR-4	OVCAR-5	OVCAR-8
TP53	ARID1A	ERBB2 (HER2)	PIK3R1	TP53	KRAS	CTNNB1
MLH1	FBXW7	TP53	TP53	BRCA2		APC
PIK3CA	TP53					KRAS
PTEN	APC					ERBB2 (HER2)

5.5 STATISTICS

Results in this thesis are presented as heatmaps, histograms, dot plots, bar diagrams and line diagrams. In heatmaps and histograms the results are calculated with a cloud based software (Cytobank) where elevated signals are displayed as colour intensities in proportion to a baseline signal, giving a visual overview of analysed data.

Most of our experiments are repeated once (n=1) or multiple times (n=1-5), making it possible to calculate the average (A)

$$A = \frac{1}{n}\sum_{i=1}^{n} x_i,$$

Were *n*, and *x* are the total number of values and each value, respectively, and the variations between the experiments (standard deviation, σ)

$$\sigma = \sqrt{\frac{1}{n}\left(\sum_{i=1}^{N}(x_i - \mu)^2\right)},$$

where *N*, *n*, *x* and μ are the total number of values, one specific value, each value and the mean of values, respectively.

6 OBJECTIVES

Ovarian cancer is the fifth leading cause of cancer deaths worldwide. A common complication with this disease is the accumulation of ascites. Ascites creates a tumour friendly microenvironment that further supports cancer progression. To better understand the tumour microenvironment we wanted to study the intracellular mitogenic signalling networks involved in multiple adherent ovarian cancer cell lines treated with malignant ascites, looking at phosphorylation patterns. The work presented in this master thesis is part of a larger project funded by the Norwegian Cancer Society with a Postdoc fellowship to Dr. Lena Eroukhmanoff to study the effects of the tumour microenvironment in ovarian cancer. As a part of this project, I characterized mitogenic signalling that mirrors the tumour microenvironment in several ovarian cancer cell lines in the presence of ascites from different patients. The objectives of my work were to:

1) Find good cell line candidates for our experiments;

2) Examine whether intracellular phosphorylation is affected by the cold trypsinization protocol, by parallel flow cytometry and Western blot experiments;

3) Ensure that 3D fluorescent cell barcoding with Alexa Fluor 488, Pacific blue and Pacific orange can be used in our experiments;

4) Study IL-6-induced intracellular phosphorylation of proteins, with focus on STAT3; and

5) Characterize intracellular phosphorylation signatures in two cell lines (SKOV-3 and OVCAR-8) treated with multiple patient samples of malignant ascites

7 MATERIALS

In this section we list the chemicals, materials, equipment and instrumentation used during the execution of this thesis.

7.1 CELL CULTURE

Table 3 Chemicals and dilutions used when working with cells. *Producer full name: LT= Life technologies, SA=Sigma-Aldrich, BC= The Biotechnology Centre of Oslo, BD= BD Bioscience*

ID	Chemicals	Producer / Cat#	Dilutions
A1	**1640 RPMI medium (1x) + GlutaMAX**	LT / 61870-010	
A2	**1640 RPMI medium + PS**		500 mL 1640 RPMI medium (A1) + 5 mL PS (A7)
A3	**1640 RPMI medium + FCS + PS**		500 mL 1640 RPMI medium (A1) + 50 mL FCS (A6) and 5 mL PS (A7)
A4	**1640 RPMI medium + PS + FCS + DMSO**		500 mL 1640 RPMI medium (A1) + 5 mL PS (A7) + 50mL FCS (A6) DMSO (A8)
A5	**TrypLE Express (1x)**	LT / 12605-010	
A6	**Trypsin (10xx) 2,5%**	LT / 15090-046	
A7	**FCS** (Fetal bovine serum)	LT / 26140-079	
A8	**PS (**Penicillin-Streptomycin)	LT / 10177012	
A9	**DMSO** (Dimethyl sulfoxide)	SA / 41640-100ML	
A10	**PBS**	BC	
A11	**Ethanol**	Kemetyl	
A12	**Barrycidal 36**	Interchem hygiene GmbH	
A13	**Relu+On Virkon**	DuPont	
A14	**Fix buffer I**	BD / 557870	
A15	**EGF**	SA / E9644	
A16	**IL-6 Blocking antibody**	MAB227	
A17	Alexa 647 CD3	LT / MHCD0320	

Table 4 Cell lines, equipment and instruments/software used when working with cell culture.

ID	Cell lines	Producer
I	SKOV-3	National Cancer Institute
II	NCI/ADR-RES	National Cancer Institute
III	OVCAR-3	National Cancer Institute
IV	OVCAR-4	National Cancer Institute
V	OVCAR-5	National Cancer Institute
VI	OVCAR-8	National Cancer Institute
ID	**Equipment**	**Producer / Cat#**
E1	50 mL sterile tubes (PP)	Sarstedt / 62.547.254
E2	15 mL sterile tubes (PP)	Sarstedt / 62.554001
E3	6 welled plate nuclon delta surface	Thermo Scientific / 140675
E4	Costar 96 welled V bottom plate	Sigma-Aldrich / CLS3894
E5	Nunc Cell Culture Treated EasYFlasks 75 cm^2	Thermo Scientific / 156499
E6	Costar Cell culture flasks 162 cm^2	Sigma-Aldrich / 3151
E7	Cryotube sterile vials	Thermo Scientific / 377267
ID	**Instrument**	**Software**
F1	Leica DMIL microscope	-
F2	Allegra X-22R centrifuge	-
F3	Eppendorf centrifuge 5415R	-

7.2 FLOW CYTOMETRY

Table 5 Chemicals used when performing flow cytometry. *Producers full name; BD=BD Bioscience, SA=Sigma-Aldrich, BC=The Biotechnology Centre of Oslo*

ID	Chemicals	Producer	Dilutions
B1	Flow wash buffer	BC	400 mL PBS (A10) + 5mL FCS (A7) + 10 % NaAzid (B2)
B2	10 % NaAzid	BC	
B3	FACS Clean	BD / 340345	
B4	BD FACS Shutdown solution	BD / 334224	
B5	BD FACS Flow	BD / 342003	
B6	BD Sheat solution	BD / 336911	
B7	Sodium hypochlorite solution	SA / 71696-5L	
B8	Perm buffer III	BD / 558050	
B9	Negative beads	BD / 51-90-9001291	
B10	Positive beads	BD / 51-90-9001229	
B11	dH_2O	BC	

Table 6 Conjugated antibodies and their dilutions. *Producer full name: BD=BD Bioscience, CST= Cell signalling technologies, SC=Santa Cruz*

Conjugated antibodies	Concentration	Antibody	FACS buffer	Producer / Cat#
IgG kappa		5 µl	20 µl	BD / 557783
Akt/PKB (pS473)		2 µl	23 µl	CST / 4075
MEK1		5 µl	20 µl	BD / 560043
NFkB (pS529)		1,5 µl	23,5 µl	BD / 558422
NFkB (pS539)		2,5 µl	22,5 µl	CST / 4887
STAT 3		4 µl	21 µl	BD / 557815
MAPKAPK-2		1 µl	24 µl	CST / 4320
Stat6		5 µl	20 µl	BD / 612601
Rb		2 µl	23 µl	BD / 558590
S6rp		1,5 µl	23,5 µl	CST / 4851
44/42 MAPK		1 µl	124 µl	CST / 4375
p38 MAPK		1 µl	49 µl	CST / 4552
STAT 1 (pY701)		5 µl	20 µl	BD / 512597
STAT 1 (pY701)		5 µl	20 µl	BD / 560190
AKT (pT308)		5 µl	20 µl	CST / 3375
STAT5		5 µl	20 µl	BD / 612597
ATF-2		1 µl	24 µl	SC / SC-8398
Histone H3		1,5 µl	48,5 µl	CST / 9716
SAPK/JNK		2 µl	23 µl	CST / 9257

Table 7 Unconjugated antibodies and their dilutions. *Producer full name: BD=BD Bioscience, CST= Cell signalling technologies, SC=Santa Cruz, AC=Abcam, I=Invitrogen*

Unconjugated antibodies	Amount antibody	Amount FACS buffer	Producer / Cat#
PLCg-1 (pT783)	1 µl	250 µl	CST / 2821
b-catenin (pS45)	1 µl	250 µl	CST / 9564
Gsk3 beta (pS9)	1 µl	125 µl	CST / 9336S
Gsk3 alfa (pS21)	1 µl	125 µl	CST / 9316
Vasp (pS157)	1 µl	500 µl	CST / 3111
Vimentin (pS56)	1 µl	125 µl	AC / Ab52942
Jak-2	1 µl	200 µl	CST / 8082S
CaMKII (pT286)	1 µl	125 µl	CST / 3361
Cdc-2 (pT161)	1 µl	125 µl	CST / 9114
HSP27 (pS82)	1 µl	125 µl	CST / 2405
PKD/PKCµ	1 µl	500 µl	CST / 2054
Vasp (pS239)	1 µl	500 µl	CST / 3114
Vav (pY174)	1 µl	500 µl	SC / SC16408-R
Goat anti rabbit A647	1 µl	8000 µl	I / A21245

Table 8 Dyes used when performing flow cytometry. *Producers full name: LT=Life technologies.*

Dye name	Producer	Concentration	Dilutions
Alexa Fluor 488	LT / A-20100	Stock	
		0	2 µL stock /dye stock) and 998 µL DMSO
		1	100 µL (concentration 0) and 900 µL DMSO
		2	100 µL (concentration 1) and 250 µL DMSO
		3	100 µL (concentration 2) and 300 µL DMSO
		4	50 µL (concentration 3) and 550 µL DMSO
Pacific Blue	LT / P-10163	0	2 µL stock /dye stock) and 498 µL DMSO
		1	100 µL (concentration 0) and 900 µL DMSO
		2	100 µL (concentration 1) and 300 µL DMSO
		3	100 µL (concentration 2) and 300 µL DMSO
		4	44 µL (concentration 3) and 355 µL DMSO
Pacific Orange	LT / P30253	0	10 µL stock /dye stock) and 90 µL DMSO
		1	90 µL (concentration 1) and 360 µL DMSO
		2	125 µL (concentration20) and 325 µL DMSO
		3	75 µL (concentration 0) and 325 µL DMSO
		4	83 µL (concentration 0) and 917 µL DMSO

Table 9 Visual observation of patient samples (ascites).

Patient samples	Visual observations	Patient samples	Visual observations
# 23	Yellow and clear	# 36	Yellow and clear
# 25	Weakly orange and clear	# 37	Yellow and clear
# 27	Weakly yellow and clear	# 38	Weakly yellow and clear
# 28	Yellow and clear	# 39	Yellow with tissue lumps
# 29	Yellow and clear	# 40	Orange and clear
# 30	Yellow and clear	# 41	Orange and clear
# 31	Yellow and clear	# 42	Orange and clear
# 32	Yellow and clear	# 43	Orange, unclear and with tissue lumps
# 33	Yellow and clear	# 44	Orange/brown and clear
# 35	Yellow and clear	# 45	Yellow and clear

Table 10 Cell lines, equipment and instruments/software used when performing flow cytometry.

ID	Equipment	Producer / Cat#
E2	15 mL sterile tubes (PP)	Sarstedt / 62.554001
E8	Costar 96 well V bottom plates	Sigma-Aldrich / CLS3894
ID	**Instruments**	**Software**
F2	Allegra X-22R centrifuge	-
F3	Eppendorf centrifuge 5415R	-
F4	Eppendorf centrifuge 5810	-
F5	Vortex V1	-
F6	BD FACSCanto II	FACSDiva
F7	BD LSRFortessa	FACSDiva

7.3 WESTERN BLOT

Table 11 Chemicals used when performing Western blot. *Producer full name; JIR=Jackson ImmunoResearch, BC=The Biotechnology Centre of Oslo, SA=Sigma Aldrich, TH=Thermo Scientific, AGFA=AGFA*

ID	Chemicals	Producer	Dilutions
C1	Lysis buffer	BC	150mM NaCl + 50 mM Tris 8.0 + 1% Trito X-100
C2	Protease inhibitor		1 tablet + 1 ml dH20 = 50x solution. Further diluted 50x in lysis buffer
C3	Loading buffer (SDS 3x)	BC	
C4	Loading buffer (SDS 1x)	BC	
C5	SDS running buffer (10x)	BC	(150 g Tris/HCL + 720g glycine + 50g SDS) diluted to 5 litre with dH_2O
C6	Towbin buffer	BC	(15g Tris/HCL + 1000mL methanol + 72g glycine) diluted to 5 litre with dH_2O, pH adjusted to 8,3
C7	TBS-T (10x)	BC	(60,5g Tris/HCL + 438,5g NaCl + 20 mL Tween 20) diluted to 5 litre with dH_2O
C8	TBS-T (1x)	BC	100 mL of 10x TBS-T + 900 mL dH_2O
C9	Ponceau S solution (0,1%)	SA / P7170-1L	
C10	Methanol	VWR / 00288	
C11	pSTAT-3 (Rabbit)	CST / 9131	
C12	pAKT (pT308) (Rabbit)	CST /	
C13	Vinculin (mouse)	SA / V9131	
C14	BSA	SA / A6003-25G	

C15	NaN_3	SA / 26628-22-8	
C16	Milk powder	Tine	
C17	5% milk solution	BC	0,5 g milk powder(C16) to 10mL 1x TBS-T
C18	Secondary antibody (mouse)	JIR / 115035-146	
C19	Secondary antibody (rabbit)	JIR / 111-035-144	
C20	Super Signal West Dura ext.	TS / 34076	
C20	G354 Rapid fixer	AGFA / 2828Q	
C21	G153 A Developer	AGFA / HT536	
C22	G153 B Developer	AGFA /HT536	
C23	Gel		Citerion with 10 % Tris-HCL polyacrylamide (18 wells)
C24	Ladder (standard)		

Table 12 Equipment and instruments/software used when performing Western blot.

ID	Equipment	Producer / Cat#
E10	Development cassette	
E11	Amersham hyperfilm MP	GM healthcare
E12	Electrophorese chamber, criterion	BIO-RAD
E13	Transfer chamber, criterion blotter (strings)	BIO-RAD
E14	Transfer membrane Immobilon	Millipore Corporation / IPVH00010
ID	**Instruments**	**Producer / Software**
F8	CURIX 60 Developer	AGFA
F9	Shaker platform STR8	Stuart Scientific
F10	Heater Dri-block DB2D	Techne
F11	Electrophorese PowerPac HC	BIO-RAD

8 METHODS

In this section we list the employed methodology. We used protocols modified by scientists in the Taskén group for all experiments. Some of these protocols are still under development.

8.1 CELL CULTURE

Adherent cells can be grown in culture flasks with a surface that is slightly hydrophilic (pulls cells towards the plastic binding surface). Different plasma membrane proteins bind the cell to the flask surface and to other cells as they expand.

To provide a good environment for the cells it is important to carefully check them in the microscope, provide them with nutrients and to maintain conditions of right pH, stable CO_2- and humidity levels. Culturing conditions may vary from cell line to cell line and it is therefore important to check this before a new cell line is used. It is also important to split cells regularly to avoid mutations and cell death.

As illustrated by the standard growth curve for adherent cells (figure 10), they go through different growth stages. In our experiments, we wanted to examine cells in their log phase. If cells were to move beyond log phase they would experience stress and activate pathways that normally are inhibited during the log phase. This could lead to increased phosphorylation of some proteins and give a false baseline in our experiments.

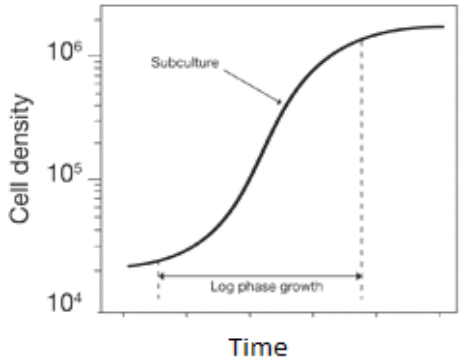

Figure 10 General cell growth curve.

8.1.1 Cell lines

In our experiments we have used multiple cell lines which were stored at -150 degrees Celsius until used. When stock cell lines were thawed and expanded a personal stock was frozen down and used in later experiments.

8.1.1.1 Passaging cell lines

1) Remove FCS medium
2) Rinse with 9 mL PBS (A10)
3) Add 2-4 mL of trypsin (A5). Trypsin need to be in contact with the entire surface were cells are attached to the- flask bottom
4) Remove trypsin
5) Incubate at 37°C with a CO_2 level at 5 % until they detach – confirm by looking at the cells in the microscope (Leica DMIL – F1)
6) Add FCS medium (A3) to quench reaction, volume is dependent on split ratio
7) Distribute medium into new bottles (E6) or a tubes (E1, E2 - for cell counting)
8) Wash with FCS medium (A3) and distribute cell suspension into one or all the flasks/tubes
9) For 162cm^3 flasks the total medium volume should be 25 mL, and for 75cm^3 flasks the total volume should be 12 mL

8.1.1.2 Cell line start-up and freezing

- Thaw cells fast in water bath and immediately transfer cells to preheated 11 mL FCS medium (A3) in culturing flasks 75cm^3 (E5) and incubate at 37°C with a CO_2 level at 5 %.
- Next day, remove medium from flask and add 12 mL new preheated FCS medium (A3)
- Change medium every day until cells have reached approximately 80 % confluence
- Passage cells 1:2 and expand further to approximately 80 % confluency, then passage cells in flask into multiple flasks (E6) (See protocol for passaging cell lines, above)

- Once cells have reached about 80 % confluency they are ready to be trypsinazed and frozen down
- Trypsinize cells with 1x trypsin (A5) until all cells detach from surface (verify in Leica DMIL microscope, F1)
- Transfer cell suspension to 50 mL tubes (E1) and spin down for 7 minutes at 4°C at 200rcf, Allgera centrifuge (F2)
- Remove medium and add new FCS medium with DMSO (A4), re-suspend cells by carefully pipetting
- Add 1 mL to 3-4 2,5 mL cryo tubes (E7) pr. 162 cm^3 flask and put on ice and transfer tubes to freezer (-150°C) for storage until needed

8.1.1.3 Setting up experiments with 6 well plates

In our experiments we have used 6 well plates (E3) with approximately 150 000 cells per well. It is important that counting is performed correctly in a Bürker chamber. It is recommended to count at least two individual times and calculate the average.

- Perform step 1-5 listed in the protocol for passaging cell lines, above
- Add FCS medium (A3) to quench reaction, volume is not important
- Transfer cell suspension into sterile tubes (E1 or E2)
- Spin down tube at 200rcf for 7 minutes, Allgera centrifuge (F2)
- Remove supernatant
- Re-suspend cell pellet in 2-12 mL FCS medium (A3) depending on the pellet size
- Mix 100 µL PBS and 100 µL cells in a 1.5 mL sterile Eppendorf tube
- Add 12,5 µL to counting chip
- Count cells in microscope (Leica DMIL – F1) and follow the guidelines, figure 10
- Repeat the two last points
- Dilute cell suspension so that there is 150 000 cells per mL in FCS medium (A3). Take into consideration how many 6 well plates (E3) that are used in the experiment

- Add 1 mL into each well and incubate at 37° with a CO_2 concentration at 5 % overnight
- Remove medium and wash with FCS free medium (A2)
- Add 1 mL FCS free medium (A2) into each well (starve the cells), and incubate at 37° with a CO_2 concentration at 5 % overnight
- Before starting experiment, check the cells in the microscope, Leica DMIL (F1), and make sure they are healthy and evenly distributed. Cells in plates should now be ready for stimulation.

8.1.2 Treatment

8.1.2.1 Treatment medium

In our experiments, we have treated cells with EGF or with ascites from multiple patients. EGF was used to investigate whether intracellular phosphorylation was affected by the established cold trypsinization protocol (EGF is known to trigger cellular responses in most cell lines). We used a concentration of 100 ng/mL in our experiments.

Ascites samples were collected at Haukeland University Hospital from patients with ovarian cancer in stage III and IV. Samples were collected at the time of surgery and before chemotherapy. The Regional Ethics Committee approved the study and all patients consented. When received, samples were logged and spun down to remove cells (tumour and immune cells), then stored at -80 °C until use.

8.1.2.2 Treatment protocol

- For each well treated, approximately 260-280 µL ascites is needed
- Thaw ascites samples in room temperature, put immediately on ice when ready
- Dilute ascites samples 1:2 in FCS free medium (A2)
- Put diluted ascites in water bath at 37°C, 3-5 minutes before treatment start
- Put prepared 6 well plates in water bath that is set to 37°C
- Remove FCS free medium from wells
- Add 0,5 mL (50 %) tempered ascites to each well, start timer
- Put plate on ice immediately after time course (after 20 and 3 minutes)

- Remove treatment medium and wash with 1,0 mL/well ice cold PBS (A10)
- Remove PBS and add 700 µL/well ice cold Trypsin (A6)
- Trypsinize cells for 20 minutes on ice
- Quench reaction by adding 600 µL /well FCS medium (A3)
- Wash cells with 1 mL pipette and transfer cells to a 1.5 mL Eppendorf tubes
- Spin down, 5 min @ 500g @ 4°C (Eppendorf centrifuge - F3)
- Resuspend cells in 1 mL ice cold PBS (A10)
- Spin down, 5 min @ 500g @ 4°C (Eppendorf centrifuge - F3)
- Resuspend cells in 100 µL ice cold PBS (A10)
- Add 100 µL FIX buffer I (A14) and incubate in water bath at 37°C for 10 minutes
- Add 800 µL ice cold PBS, spin down for 5 min @ 700g @ 4°C (Eppendorf centrifuge - F3)
- Wash cells with 1 mL ice cold PBS (A10)
- Resuspend cells in so that the total volume is 200 µL with ice cold PBS (A10)
- Cells are now ready for fluorescent cell barcoding

8.2 FLOW CYTOMETRY

Flow cytometry is a technique that can measure physical cell properties as single cells flow past one or multiple light beams. Scattered and emitted light can be detected and converted to electronic signals. Then computer software can convert these signals into readable data that contains information about physical characteristics of each cell in the sample, including cell size, granularity and relative fluorescent intensity. With flow cytometry a whole spectre of proteins can be investigated simultaneously within single cells, making it possible to draw maps of protein status within individual cells at specific time points. This makes it possible to obtain both qualitative and quantitative information about intracellular molecules and/or cell surface receptors in one single cell. Other analytical methods like Western blot are usually used for investigating one or a few proteins within a cell population.

In the last decade there has been improvement within flow cytometry and immunostaining methods (staining specific targets with antibodies), which has led to the rise of phosphoflow cytometry. This technique makes it possible to study phosphorylation of intracellular proteins that are essential in signalling transduction within individual cells using phospho-epitope specific antibodies [29]. Furthermore, introduction of fluorescent cell barcoding (FCB) has revolutionized the method by allowing high throughput analysis, making it possible to analyse multiple cell populations in one sample. In the future, phosphoflow cytometry can give us an increased global understanding of the signal transduction dynamics at single cell levels [29].

In our experiments, before analysing samples by phosphoflow cytometry, cell populations were treated (activating signalling transduction). After this, cell populations were barcoded, combined and stained with protein specific antibodies that were conjugated to fluorochromes.

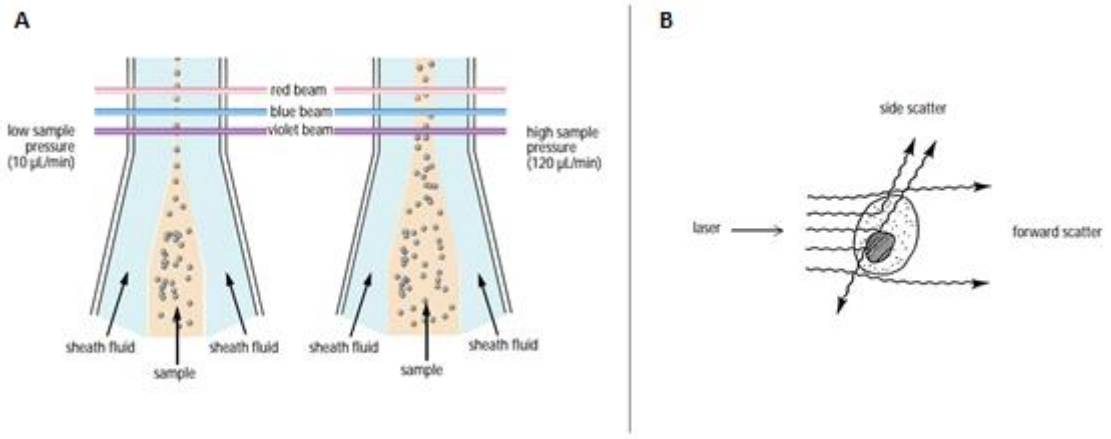

Figure 11 Flow cytometry (BDCanto II) Sample flow chamber (A) and side/forward scatter (B), from [30, 31].

In flow cytometry, samples (containing cells) are injected into the middle of the sheath flow (Figure -11A). If the density and/or velocity of the sample fluid and the sheath fluid differ enough they will not mix (laminar stream), creating a two layer fluid flow. Sheath flow carries cells towards a hydrodynamic focus point where one or multiple lasers are aimed. This focus point is created by increasing or decreasing sample pressure, making it possible to regulate the diameter (Figure 11A). Increased pressure will provide a higher flow rate and diameter. This means that multiple cells will be exposed to the laser beams at once, leading to a lower resolution [30, 31]. By controlling the flow rate it is possible to acquire a flow diameter where there is only room for one cell, thereby making it possible to measure single cells (Figure 11A).

In BD FACSCanto and BD FACSFortessa there are three lasers; blue laser (488nm), red laser (640nm) and violet laser (405nm). When one or multiple laser beams strike a single cell in the measuring chamber, some light will be scattered and some energy will be absorbed. If fluorescent antibodies are used to stain cells or cellular components, photons are absorbed causing electrons to jump to a higher energy state (electrons are excited). After some time, electrons will return to their ground state, leading to the emission of quantum light, which is known as fluorescence. The emitted wavelength is usually longer than the absorbed wavelength, and this makes it possible to use the same laser on multiple fluorochromes. For example, fluorochromes PerCP and FITC both absorb blue light at 488 nm but PerCP emits red light at 675nm and FITC emits green light at 530nm. Scattered and emitted light passes through a number of lenses and optical filters before reaching the detectors (Figure 12). Their main function is to modify spectral distribution by sorting and guiding specific intervals of wavelength (the emitted light of a specific fluorochrome) to its specific detector.

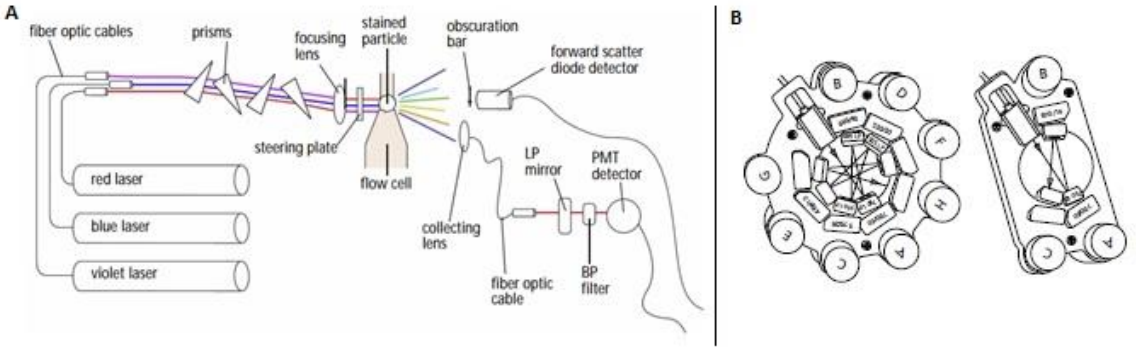

Figure 12 BD FACSCanto and BD LSRFortessa light pathways from laser to detector (A), and photomultiplier tube configuration, from [30, 31].

Scattered and emitted fluorescent light can be detected by two different detector systems (Figure 12). The first detector array is a photodiode that can detect strong signals, like forward scatter (FSC). The other detector system is PMTs (photomultiplier tubes), which can detect weaker signals like fluorescence light or side scatter (SSC) [30, 31]. Forward scatter reveals information about cell size and side scatter gives information about internal granularity and complexity of a single cell (Figure 11b). BD FACSCanto and BD FACSFortessa are equipped with one photodiode that detects FCS, one PMT that detect SSC, and 6-10 PMTs each that together can measure a wide range of wavelengths of fluorescent light.

8.2.1 Spillover and compensation

One of the major challenges within multicolour flow cytometry is when emission from one fluorochrome is detected in a detector that is designed for another fluorochrome; this is known as spillover and can cause significant optical background [32].

Detectors are set to measure between specific wavelengths, but since fluorochromes emit light over a range of wavelengths this will cause a physical overlap in the emission spectra of other fluorochromes. Figure 13A shows the detection of a specific fluorochrome in the FITC channel, but due to the brightness of the fluorochrome there is also detection in the PE channel. This means that the area detected will be smaller, and the calculated fluorescence response will be inaccurate.

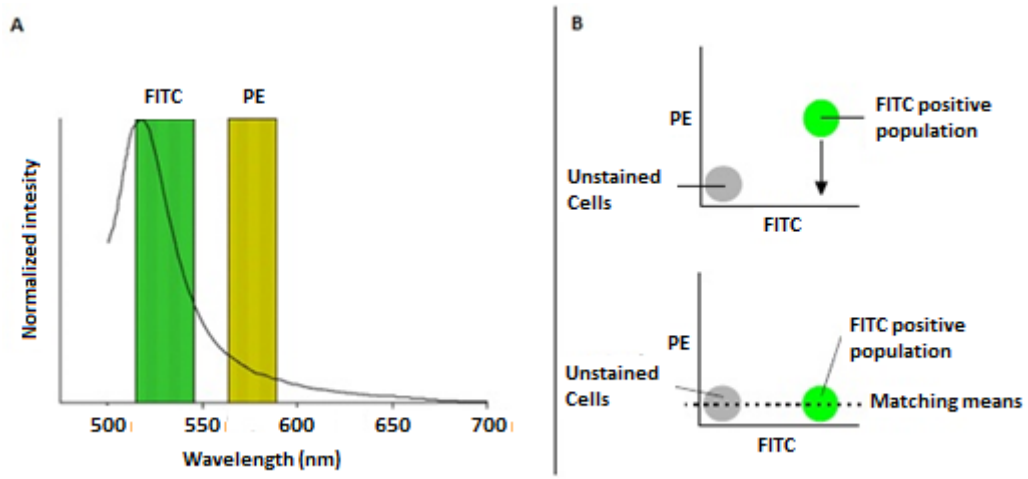

Figure 13 Fluorochrome spillover in PE channel (A) and compensation by unstained and stained cells (B), from [30, 31].

To solve this problem a mathematical compensation technique has been developed were the percentage spillover is moved to the right channel. This is done by running a sample containing single stained cells and unstained cells for all fluorochromes that are used in the experiment. By manually setting the window for each fluorochrome the program can compensate and the problem is solved (figure 13B).

8.2.2 Fluorescent cell barcoding

In most of our experiments we have used 3D fluorescent cell barcoding to distinguish between different cell populations (for example cells that have been treated with different patient samples of ascites and/or for different time periods). Fluorescent cell barcoding (FCB) makes it possible to use multiple cell populations in one sample. We have used three fluorescent dyes for FCB in our experiments, Alexa Fluor 488, Pacific blue and Pacific orange.

- **Pacific Orange** is an amine-reactive succinimidyl ester that is excitable with the violet laser at 405 nm. Maximum emission wavelength is approximately 551 nm
- **Pacific Blue** is an amine-reactive succinimidyl ester that is excitable with the blue laser at 405 nm. Maximum emission wavelength is approximately 455 nm
- **Alexa Fluor 488** is an amine-reactive succinimidyl ester that is excitable with the violet laser at 495 nm. Maximum emission wavelength is approximately 519 nm

By distributing four different concentrations of Alexa Fluor 488 into multiple wells and adding different concentration combinations of Pacific blue and Pacific orange, we could run up to 64 cell populations in one experiment (Figure 14). It is important that dyes are protected from light exposure as much as possible to ensure separation of each cell population after analyses.

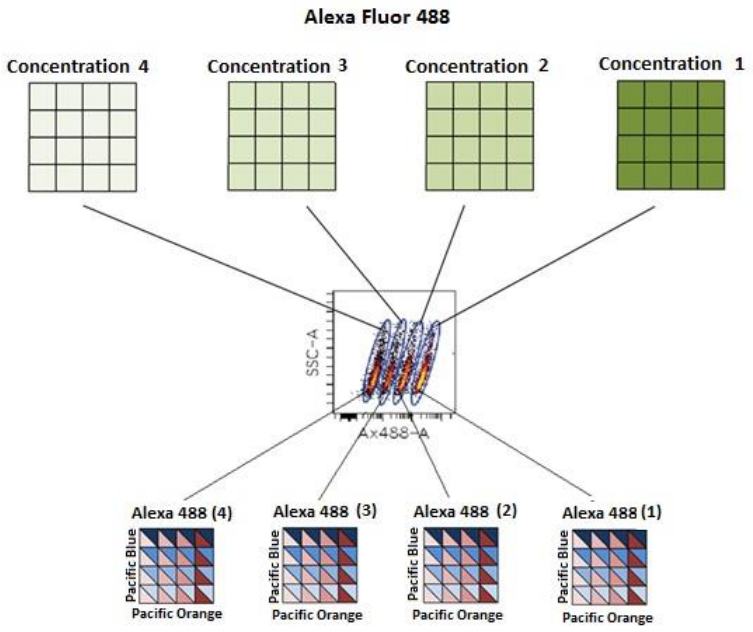

Figure 14 Example on 3D fluorescent cell barcoding.

8.2.2.1 Fluorescent cell barcoding - samples

- Transfer 5 µL of Pacific orange concentration 1-4 into 4 x 16 wells (figure 11)
- Transfer 5 µL with different concentrations of AX and PB 4 x 16 wells (figure 11)
- Transfer 200µL cell suspensions into wells in the FCB (fluorescent cell barcoding) plate (E8)
- Incubate at room temperature for 30 minutes (DARK)
- Spin down, 5 min @ 700rcf (Eppendorf centrifuge – F4)
- Wash with 200µL flow wash buffer (B1) and spin again with the same parameters
- Re-suspend cells in 200µL and combine FCB populations in a 15 mL tube (E2)
- Wash wells with flow wash buffer (B1). The total volume should be around 3 mL
- Spin down, 7 min @ 700rcf (Allgera centrifuge - F2), remove supernatant
- Vortex pellet (Vortex V1) so that the solution is homogenous
- Add 300-500 µL of perm buffer III (B8) per 15 mL tubes and store for -80° for minimum 30 minutes (up to three months)

8.2.2.2 Fluorescent cell barcoding - compensation controls

- For compensation control it is possible to use untreated cells
- Save some of the untreated cells (unstained cells)
- Transfer 5 µL of concentration 1 (highest) of each dye to individual wells
- Add 200 µL untreated cells to each well and mix well
- Incubate at room temperature for 30 minutes (DARK)
- Spin down, 5 min @ 700rcf, Eppendorf centrifuge (F3)
- Wash with 200 flow wash buffer and spin again with the same parameters
- Re-suspend cells in 200 µL flow wash buffer (B1) and transfer each single stained population to individual Eppendorf tubes, wash each well once
- Add untreated cells (1:3 3D fluorescent cell barcoding is used)
- Spin down, 5 min @ 700rcf, Eppendorf centrifuge (F3)
- Remove supernatant
- Vortex pellets so that the solution is homogeneous
- Add 100 µL of perm buffer III (B8) per Eppendorf tube and store for -80°C for minimum 30 minutes (up to three months)

8.2.3 Antibodies and staining

Antibodies, also known as immunoglobulins, are a part of the adaptive immunity [33]. Their function is to recognize and flag foreign objects (like viruses and bacteria) for further elimination by the immune system. The general structure is made up by one heavy chain and one light chain. The different domains are crucial when it comes to specificity. The main structure of antibodies consists of one light chain and one heavy chain; marked in green and blue (Figure 15).

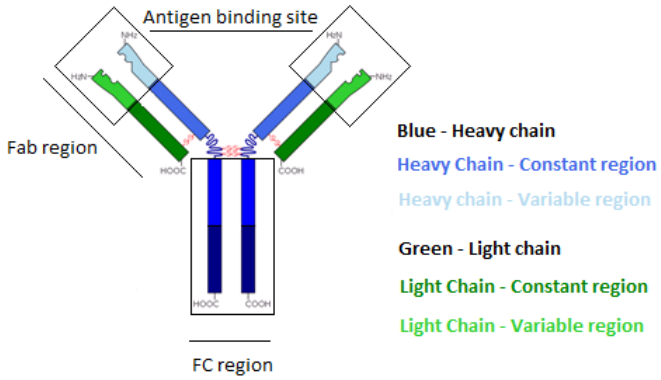

Figure 15 Simplified structure of an antibody, modified from [1].

In each chain, there is one constant region, similar in all antibodies within the same isotype, and one variable region that is antigen-specific. The Fab region (fragment antigen binding) functions as the binding site for antigens while the FC region (fragment crystallisable) is where the effector domain lies. This site can bind to other immune cells, and activate the complementary immune response [33].

Our understanding of their structure has made it possible to develop antibodies that can recognize and bind to specific phosphorylated states of proteins (known as phopho-specific antibodies). By conjugating fluorochromes to these antibodies, they can be detected by multiple analytical methods, including flow cytometry.

The method involving the use of antibodies to detect specific proteins is called immunostaining. In flow cytometry and Western blot there are two types of antibodies that frequently are used (Figure 16). The first one is attached to a fluorochrome (conjugated antibodies) and can bind directly to specific sites on target of interest. The other antibody type has no fluorochromes attached (unconjugated antibody) and can bind to specific sites on target of interest. However, to be able to detect signals a secondary antibody is required. This antibody is attached to a flourochrome and can bind to specific sites on the FC region of a primary antibody.

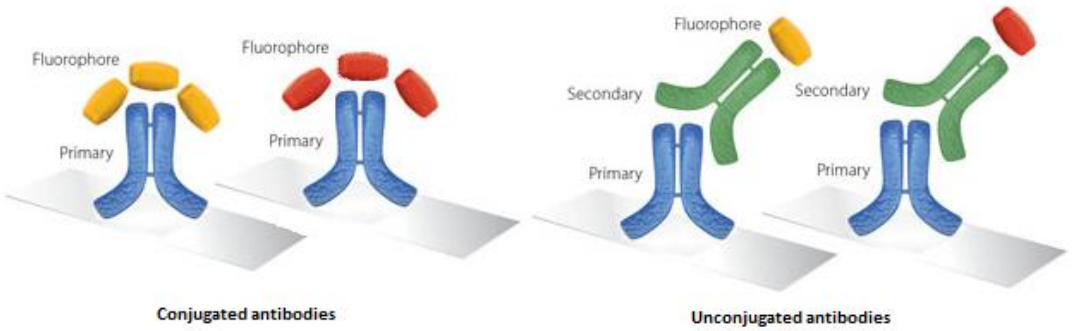

Figure 16 Conjugated and unconjugated antibodies, modified from [34].

Activation of intracellular signalling pathways is known to be mediated by protein phosphorylation, leading to the transcription of different genes that promotes cellular functions. Phospho-specific antibodies make it possible to tag these phosphorylated proteins so that active signalling pathways can be detected [35].

8.2.3.1 Antibody staining procedure

Conjugated antibodies

- Thaw cells, including compensation controls and unstained cells.
- Add flow wash buffer so that volume is 3 mL (samples) and 1 mL (compensation controls)
- Spin down at 700rcf for 7 minutes, Allgera centrifuge (F2)
- Wash two more times with flow wash buffer (B1)
- Resuspend cells in flow wash buffer (B1), volume is dependent on how many antibodies you want to analyse (for example 5 antibodies = 5 x 25µL = 125µL + extra volume to check instrument parameters)
- Add 25µL cell suspension in each well, one for each antibody, in a 96 well V bottom plate (E8)
- Then add 25µL of each antibody in pre-marked wells
- Incubate in the dark at room temperature for 30 minutes
- Wash two times with flow wash buffer (B1)

First time with 150µL flow wash buffer (B1), spin down at 700rcf for 5 min, Eppendorf centrifuge (F4). The second time with 200µL flow wash buffer (B1) at 700rcf for 5 min, Eppendorf centrifuge (F4). To remove fluids after each spin flip the plate hard and only once.

- Resuspend in 200µL flow wash buffer (B1), samples is now ready for analysis

Unconjugated antibodies

- To dilute antibodies use 1,5 mL test tubes, dilute with flow wash buffer (B1)
- Add 25µL diluted antibodies into pre-marked wells, in a 96 welled V bottom plate (E8)
- Add 25µL of cell suspension in each well, one for each antibody, mix well with the pipette
- In the well that is marked secondary alone (Goat anti Rabbit Alexa Fluor 647), add flow wash buffer(B1) as antibody
- Incubate dark at room temperature for 30 minutes
- Wash two times with flow wash buffer (B1), follow the washing step listed under conjugated antibodies
- Then add 50µL of pre-diluted secondary alone, mix by pipetting
- Incubate in the dark at room temperature for 30 minutes
- Wash two times with flow wash buffer as listed under conjugated antibodies
- Resuspend in 200µL flow wash buffer (B1), samples are now ready for analysis

Beads

- Beads are prepared in an Eppendorf tube
- Add 100µL flow wash buffer (B1)
- 1 drop negative beads (B9), vortex before use
- 1 drop positive beads anti-mouse (B10)
- 2 µL antibody (mouse) example Alexa Fluor 647 CD3 (listed under dyes)
- Mix together and incubate at room temperature in the dark for 15 minutes
- Add flow buffer so that the total volume is about 1mL
- Spin down at 700rcf for 7 min, Eppendorf centrifuge (F3)
- Resuspend pellet in 0,5 mL flow wash buffer
- Beads are ready for analysis

Compensation control and unstained cells

- Add flow was buffer (B1) to compensation controls and unstained cells so that the total volume is 1mL, spin down at 700rcf for 5 min, Eppendorf centrifuge (F3)
- Resuspend pellet in 100-150µL flow wash buffer (B1)
- Cells are ready for analysis

8.3 CYTOBANK – ASSESSING RESULTS

There are a few software utilities that can be used to analyse results obtained by flow cytometry, Cytobank is one of them. This cloud-based software makes it possible to generate information about cell properties and to share the results with other researchers.

First, the data files generated from flow cytometry experiments need to be uploaded to the Cytobank server. In most cases the interest is to study live, singlet cells, thereby duplicates and dead cells need to be excluded from main cell populations.

This is done by setting FSC-A on the Y axis and SSC-A on the X-axis and gating the live cells (dead cells will be in the population with low FSC-A and SSC-A), shown in figure 17A. Then duplicates are excluded by gating singlet cells according to the parameters shown in figure 17B.

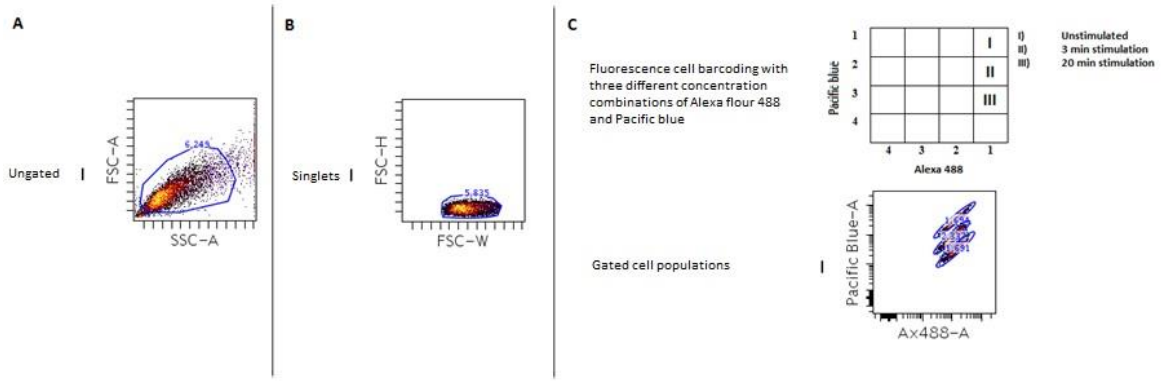

Figure 17 Cytobank gating of live cells (A), singlets (B) and fluorescence cell barcoding combinations and their gated cell populations (C).

When singlet cells are identified, the different cell populations within the sample can be gated/identified. Further gating strategies depend on whether there has been used one, two or three dyes in the experiment. Figure 17C shows an example of 2D staining with Pacific blue and Alexa Fluor 488.

When these settings are made, it is possible to study properties within each live/singlet cell population. Some of the information that can be studied more closely is number of live/dead/duplicated cells in a sample and fluorescence levels of specific targets. The result output can be presented in many different formats. In our experiments we use manly heatmaps, overlaying histograms and tables that can be used for making different types of diagrams, figure 18.

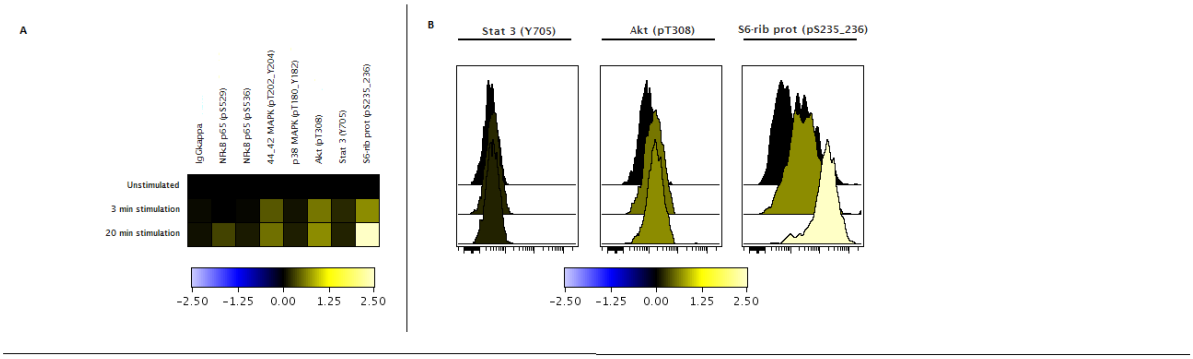

C

	IgGkappa - Panel 1	NFkB p65 (pS529) - Panel 2	NFkB p65 (pS536) - Panel 3	44_42 MAPK (pT202_Y204) - Panel 6	p38 MAPK (pT180_Y182) - Panel 7	Akt (pT308) - Panel 8	Stat 3 (Y705) - Panel 4	S6-rib prot (pS235_236) - Panel 5
Unstimulated	0.0	0.0	0.0	0.0	0.0	0.0	0.0	0.0
3 min stimulation	0.05	0.0	0.03	0.43	0.09	0.58	0.2	0.69
20 min stimulation	0.08	0.33	0.13	0.55	0.15	0.69	0.17	2.49

Figure 18 Some of the options for presenting results in Cytobank. Heatmap (A), overlaying histograms (B) and table (C).

8.4 WESTERN BLOT

Western blot is one of the most used analytical techniques to separate and detect specific proteins in a sample. In our experiments we have used cell lysates. We performed the experiment with an equal amount of cells in each well and cells were lysed directly after stimulation. Therefore, we did not measure protein concentration.

Preparation of Lysate

- Stimulate cells with EGF 100ng/ml (A15) in 6 well plates for 0, 3, 30 min (150 000 cells/well, 2h serum starvation) in incubator at 37°C
- Put plate on ice, remove treatment medium and add 800µl PBS (A10) per well. Scrape off the cells and transfer to pre-cooled Eppendorf tubes. Rinse well with 500µl PBS (A10) and transfer to Eppendorf tubes
- Spin down cells, 500rcf for 10 min at 4°C, Eppendorf centrifuge (F3)
- Discard supernatant, lyse cells in 50µl lysis buffer (C1), containing recently added protease inhibitor, for 10 min on ice
- Spin Down at 16000rcf for 10 min at 4°C, Eppendorf centrifuge (F3)
- Transfer the supernatant to new pre-cooled Eppendorf tubes
- Store at -20°C

8.4.1.1 SDS-Page

There are many types of gel systems available. Most of these use two different acrylamide gels: stacking and separating gels. The stacking gel has a PH around 6,8 and a lower polyacrylamide concentration and is buffered with Tris-HCL that supports band formation but functions poorly when it comes to separating proteins [36]. The separating gel has a pH around 8,8 and a higher polyacrylamide concentration and is buffered with Tris-HCL making it possible to separate proteins after size [36]. A higher concentration of polyacrylamide leads to a narrower passageway for proteins, so that bigger proteins will use more time through the gel and small proteins will migrate faster. Therefore it is important to choose a gel with a polyacrylamide concentration adapted to the size of the sample proteins.

After SDS chamber with running buffer/samples are prepared the voltage is switched on and the negative charged glycine molecules in the running buffer (buffered with Tris-HCL and a pH at 8,3) move away from the cathode (which is negatively charged). Once they have passed the sample and go into the stacking gel they lose their charge and slow down. This happens due to the change in pH (from pH 8,8 to pH 6,8), and since glycine is a zwitter ion it exists with a negative charge in higher pH and becomes neutral at lower pH values. The negatively charged Cl ions in the separating gel start moving away from the negative electrode (cathode). This results in a narrow area where the electrical resistance is very high (low conductance) in the upper part of the stacking gel. Due to the denaturation of the proteins they are negatively charged. The narrow area with a low conductance makes the proteins move forward into the stacking gel and separation begins. As proteins migrate through the gel they will separate according to their size and form bands. The extent of one band can be related to the amount of protein with that specific size.

Gel electrophoresis

- Thaw cell lysates at RT
- Add 20µl 3x loading buffer (C3) to 40µL lysates amount and incubate in heat-block (95°C) for 5min. Colour on loading buffer will fade over time, use recently made buffer. Caps can pop up leading to a reduction in the volume, press caps back on!
- Quick spin
- Pick a suitable gel, for example criterion with 10% Tris-HCL polyacrylamide with 12 or 18 wells (C23).
- Install prepared gel into the chamber and remove green plastic wells. Fill the chamber with 10x running buffer (C5)
- Load 10 µl 1x SDS (C4) in all empty wells to keep gel from changing shape
- Load 10 µl ladder (C24) into two wells, one in the first well and one of the last well
- Load appropriate amount of sample lysate into wells, 5 µl less than the total volume range in each well (18 wells – 25 µl and 12 wells - 40 µl)
- Put the lid on; black-black, red-red. Start with 100V for approximately 10 minutes, then press pause and increase to 150V for another 1.20 hours
- Stop gel electrophorese after tracking dye has run out of gel

The proteins on the gel need to be transferred to a membrane, ether nitrocellulose or PVDF (Figure 19). The transfer is performed wet with an electric field perpendicular to the gel surface. Gel, transfer membrane, filter papers and pads are put together in a sandwich by the help of a support grid. It is important that it is tight and that all bubbles are removed to obtain a good transfer of proteins.

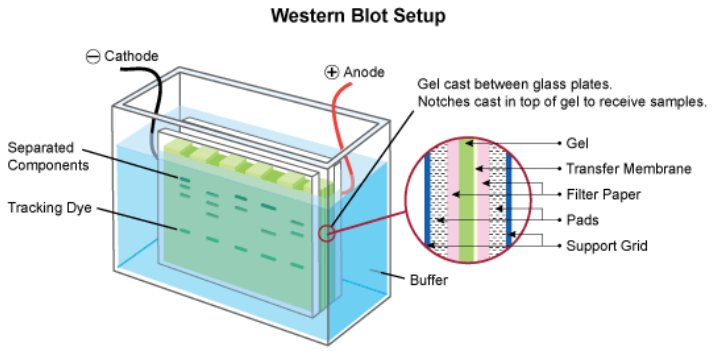

Figure 19 Western blot membrane transfer setup, from [37].

Membrane Transfer

- Sponges and filter papers are soaked in Towbin buffer (C6). Depending on the thickness of the sponges use 2 – 4 or more if necessary
- Cut four filter papers in appropriate size (fit gel size), and put them in Towbin buffer (C6)
- Setup: Red side, 2 x sponges, 2 x filter paper, membrane, gel, 2 x filter paper, 2 sponges. Keep wet and avoid bubbles
- Cut filter membrane a little smaller than the filter papers. Activate membrane by soaking it in methanol (C10). Pour methanol back into flask, put membrane in Towbin buffer (C6) together with sponges and filter papers
- Add cold Towbin buffer (C6) into the chamber and one ice block
- Break the plastic around the gel and cut wells and sides. When transferring gel dip gloved fingers in Towbin buffer, be careful it can stick and break
- Put the lid on; black-black, red-red and run for 1 hour at 100V
- Dry membrane completely
-

The next step is to prevent unspecific binding of antibodies to the membrane by performing a blocking. Depending on the antibodies used, a blocking method is chosen. One blocking method is to dry the membrane completely before adding antibodies. Then the membrane is stained in two steps, first with a primary antibody specific for the proteins and then with a secondary antibody that is linked to biotin or to a reporter enzyme like horseradish peroxidase (Figure 22). The washing steps

between primary- and secondary antibody staining limits background noise, due to the removal of unbound antibodies.

Primary antibody staining

- Transfer membrane into plastic box, rinse with 1x TBS-T (C8)
- Stain with Ponceau S solution (C9) for 1-2 minutes, pour it back into flask, rinse 3x with 1x TBS-T (C8)
- Cut membrane if necessary and let it dry completely
- Add 10ml of primary antibody, (1µL antibody diluted in 10 mL of solution: 3 % BSA (C14) and 0,02 % NaN_3 (C15) in 1x TBS-T buffer (C8)) and shake ON at 4°C overnight

Secondary antibody staining

- Pour off and save primary antibody solution (can often be used multiple times, store at 4°C)
- Cover membrane thoroughly with 1x TBS-T (C8) and place on shaker for 5 min at RT. Repeat for a total of 3 washes
- Prepare buffer for secondary antibody (1 µL to 10 mL 5% milk solution (C17))
- Add secondary antibody to membranes and shake at RT for 1 hour

When a chemiluminescence agent is added to the membrane (Figure 20), the reaction between the secondary linked labels leads to a product that produces luminescence in proportion to the amount of protein. Luminescence light is transferred and captured on an x-ray film, then developed.

Exposure and development of x-ray film

- Pour off and save secondary antibody (can often be used multiple times, store at -20°C)
- Wash membrane three times with 1x TBS-T (C8) and place on shaker for 5 min at RT
- Add buffers (C20), premixed 1:1, and make sure that it covers the hole membrane
- Take membrane out and install them into a cassette (E10)
- In the darkroom; take a film (E11), cut in two if possible and expose for different time-points
- Put films into developer

9 RESULTS

In this section we present the results obtained during the execution of this thesis.

9.1 COLD TRYPSINIZATION OF OVARIAN CANCER CELL LINES

In our first set of experiments, we wanted to find multiple ovarian cancer cell lines that were compatible with our cold trypsinization protocol. We tested six ovarian cancer cell lines to see if they detached from the plate surface after 20, 30 and 60 minutes of cold trypsinization (Table 13). Five of the cell lines tested detached already after 20 minutes, including; OVCAR-3, OVCAR-5, OVCAR-8, NCIADR-RES and SKOV-3 cells. One cell line (OVCAR-4) was disregarded in further experiments since it did not detach from the plate surface.

Table 13 Cold trypsinization performed on different ovarian cancer cell lines.
Detachment of cells was verified in microscope at time points 20, 30 and 60 minutes

Cell line	20 min	30 min	60 min
OVCAR-3	Yes	Yes	Yes
OVCAR -4	No	No	No
OVCAR-5	Yes	Yes	Yes
OVACR-8	Yes	Yes	Yes
NCI/ADR-RES	Yes	Yes	Yes
SKOV-3	Yes	Yes	Yes

9.2 OVARIAN CANCER CELL LINES TREATED WITH EGF (EPIDERMAL GROWTH FACTOR)

Next, we wanted to check the phosphorylation response of cell lines after cold trypsinization. We treated SKOV-3 and OVCAR-8 cells for different time periods with EGF, a growth factor to which the ovarian cancer cell lines were expected to respond, and analysed samples by phosphoflow cytometer. We showed that multiple intracellular proteins were phosphorylated upon treatment with EGF (100ng/mL) in both SKOV-3 and OVCAR-8 cells (Figure 21). SKOV-3 cells displayed an increased phosphorylation of S-6 ribosomal protein, STAT3, 44_42 and AKT (pT308) after 3 minutes stimulation.

After 20 minutes stimulation, increased phosphorylation of S-6 ribosomal protein, NFkB (pS529), 44_42 MAPK and AKT (pT308) was observed (Figure 21). The strongest phosphorylation response of SKOV-3 cells was AKT (pT308) after 20 minutes stimulation.

Phosphorylation signals of proteins in OVCAR-8 cells were overall weaker than in SKOV-3 cells. We also observed an increased phosphorylation response in 44_42 MAPK in OVCAR-8 cells after 3 minutes EGF-stimulation. NFkB(pS529), NFkB(pS529), STAT3, p38 MAPK and AKT(pT308) displayed a weak phosphorylation response after 3 and 20 minutes stimulation (Figure 21). The strongest phosphorylation response of OVCAR-8 cells was S-6 ribosomal protein after 20 minutes stimulation.

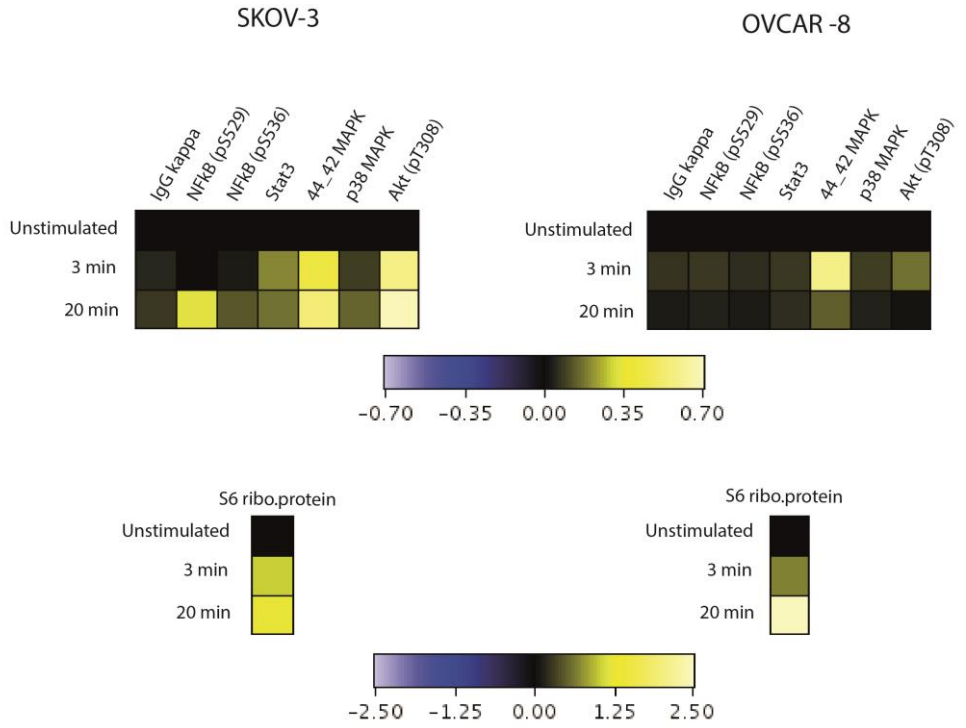

Figure 21 Heatmap of EGF-induced phosphorylation signals in SKOV-3 and OVCAR-8 cells. *Cells were stimulated with 100 ng/mL EGF for to different time period (3 and 20 minutes). Results were calculated in Cytobank with arcsinh ratio of medians, and they were normalized to the first row (untreated cells). The data was collected from one single experiment where samples were analysed by phosphoflow cytometry.*

In order to validate the cold trypsinization protocol, we wanted to compare phosphoflow cytometry results with an independent method, Western blot. Figure 22 shows the Western blot results from a stimulation experiment with the same cell lines (SKOV-3 and OVCAR-8) and with the same treatment parameters (untreated, 3 min stimulation with 100ng/ml EGF and 20 min stimulation with 100 ng/mL EGF) as in the experiment analysed by phosphoflow cytometry. Experiments analysed by Western

blot were executed with an equal amount of cells in each well and lysed directly after stimulation. Protein concentration was for this reason not measured.

Vinculin is a housekeeping gene that we used to validate the protein amount in each sample. Its protein size is 125 kDa, and for this reason we assumed that the band displayed between 100 and 150kDa was Vinculin. The protein amount looked similar in all lanes, but perhaps with a slightly higher protein amount present in two samples; 20 minutes stimulation (SKOV-3 cells) and untreated (OVCAR-8 cells).

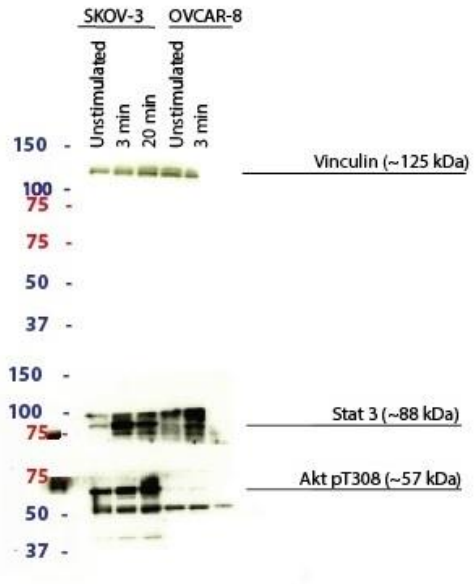

Figure 22 Western blot of proteins investigated in SKOV-3 and OVCAR-8 when treated with EGF. *SKOV-3 and OVCAR-8 cells were stimulated for 3 and 20 minutes with an EGF concentration of 100 ng/mL. Proteins investigated were pAKT (pT308), pSTAT3 and Vinculin. The data was collected from one single experiment where samples were analysed by Western blot.*

In the area where pAKT (pT308) appeared, there were two bands. The protein size for pAKT (pT308) is approximately 57 kDa, therefore we assumed that the top band was pAKT according to the ladder. Increased AKT (pT308) phosphorylation was observed in SKOV-3 cells stimulated with EGF for 3 minutes, and phosphorylation continued to increase over time. In OVCAR-8 cells there was a weak phosphorylation signal in AKT (pT308).

Multiple bands were observed in the area where pSTAT-3 was expected to appear. However, we assumed that the strongest band (in the middle) was closest to the protein size of pSTAT-3 (88kDa). We found that there was an increased STAT-3 phosphorylation in both SKOV-3- and OVCAR-8 cells stimulated with EGF for 3 minutes, and after 20 minutes stimulation the signal had decreased slightly.

The phosphorylation intensity of STAT-3 seemed overall stronger after EGF treatment of SKOV-3 cells, compared to OVCAR-8 cells.

9.3 FLUORESCENT CELL BARCODING

To verify that 3D barcoding with Alexa Fluor 488, Pacific Blue and Pacific Orange would give a good separation of multiple samples we performed a barcoding test with SKOV-3 cells (Figure 23). Cells were fixed before barcoding reagents were added. Results show that it is possible to separate all populations within the sample.

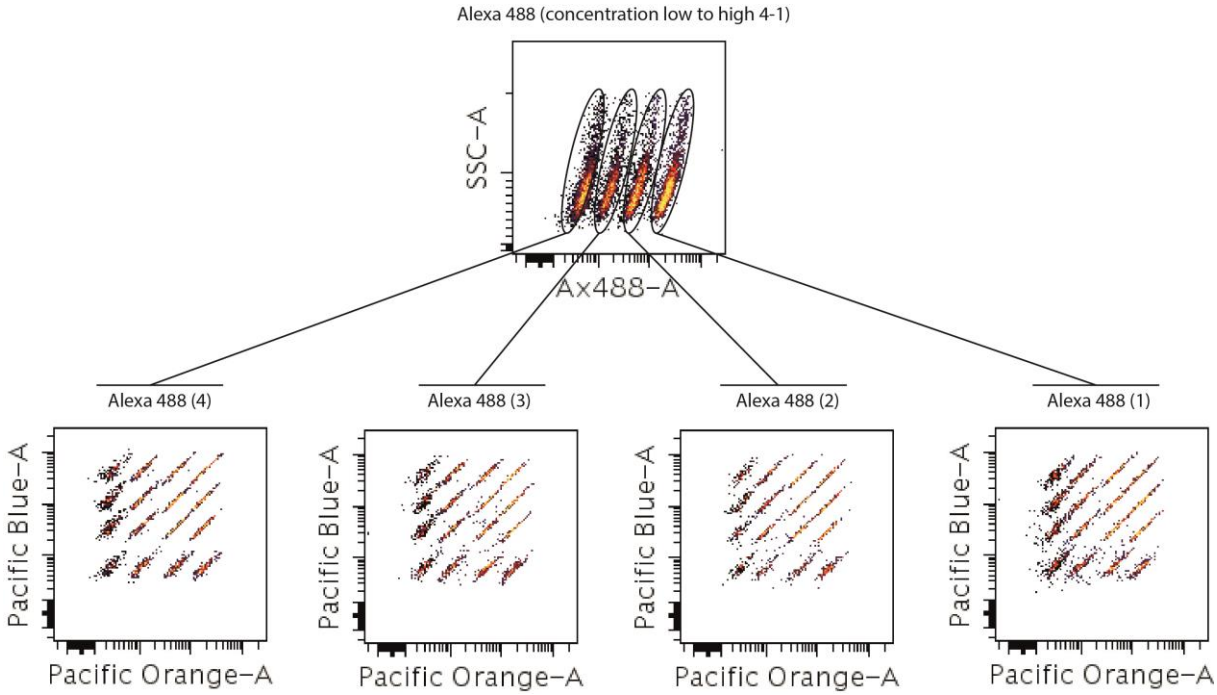

Figure 23 3D fluorescent cell barcoding with SKOV-3 cells. *Cells were stained with different concentrations of Alexa 488, Pacific Orange and Pacific Blue (Concentrations are listed under materials). The sample was analysed by flow cytometry and results are presented as dot plots.*

9.4 ASCITES TITRATION

Since components in ascites (growth factors, cytokines and more) can affect intracellular phosphorylation differently depending on their concentration, we performed a titration with six ascites concentrations from patient #40.

The three cell lines (OVCAR-5, OVCAR-8 and NCI/ADR-RES) were treated for 30 minutes with ascites concentrations of 0 %, 4%, 20 %, 40 %, 80 % and 100%. Results show similarities between the phosphorylation patterns of the investigated proteins in all three cell lines (Figure 24).

STAT3 phosphorylation appeared to increase with increased ascites concentration in OVCAR-5-, OVCAR-8- and NCI/ADR-RES cells.

Increased phosphorylation of S-6 ribosomal protein was observed between ascites concentrations; 0 % up to approximately 20 %. In concentrations higher than this, the signal was partially saturated in all three cell lines. AKT (pS473) phosphorylation increased when exposed to ascites concentration from 0 % up to approximately 20 %. In concentrations higher than this, the signal partially saturated in both OVCAR-5- and OVCAR-8 cells.

NCI/ADR-RES cells displayed an increased phosphorylation of AKT (pT308) between ascites concentrations; 0 % up to approximately 20 %. In ascites concentrations from approximately 20% to 80 % the phosphorylation signal decreased, and in higher concentrations the signal was partially saturated. For more data, see appendix I.

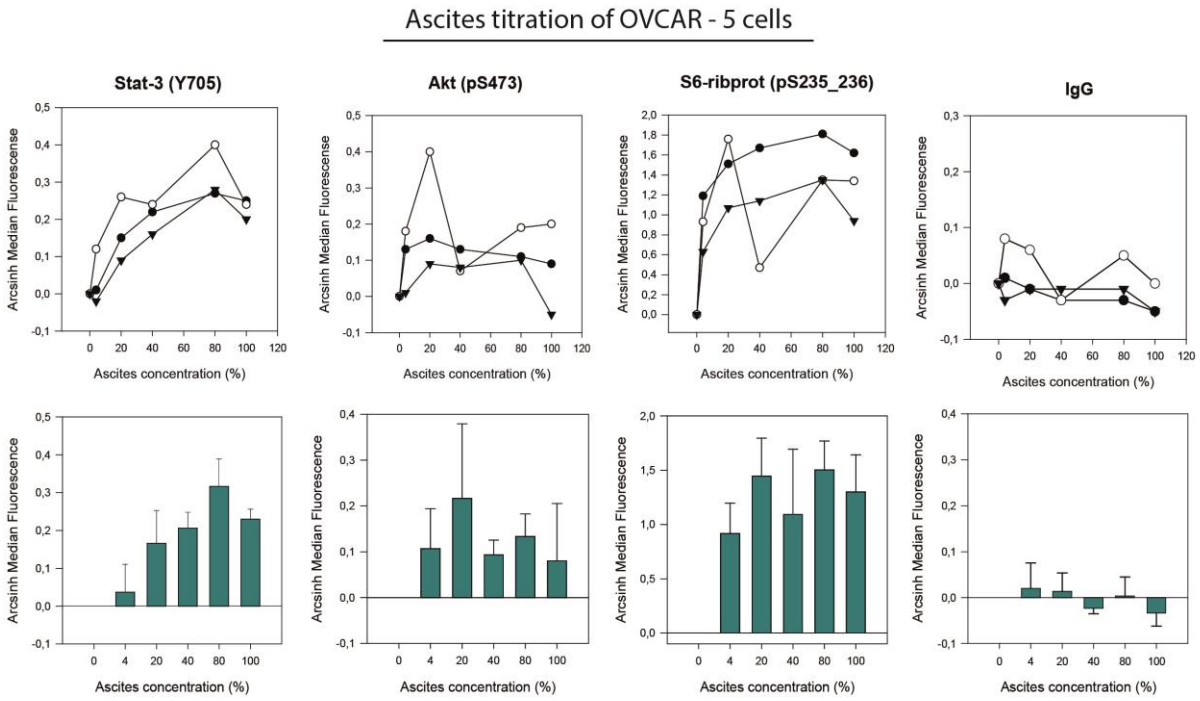

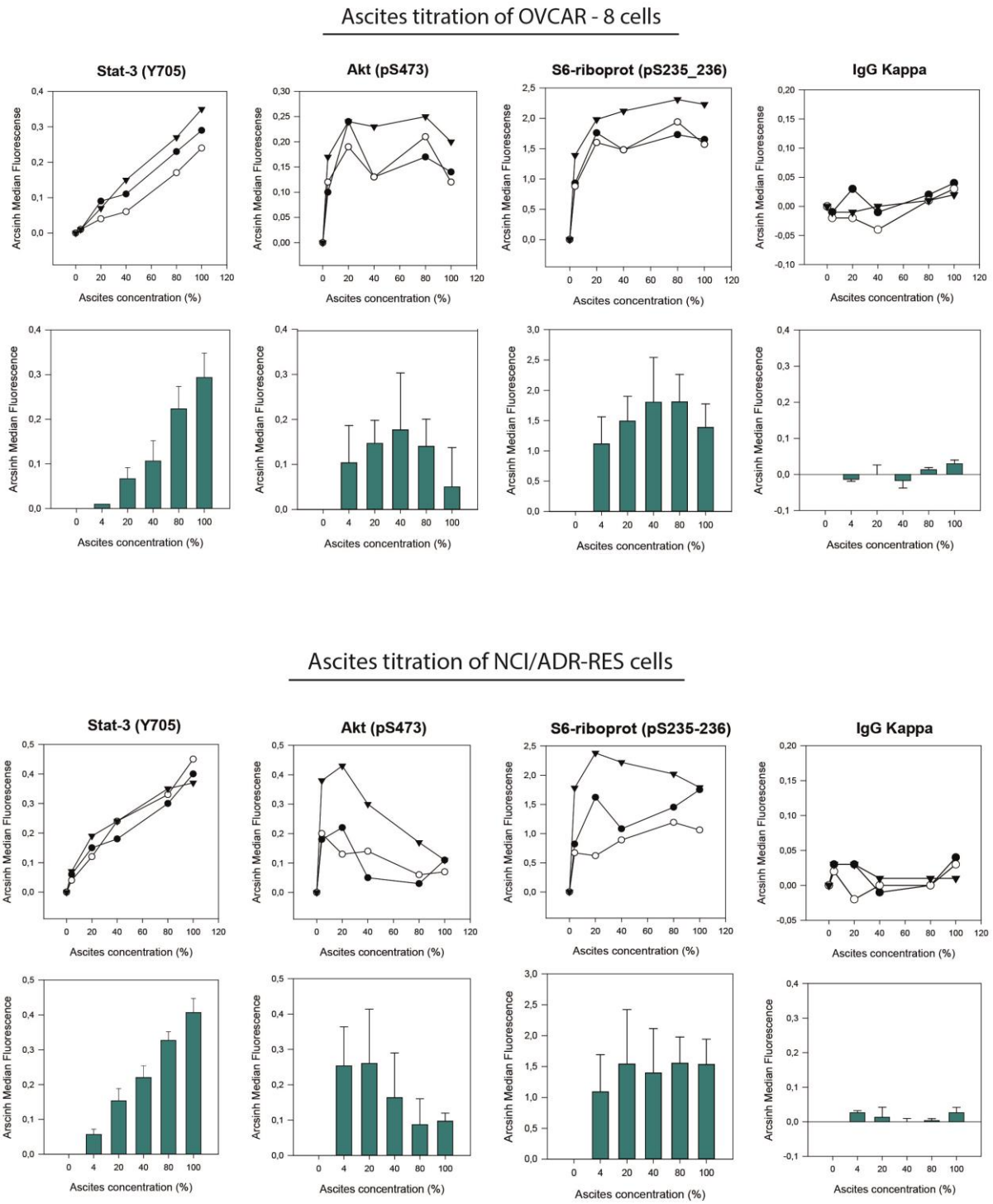

Figure 24 Ovarian cancer cell lines treated for 30 minutes with different concentrations of ascites. *OVCAR-5 (A), OVCAR-8 (B) and NCI/ADR-RES (C) were treated for 30 minutes with ascites from patient #40 with the following concentrations; 0%, 4%, 20%, 40%, 80% and 100%. Result were analysed by phosphoflow cytometry and calculated in Cytobank with arcsinh ratio of medians, and they were normalized to the first row (untreated cells). The horizontal axis is given in units of ascites concentration, while the vertical axis in units of arcsinh medium fluorescence. Upper panels show line diagrams of three experiments while the lower panels show bar diagrams with the average of three experiments with standard deviation.*

9.5 ASCITES-INDUCED PHOSPHORYLATION AT DIFFERENT TIME POINTS

Next, we wanted to examine how ascites-induced phosphorylation of several proteins varied over a longer time. SKOV-3 cells were treated with 50 % ascites from patient #40 at five time points (0, 30, 60, 90 and 120 minutes). Results displayed are only a selection of the investigated proteins, for more data see Appendix II.

In the time interval that we investigated, the phosphorylation levels of multiple proteins increased and peaked at approximately 30 minutes. With one exception, STAT1 (pY701), which showed a slightly decreased phosphorylation signal between 0 and 30 minutes (Figure 25). Proteins that are not displayed here (appendix II) showed similar responses, with a phosphorylation peak at approximately 30 minutes.

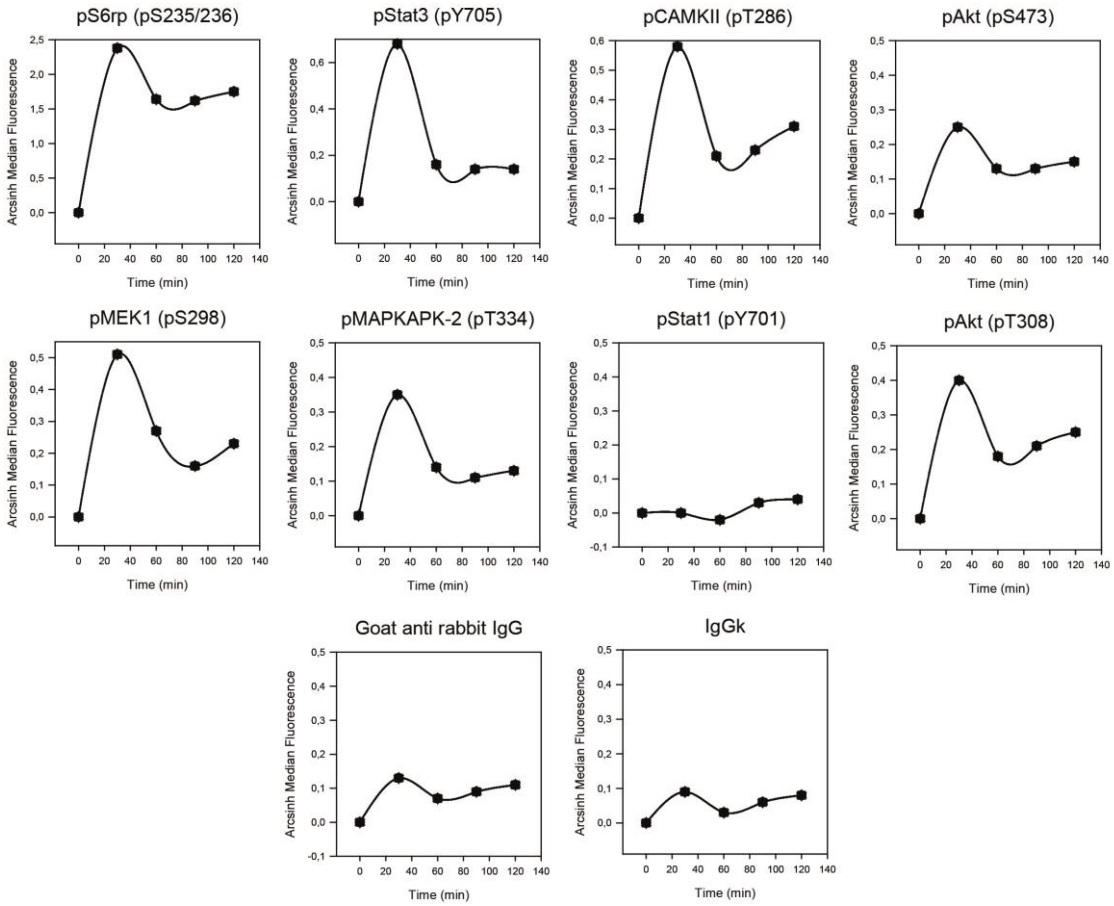

Figure 25 Phosphorylation signal of intracellular proteins at different time points, displayed in SKOV-3 cells when treated with ascites. *Treatment was performed at five different time periods (0, 30, 60, 90 and 120 minutes) with SKOV-3 cells. Cells were treated with 50 % ascites from patient #40. Result were analysed by phosphoflow cytometry and calculated in Cytobank with arcsinh ratio of medians, and they were normalized to the first row (untreated cells). The horizontal axis is given in units of time, while the vertical axis in units of arcsinh medium fluorescence.*

9.6 TREATMENT OF NCI/ADR-RES CELLS WITH ASCITES FROM PATIENT #35 AND #40

Next, a panel of 33 phospho-proteins was used to map the intracellular signalling patterns in NCI/ADR-RES cells treated with two different patient samples; ascites #35 and #40. We used a concentration of 50% ascites and investigated protein phosphorylation at three different time points, 0, 3 and 20 minutes. Patient #35 and #40 showed a strong phosphorylation of the S-6 ribosomal protein, and therefore the bar diagram is presented with two different scales (Figure 27 and 29). The results presented here is only a selection, for more see Appendix III and IV.

Experiments performed with ascites from patient #35 showed that the S-6 ribosomal protein and STAT-3 display increased phosphorylation from 0-3 minutes and between 3-20 minutes (Figure 26). CAMKII showed an increased response from 0-3 minutes in three of the experiments, and between 3-20 minutes the phosphorylation level decreased in all four experiments (Figure 27).

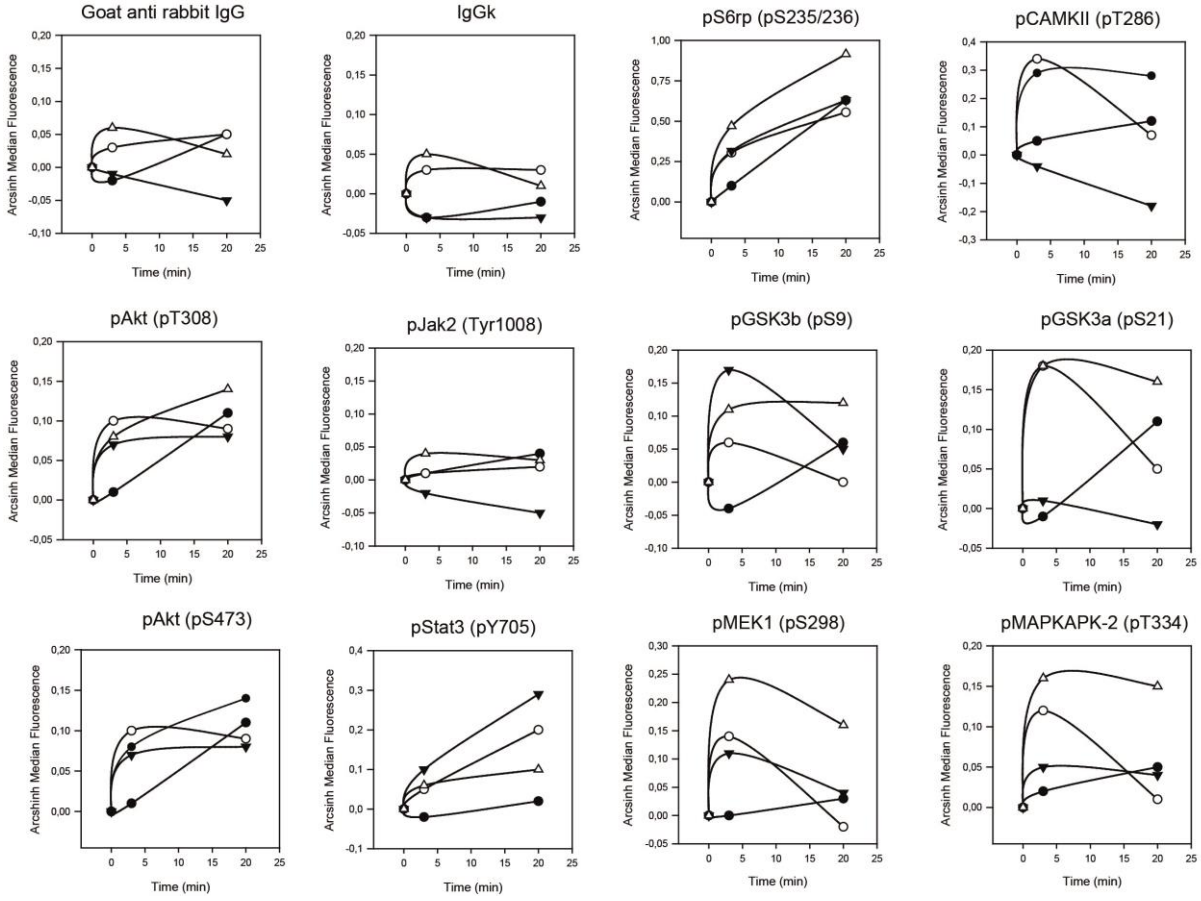

Figure 26 Phosphorylation signals of intracellular proteins in NCI/ADR-RES cells when treated with ascites from patient #35. *Treatment with 50 % ascites from patient #35 on NCI/ADR-RES with three time courses; 0, 3 and 20 minutes. Illustration displays a selection of proteins investigated with values from all four experiments. Samples were analysed by phosphoflow cytometry and calculated in Cytobank with arcsinh ratio of medians, and they were normalized to the first row (untreated cells). The horizontal axis is given in units of time, while the vertical axis in units of arcsinh medium Fluorescence.*

Other proteins, MEK1, MAPKAPK-2, GSK3-alfa, GSK3-beta, AKT (pS473), AKT (pT308), showed a minor increased phosphorylation between 0-3 minutes. The phosphorylation response for negative controls (IgG kappa and Goat-anti rabbit IgG) varied somewhat between experiments, within a fluorescence signal range of approximately -0,4 to 0,6.

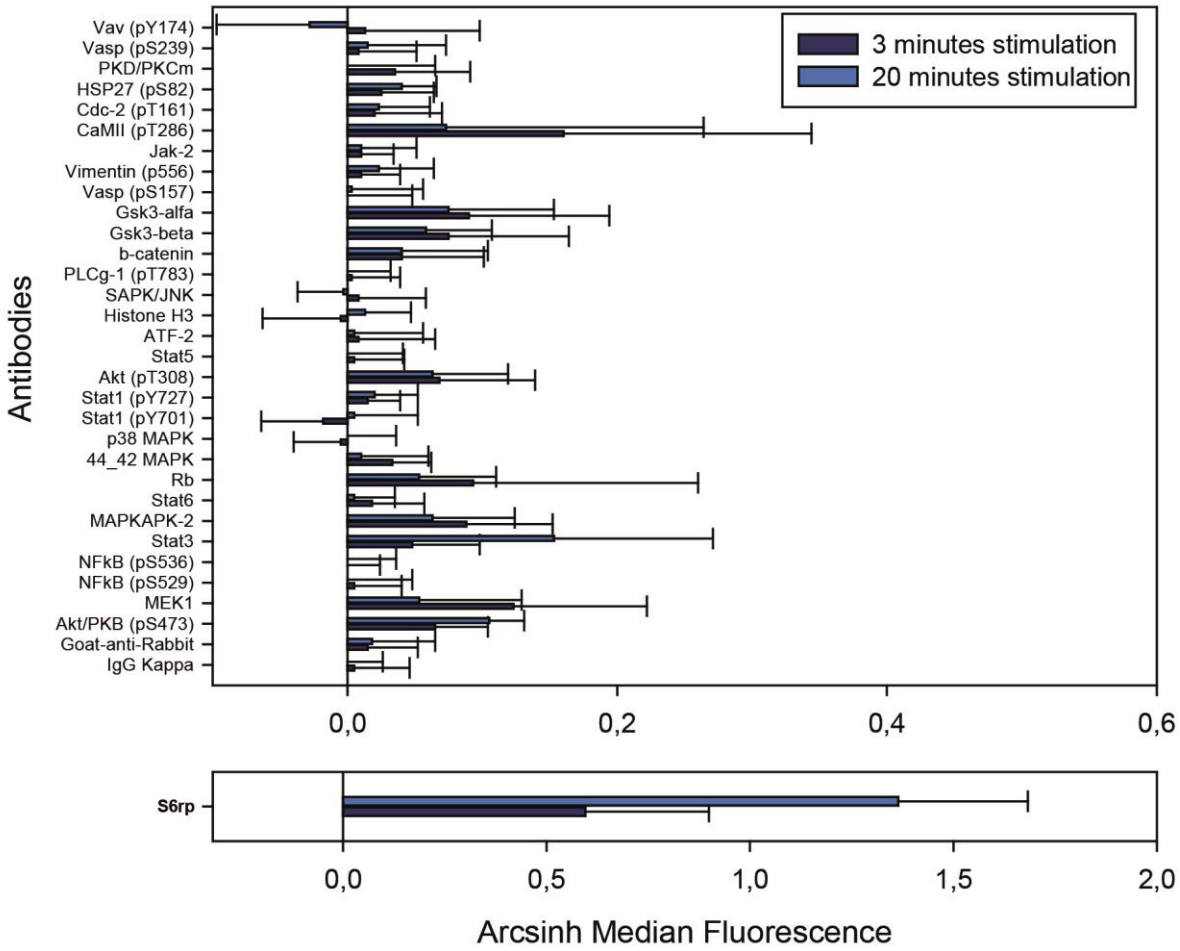

Figure 27 Average phosphorylation signals of intracellular proteins in NCI/ADR-RES cells when treated with ascites from patient #35. *Treatment with 50 % ascites from patient #35 on NCI/ADR-RES with three time courses; 0, 3 and 20 minutes. Illustration display all experiments and proteins investigated, with average and standard deviation bars. Result were analysed by phosphoflow cytometry and calculated in Cytobank with arcsinh ratio of medians, and they were normalized to the first row (untreated cells). Horizontal axis is given in units of time, while the vertical axis in units of arcsinh medium fluorescence.*

One of the experiments performed with ascites from patient #40 showed an overall stronger phosphorylation level in multiple proteins compared to the two other experiments. The results from the remaining experiments seemed to follow the same path, but phosphorylation signals varied somewhat between the proteins that were investigated. S-6 ribosomal protein and STAT-3 presented with an increased phosphorylation response from 0-3 minutes and between 3-20 minutes (Figure 28). CAMKII shows an increased response level after 3 minutes stimulation, which decreases at 20 minutes.

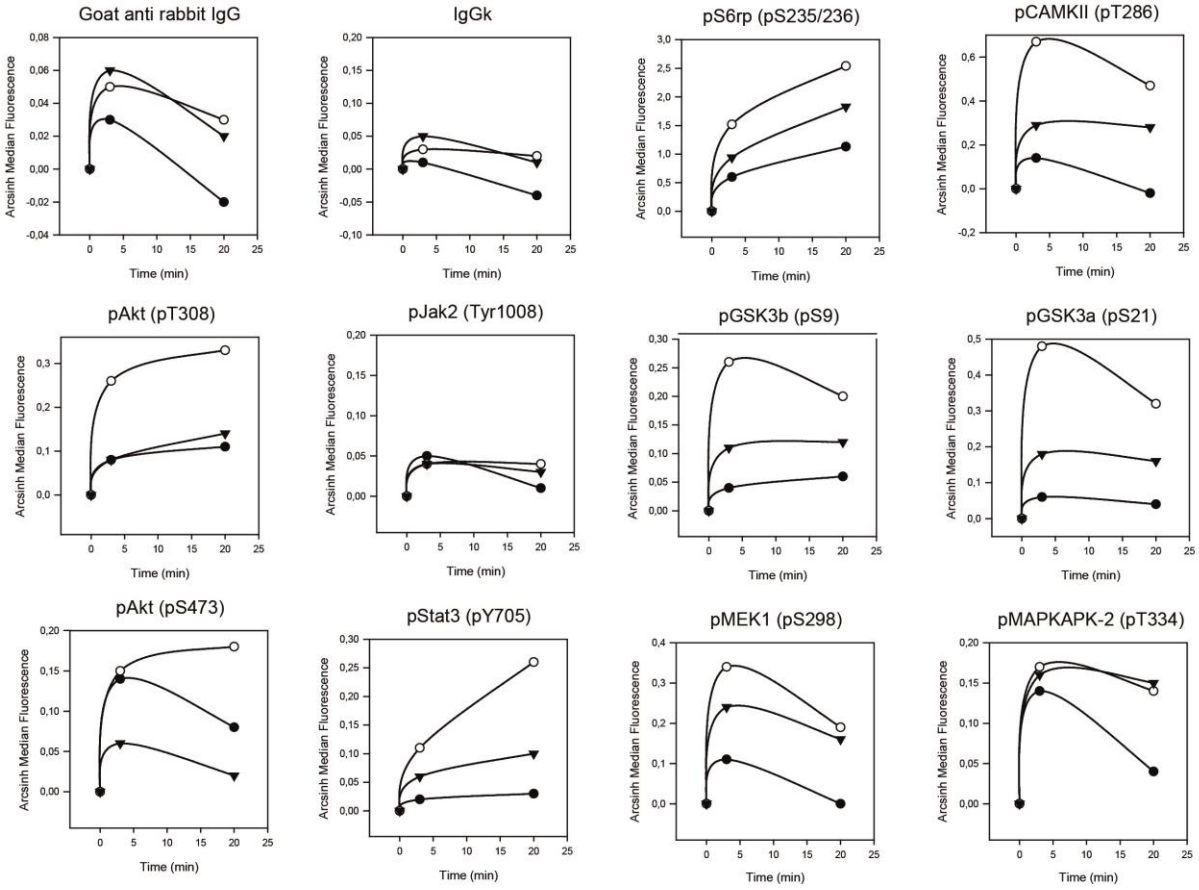

Figure 28 Phosphorylation signals of intracellular proteins in NCI/ADR-RES cells when treated with ascites from patient #40.*Treatment with 50 % ascites from patient #40 on NCI/ADR-RES with three time courses; 0, 3 and 20 minutes. Illustration displays a selection of proteins investigated with values from all three experiments. Samples were analysed by phosphoflow cytometry and calculated in Cytobank with arcsinh ratio of medians, and they were normalized to the first row (untreated cells). The horizontal axis is given in units of time, while the vertical axis in units of arcsinh medium fluorescence.*

Other proteins, like MEK1, MAPKAPK-2, GSK3-alfa, GSK3-beta, AKT (pS473), AKT (pT308) and HSP 27, show an increased phosphorylation after 3 minutes stimulation. Between 3 and 20 minutes the phosphorylation response of these proteins varied (decreased or increased slightly) (Figure 28 and 29). The negative controls (IgG kappa and Goat-anti rabbit IgG) varied somewhat between

experiments, with a variation of phosphorylation level with approximately 0 and 0,6 arcsinh median fluorescence.

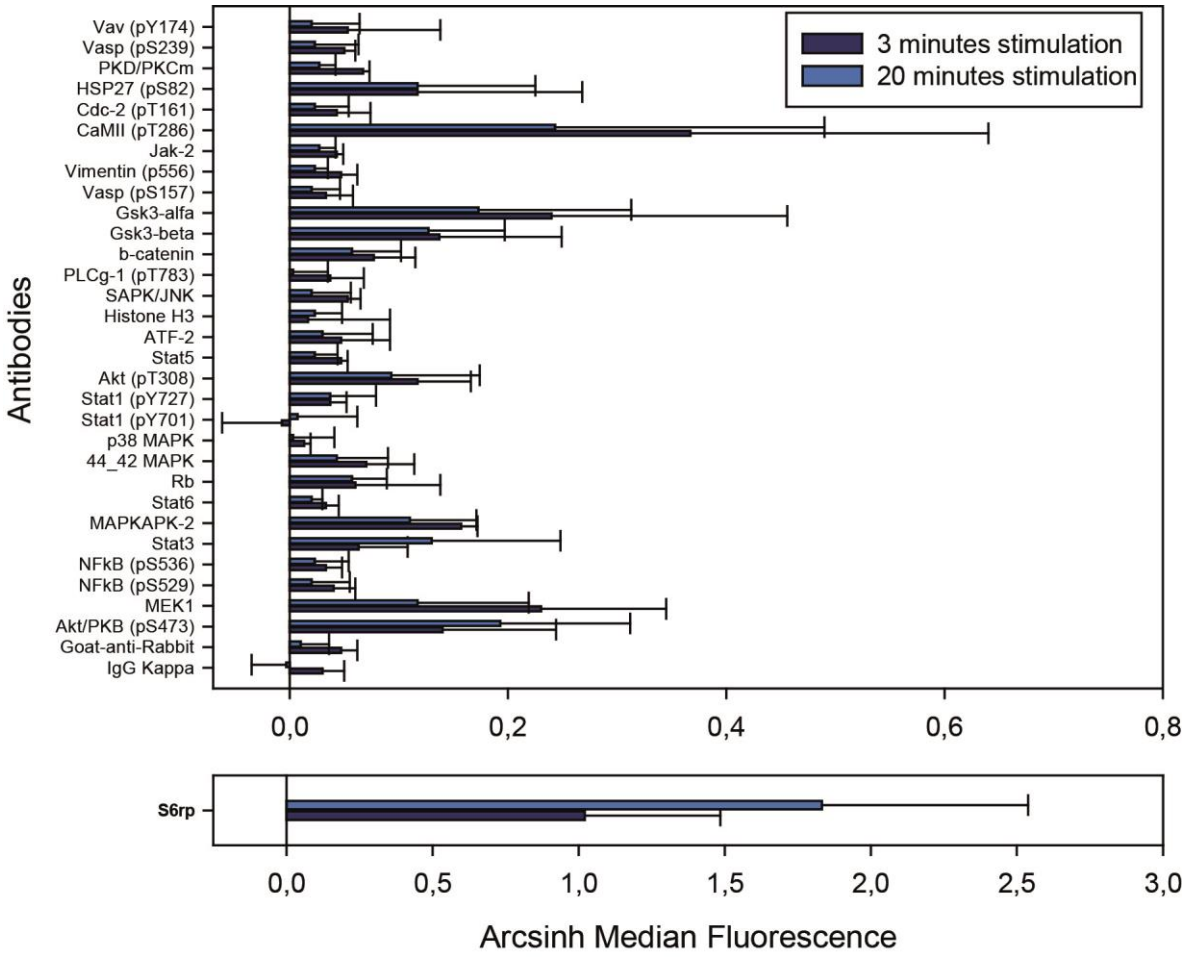

Figure 29 Average phosphorylation levels of intracellular proteins in NCI/ADR-RES cells when treated with ascites from patient #40.*Treatment with 50 % ascites from patient #40 on NCI/ADR-RES at three time points; 0, 3 and 20 minutes. Illustration displays of all experiments and proteins investigated, with average and standard deviation bars. Result were analysed by phosphoflow cytometry and calculated in Cytobank with arcsinh ratio of medians, and they were normalized to the first row (untreated cells).*

Treatment of NCI/ADR-RES cells with ascites from patient #35 and #40 showed that the same proteins were phosphorylated with the same pattern. However, the overall average of phosphorylation intensity of proteins investigated appeared to be stronger when treated with ascites from patient #40 (Figure 27 and 29).

9.7 INVESTIGATION OF IL-6-INDUCED PHOSPHORYLATION IN SKOV3 CELLS, WITH FOCUS ON STAT3

Studies have shown that there are elevated levels of IL-6 in malignant ascites [12, 17]. In order to investigate the potential role of IL-6, we wanted to study the phosphorylation signature of SKOV-3 cells treated with ascites, in presence and/or in absence of an IL-6R blocking antibody. Our primary focus was STAT-3 phosphorylation, -since IL-6R activation is known to initiate JAK kinase signalling leading to phosphorylation of STAT-3 [16]. We also wanted to investigate how dominant a potential IL-6 treatment would be, and how it would affect the phosphorylation pattern of other proteins. We treated SKOV-3 cells with ascites from patient #40 and used five different conditions; untreated, 50% ascites only, and 50 % ascites with addition of different concentration of IL-6R blocking antibody; 0,1 µg/, 1,0 µg/mL and 10 µg/mL. Two time points were used, 3 and 20 minutes. Additional data for 3 minute treatment and for treatment with all three concentration of IL-6R blocking antibody in the absence of ascites can be seen in appendix V.

After 3 minutes treatment the phosphorylation signals were overall weak (Figure 30). Phosphorylation levels in most of the investigated proteins decrease to near or under basal levels (phosphorylation signals of untreated cells) after they had been treated for 3 minutes with 10µg/mL blocking antibody. STAT3 showed decreased phosphorylation levels with increased IL-6R blocking antibody concentration, when treated for 3 minutes.

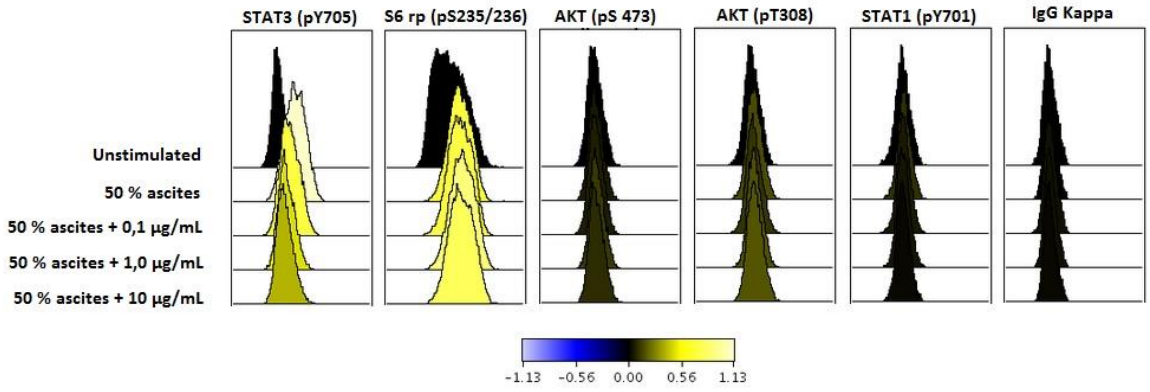

Figure 30 Phosphorylation signal of proteins treated for 20 minutes with different conditions*. SKOV-3 cells were treated with different conditions 20 minutes with ascites from patient #40. Conditions; untreated, 50% ascites only, and 50 % ascites with addition of different concentration of IL-6R blocking antibody; 0,1 µg/, 1,0 µg/mL and 10 µg/mL. Result were analysed by phosphoflow cytometry and calculated in Cytobank with arcsinh ratio of medians, and they were normalized to the first row (untreated cells). Results are displayed as histograms were the scale is given in arcsinh medium fluorescence.*

In contrast, the phosphorylation level of S-6 ribosomal protein level increased when treated for 3 minutes with 50% ascites in the presence of 0,1 and 1 µg/mL blocking antibody. Compared to the other proteins the S-6 ribosomal protein displayed a strong phosphorylation signal.

With increased IL-6R blocking antibody concentration, the phosphorylation signal in STAT-3 decreased in samples treated for 20 minutes, shown in histograms (Figure 30). After 20 minutes of treatment with 10,0 µg/mL IL-6R blocking antibody, the phosphorylation of STAT-3 was almost completely blocked (Figure 30). Upon 20 minutes treatment of SKOV-3 cells, with the exception of STAT-3 and S-6 ribosomal protein, the investigated proteins presented an overall weak phosphorylation response, and seemed unaffected by the IL-6 blocking antibody.

We also analysed SKOV-3 cells that were exposed to the IL-6R antibody, with no addition of ascites (results in appendix V). These results showed decreased phosphorylation signal in multiple proteins.

9.8 TREATMENT OF SKOV-3 CELLS WITH ASCITES SAMPLES FROM 20 PATIENTS

Next, we wanted to investigate ascites-induced phosphorylation patterns in multiple patient samples. We treated SKOV-3 cells with 50 % ascites at two different time points, 3 and 20 minutes, with ascites from 20 different patients. To be able to investigate 33 intracellular proteins in 20 patient samples, we divided the experiment into three parts. In each experiment we used all patient samples and studied phosphorylation of approximately 12 proteins. We analysed pSTAT-3 in all three experiments as a reference and used IgG kappa and secondary alone (Goat-anti rabbit IgG) as negative controls for conjugated- and unconjugated antibodies, respectively. In this experiment we started treatment with ascites from #23 and finished with ascites from #45, meaning that samples treated early morning were fixated and stored at 4˚C until all samples were ready for barcoding and permeabilization.

Figure 31 and 32 show heatmaps of phosphorylation levels of intracellular proteins after 3 and 20 minutes treatment of SKOV-3 cells with ascites form 20 patients. Multiple proteins were phosphorylated upon stimulation, but the intensity varied between treatment times and patient samples.

Elevated phosphorylation in multiple proteins can be observed after 3 minutes treatment of SKOV-3 cells (Figure 31). In cells that were treated with all patient samples, it appeared that the S-6 ribosomal protein gave the overall strongest phosphorylation signal after 3 minutes treatment. However, the phosphorylation levels in patients #28, #30 and #32 were overall weak. Rb and GSk3-alpha appeared to decrease in phosphorylation response (compared to untreated) after 3 minutes treatment in most of the patient samples.

Ascites from patient #40 induced phosphorylation in all the proteins that were examined. The weakest overall responses of phosphorylated proteins were seen after 20 minutes treatment with ascites from patient #28, #30 and #32.

Cells that were treated with ascites from different patients exhibited increased phosphorylation of STAT-3, both after 3 and 20 minutes (Figure 31 and 32). The phosphorylation pattern of STAT-3 in all three experiments was similar (Figure 31 and 32). Cells treated with all patient samples showed a “distinct” increase of phosphorylation between 3 and 20 minutes (Figure 33A/B). Observing the phosphorylation pattern of all the proteins investigated at 3 and 20 minutes treatment of SKOV-3 cells, it was clear that STAT3 acts independently of other proteins (Figure 31 and 32).

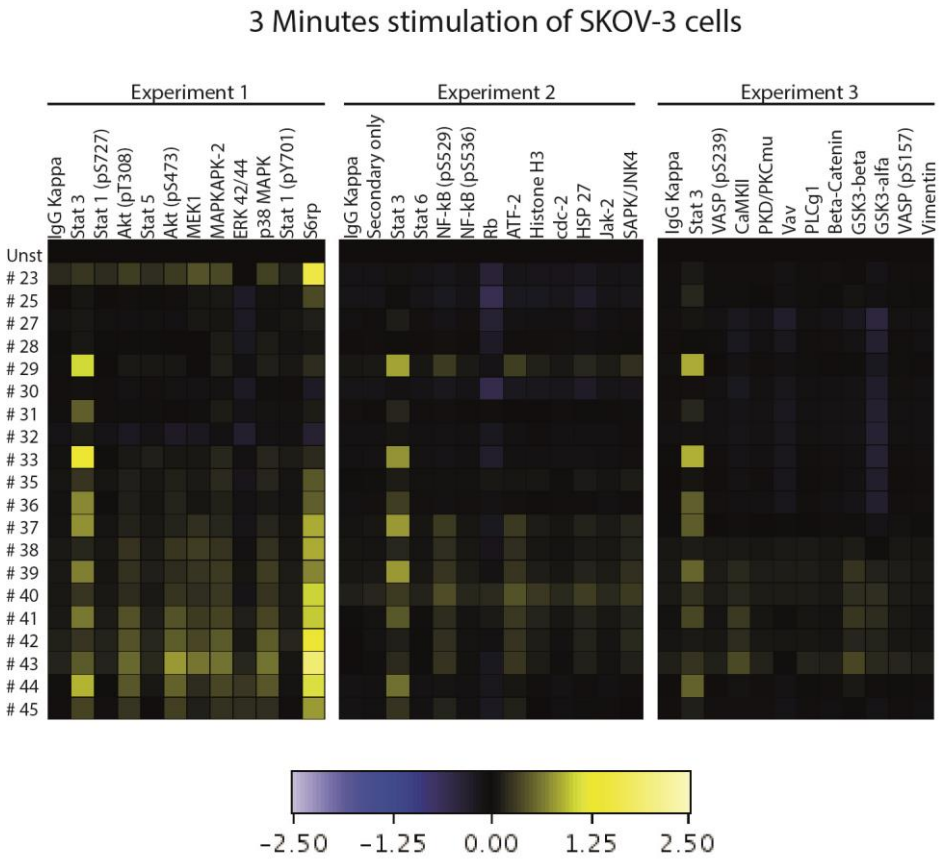

Figure 31 ***Ascites-induced phosphorylation of investigated proteins in SKOV-3 cells after 3 minutes stimulation. Cells were treated with 50 % ascites from 20 patients for 3 minutes.*** *Experiment was divided into three parts and STAT 3 was used as a positive control and in all three experiments. IgG kappa and Goat-anti rabbit was used for negative controls for conjugated and unconjugated antibodies, respectively. Result were analysed by phosphoflow cytometry and calculated in Cytobank with arcsinh ratio of medians, and they were normalized to the first row (untreated cells), displayed as a heatmap. The scale is given as arcsinh medium fluorescence, while the "vertical axis" displays patient samples.*

After 20 minutes treatment of SKOV-3 cells, phosphorylation levels of STAT1 (pY701) differed more between the patients samples than the other proteins that were investigated (Figure 32).

Almost no phosphorylation response was observed in the following proteins; VASP (pS239), VASP (pS157), Vimentin, Vav and STAT-6 after treatment of SKOV-3 cells with ascites from any of the patient samples.

The overall phosphorylation response after cells were treated with ascites from patient #35 was overall weak, with the exception of increased signals in STAT-3, STAT-1 (pY701) and S-6 ribosomal protein (Figure 31 and 32).

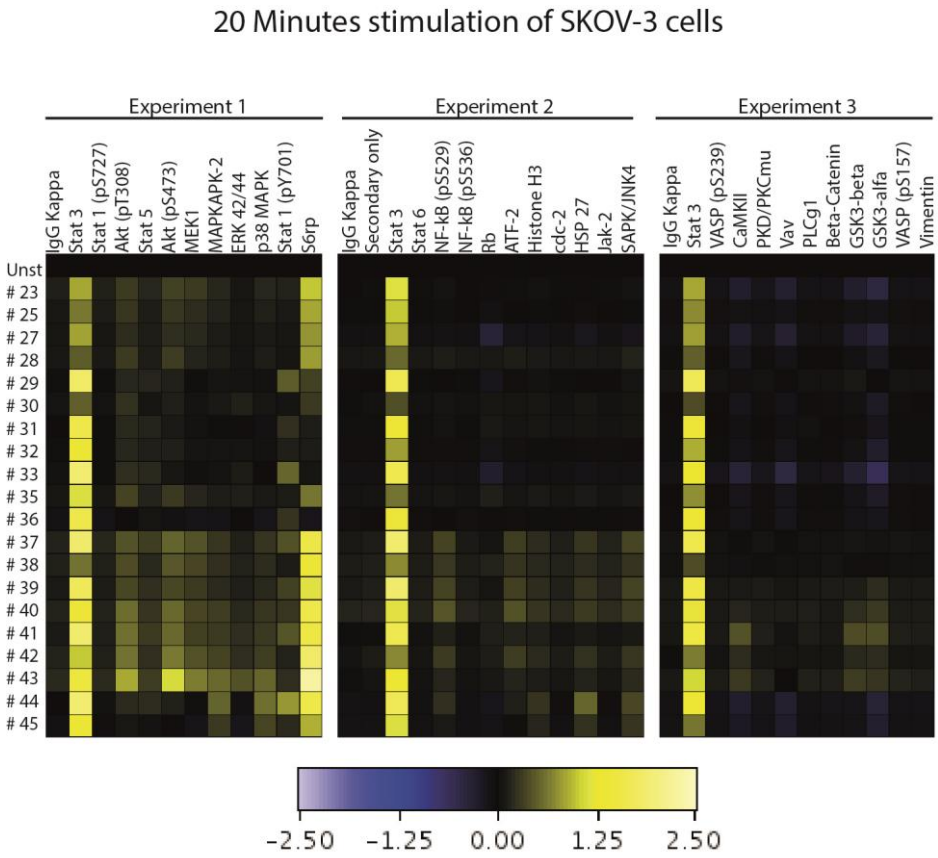

Figure 32 ***Ascites-induced phosphorylation of investigated proteins in SKOV-3 cells after 20 minutes stimulation. Cells were treated with 50 % ascites from 20 patients for 20 minutes.*** *Experiment was divided into three parts and STAT 3 was used as a positive control and in all three experiments. IgG kappa and Goat-anti rabbit was used for negative controls for conjugated and unconjugated antibodies, respectively. Result were analysed by phosphoflow cytometry and calculated in Cytobank with arcsinh ratio of medians, and they were normalized to the first row (untreated cells), displayed as a heatmap. The scale is given as arcsinh medium fluorescence, while the "vertical axis" displays patient samples.*

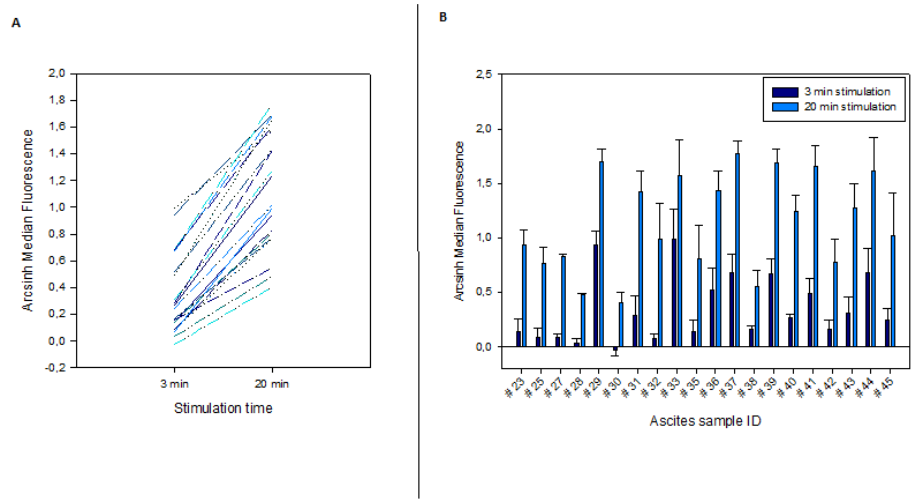

Figure 33 ***Ascites-induced STAT-3 phosphorylation in SKOV-3 cells that were treated for 3 or 20 minutes.*** *Treatment was performed with 50% ascites from 20 different patients. Samples were analysed by phosphoflow cytometry. Left panel shows the average trend of STAT 3 phosphorylation where each line represent signal in SKOV-3 cells treated with ascites from one patient sample in all tree experiments, Right panel shows average for each patient displayed as bars, with standard deviation bars.*

9.9 TREATMENT OF OVCAR-8 WITH 18 ASCITES SAMPLES

Next, we wanted to investigate ascites-induced phosphorylation patterns in another ovarian cancer cell line. We treated OVCAR-8 cells at two different time points, 3 and 20 minutes, with a total of 18 ascites samples from different patients. To be able to investigate 33 intracellular proteins in 18 patient samples, we divided the experiment into three parts. In each experiment we used all patient samples and studied phosphorylation of approximately 12 proteins. We analysed pSTAT-3 in all three experiments as a reference and used IgG kappa and secondary alone (Goat-anti rabbit IgG) as negative controls for conjugated- and unconjugated antibodies, respectively. However, due to a barcoding problem in one experiment, the results from the last 12 antibodies are not used as a part of this Thesis. Also, ascites from patient #44 and #45 were not included, because the cells treated with these ascites detached during treatment. In this experiment we started treatment with ascites from #43 and finished with ascites from #23. Samples treated early morning were fixed and stored at 4˚C until all samples were ready for barcoding and permeabilization.

After 3 minutes of treatment with any of the patient samples, STAT-1 (pY701 and pS473), NFkB (pS529 and pS539), STAT-5, STAT-6, Cdc-2, SAPK/JNK and Jak-2 showed a weak phosphorylation signal, while S-6 ribosomal protein displayed the strongest phosphorylation signal among the proteins investigated (Figure 34). When we treated SKOV-3 cells with ascites from patient #37 and #38, all the proteins that were examined displayed an overall weaker phosphorylation level (Figure 34).

After 20 minutes of treatment, STAT-1 (pS473), NFkB (pS529 and pS539), STAT-5, STAT-6, Cdc-2, SAPK/JNK and Jak-2 presented with the weakest phosphorylation signals of all the proteins investigated. The S-6 ribosomal protein displayed an overall strong phosphorylation response, after stimulation with ascites from all the patients (Figure 34).

The strongest overall phosphorylation signal was observed when OVCAR-8 cells were treated with ascites from patient #30. While ascites from patients #35, #42 and #43 induced an overall weak phosphorylation of the proteins that were investigated.

Ascites from all patients induced an increased phosphorylation of STAT-3 between 3 and 20 minutes (Figure 35A/B). The strongest STAT-3 phosphorylation level was seen after 20 minutes treatment with ascites from patient #33, compared to the other patient samples.

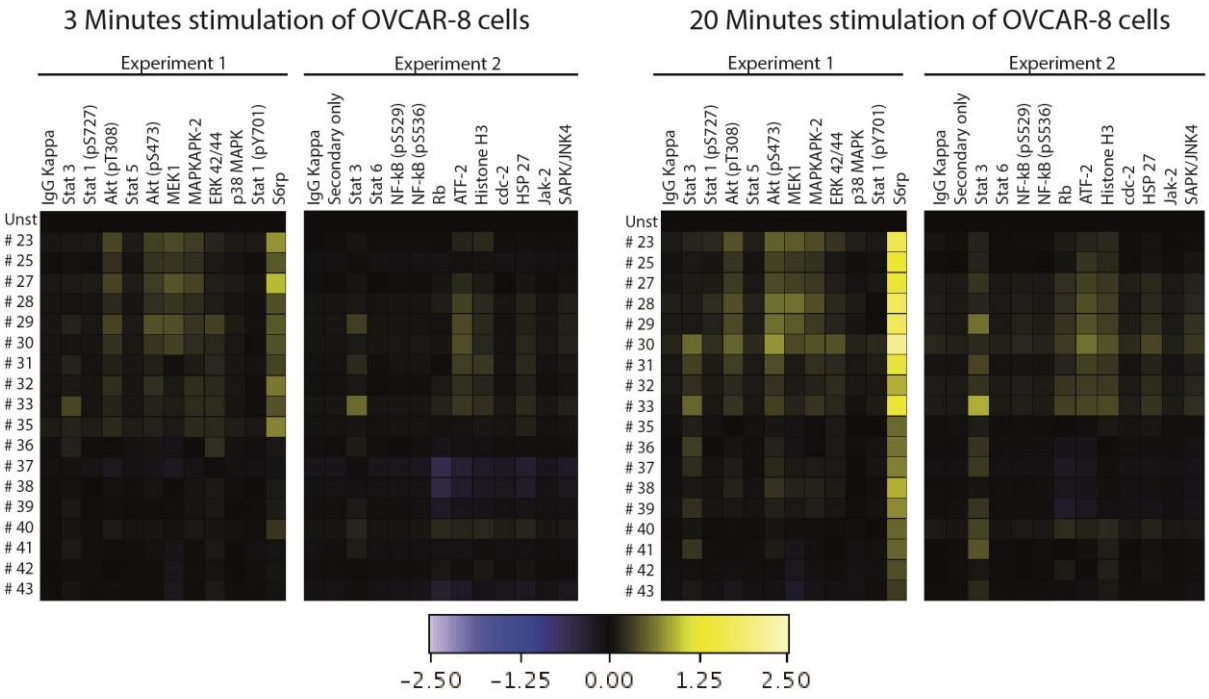

Figure 34 ***Ascites-induced phosphorylation of investigated proteins in OVCAR-8 cells. Cells were treated with 50 % ascites from 18 patients for 3 and 20 minutes.*** *Experiment was divided into three parts and STAT 3 was used as a positive control and in all three experiments. IgG kappa and Goat-anti rabbit was used for negative controls for conjugated and unconjugated antibodies, respectively. Result were analysed by phosphoflow cytometry and calculated in Cytobank with arcsinh ratio of medians, and they were normalized to the first row (untreated cells), and displayed as a heatmap. The scale is given as arcsinh medium fluorescence, while the "vertical axis" displays patient samples.*

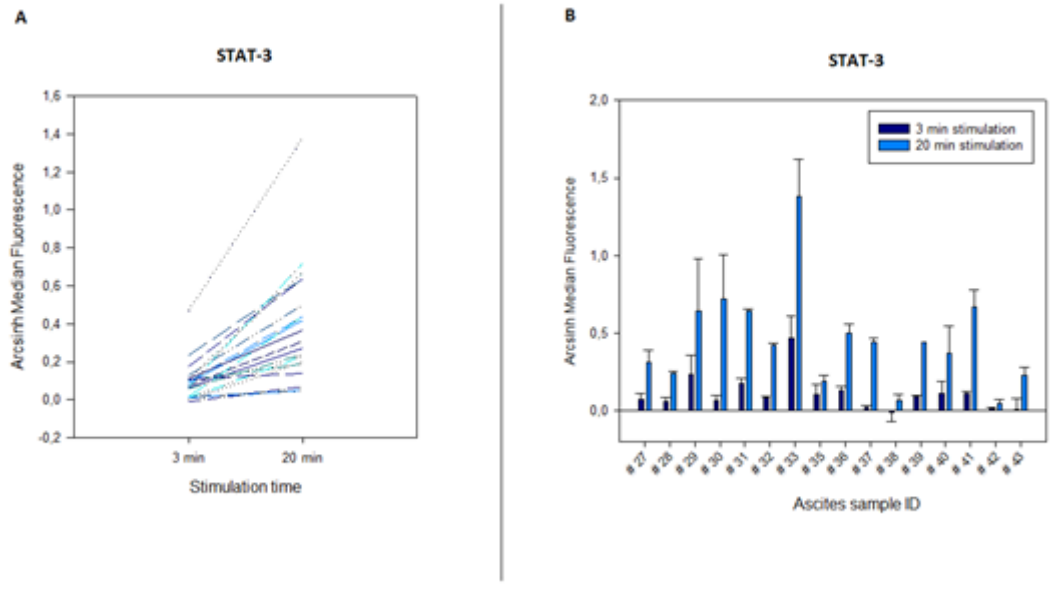

Figure 35 ***Ascites-induced STAT-3 phosphorylation in OVCAR-8 cells that were treated for 3 and 20 minutes.*** *Treatment was performed with 50% ascites from 18 patients. Samples were analysed by phosphoflow cytometry. Left panel shows the average trend of STAT 3 were each line represent signal in OVCAR-8 cells treated with one patient sample in all tree experiments, Right panel shows average phosphorylation signal for each patient after 3 and 20 minutes treatment with ascites. Results are displayed as bars with standard deviation.*

10 DISCUSSION

Cancer in the ovaries is the fifth leading cause of cancer deaths worldwide. We need new therapeutic drugs and screening techniques that can detect ovarian cancer at an early stage and give patients a more personalized treatment, which can lead to better prognosis and better life quality for patients. Therefore we need to enhance our understanding of ovarian tumour biology and how it interacts with its surroundings. In this Thesis we have studied the phosphorylation patterns of intracellular proteins when ovarian cancer cells have been treated with ascites derived from different patients.

10.1 CELL LINES

Cold trypsinization is a method developed in the Taskén laboratory that is used to detach treated adherent cell lines, while the intracellular signalling is "frozen". The downside with this method is that due to the low temperature there is a need for a stronger trypsin concentration and a relatively long trypsination time, which can damage cell membranes or lead to cell death. Therefore we needed to investigate whether selected ovarian cancer cell lines could detach with a higher concentration of trypsin without affecting cell integrity and intracellular signalling. We examined six cell lines and five of these detached already after 20 minutes stimulation. One of the cell lines did not detach (OVCAR-4) and was disregarded in further experiments. Furthermore, we needed to assess whether the protocol affected phosphorylation patterns.

10.2 EGF STIMULATION

EGF is known to activate multiple signalling pathways upon binding to its specific receptor. We wanted to validate that the cold trypsinization and the phosphoflow cytometry protocol did not affect phosphorylation of intracellular proteins. Therefore we treated two cell lines (OVCAR-8- and SKOV-3) with EGF and analysed samples by phosphoflow cytometry and with an independent method, Western blot. Results from the Western blot shows multiple bands in the area where pAKT (pT308) and pSTAT3 should form, according to their size. This indicates that we have multiple unspecific bindings to other intracellular epitopes. Unspecific binding can be caused by addition of wrong concentrations of antibodies and/or due to insufficient blocking or another third variable. The experiment was only performed once, therefore further analysis should be performed and our validation method (Western blot) should be improved.

10.3 ASCITES TITRATION

The concentration of ascites used will affect the phosphorylation patterns in the cell lines, due to the presence of different amounts of cytokines and growth factors. The phosphorylation intensity also varies due to different mutations found within the cell lines. We initially studied phosphorylation of nine proteins and together they provided a good indication to which concentration we should use in further experiments. We performed experiments with multiple ascites concentration from patient #40 with three cell lines.

Another important aspect to consider is the amount of ascites available for experimental use. Malignant ascites may be quite abundant, but the volume of ascites obtained from each patient vary from under 1 mL to 200 mL or more. It is also important not to deplete the patient samples used in the initial experiment, so that further analysis can be performed. We found that a concentration of 50% ascites gave a suitable phosphorylation response in the cell lines that were investigated (OVCAR-5, OVCAR-8 and NCI/ADR-RES). Ascites titration of SKOV-3 cell lines was already performed before my master thesis started and presented with the same pattern. Initially we treated cells with different concentrations of ascites from one patient. There is a possibility that different patient samples (ascites) contain other components and/or different concentrations of cytokines, growth factors and more, and could therefore have other optimal concentrations. However, since one of our objectives was to characterize intracellular phosphorylation signatures in patient samples, equal concentrations of ascites needed to be used. This made it possible to compare phosphorylation patterns in between the patient samples.

10.4 TREATMENT TIME

Intracellular phosphorylation of proteins varies in intensity over time because- the proteins need different activation time. Therefore we performed an experiment where we treated one cell line (SKOV-3) for multiple time periods. A longer time interval (24 hours) was also investigated, but the phosphorylation proved to be weak. The results indicated that a treatment time between 0 and 30 minutes gave us a good overview of the intracellular phosphorylation status of the ovarian cancer cells. Different mutations within cell lines can potentially cause changes in the phosphorylation time and therefore affect this interval. However, previously performed experiments (before my Thesis) on other cell lines revealed that most of the proteins exhibited strong phosphorylation signals within the interval 0-30 min.

10.5 TREATMENT OF NCI/ADR-RES CELLS WITH TWO PATIENT SAMPLES

We performed experiments on NCI/ADR-RES cells with ascites from two different patients to see if they would exhibit a high diversity in the phosphorylation patterns. We also wanted to see how phosphorylation levels varied between experiments when treated with the same ascites samples. Comparing the two patient samples (ascites from patient #35 and #40) we could see that there was a correlation between the proteins that were clearly phosphorylated. However, the intensity of the phosphorylation signal in each protein varied between the two patient samples. This indicates that the same components (cytokines and growth factors) are represented in the ascites but possibly at different concentrations. We performed four experiments with ascites from patient #40 and three experiments with ascites from patient #35.

When comparing the different experiments with the same patient samples we can clearly see that the phosphorylation response varies between the experiments, resulting in a somewhat high standard deviation for most of the investigated proteins. Such variation can be caused by a number of factors, for example the cell status upon stimulation, use of different equipment (like pipettes), degradation of components in the patient samples, and variations in phosphoflow cytometry. However, within each of these experiments the data appear to follow the same phosphorylation pattern.

10.6 IL-6R BLOCKING ANTIBODY, EFFECTS ON SKOV-3 CELLS

Recent studies have revealed that elevated levels of IL-6 are found in malignant ascites. IL-6 is known to activate the JAK/STAT pathway upon binding to the IL-6R. We wanted to examine how dominant IL-6 is when it comes to the phosphorylation of STAT3, and to investigate whether other intracellular proteins were affected.

By using an IL-6R blocking antibody, that prevents IL-6 from binding and activating JAK/STAT pathway, we could see that the STAT-3 phosphorylation signal decreased with increased concentration of IL-6R blocking antibody. This was seen in multiple experiments, only one of which is shown in this thesis.

SKOV-3 cells were also exposed to IL-6R blocking antibody in the absence of ascites for 3 minutes, and these results show that the phosphorylation in most of the proteins decreased. This might indicate that the IL-6R blocking antibody affects the basal phosphorylation signal of some proteins, meaning that the overall treatment effect with 50% ascites (included IL-6R blocking antibody) can be weaker than treatment with only 50% ascites. However, this is inconsistent with data from previously performed experiments (before my Thesis), where the IL-6R blocking antibody in absence of ascites

did not affect STAT-3 phosphorylation. Therefore more experiments need to be performed before this can be confirmed.

STAT3 was partially blocked with a concentration of 10 µg/mL blocking antibody, meaning that compared to the basal level (untreated cells) there was still an increased phosphorylation. This suggests that we either did not use a maximally effective concentration of IL-6R blocking antibody and/or that other components (cytokines, growth factors) in ascites can activate this pathway, for example LPA and EGF. The S-6 ribosomal protein appeared to give a strong phosphorylation response, and in the presence of IL-6R blocking antibody an increase in phosphorylation could be observed.

It can be discussed if other proteins show a similar phosphorylation pattern as STAT3. However, the overall phosphorylation signals of these proteins are so weak that it is difficult to say if these changes are due to the method, the IL-6R blocking antibody or a third variable.

10.7 ASCITES SCREEN OF SKOV-3- AND OVCAR-8 CELLS

Malignant ascites contains different components that affect the overall phosphorylation pattern within ovarian cancer cells. This composition may vary between patients depending on multiple factors, including; individual biochemical differences, staging and tumour type.

We wanted to investigate how ascites samples from different patients would affect multiple ovarian cancer cell lines. These cell lines contain different mutations that could influence how they respond upon ascites stimulation, leading to the activation of multiple pathways with different phosphorylation intensities.

SKOV-3 cells were treated with ascites from all patients so that we could compare the effects of individual samples on phosphorylation patterns. Due to the time consumption we divided experiment into three parts, with approximately 12 phospho-proteins in each analysis. We performed treatment with ascites from patient #23 to #36, and we also prepared untreated cells early in the day. These samples were fixed and stored at 4˚C until samples from treatment of patients #37 to #45 were ready for fluorescent cell barcoding.

Results show that multiple proteins were phosphorylated after 3 and 20 minutes stimulation, but the strongest phosphorylation intensity was observed after 20 minutes stimulation. Two of proteins presented an overall strong phosphorylation, STAT-3 and S-6 ribosomal protein. STAT-3 appeared to be regulated independently of other proteins, meaning that a strong phosphorylation in STAT-3 did not correlate with increased levels of phosphorylation of other proteins. STAT-1 displayed increased

phosphorylation after treatment with some of the patient samples; this was paralleled by a strong phosphorylation also of STAT-3 with the same samples.

However, high levels of phosphorylation were observed in STAT-3 without a significant increase in the phosphorylation level of STAT-1. While STAT-3 activates cell survival in tumour cells, STAT-1 is known to activate anti-proliferative and pro-apoptotic responses. This relationship in ascites might be interesting to investigate further. STAT-3 phosphorylation was measured in all three experiments, as a reference value, and it correlated well between the experiments.

AKT exhibited a stronger phosphorylation signal upon treatment of SKOV-3 cells with many of the patient samples. Phosphorylation responses of other proteins varied more between patients, and exhibited an overall weaker response than STAT-3 and the S-6 ribosomal protein.

Ascites from patient #36 exhibited weak overall phosphorylation signals after stimulation, with the exception of STAT3. This sample was obtained from a patient with non-malignant ascites.

As presented in the heatmap of SKOV-3 data (Figure 31), especially after 20 minutes stimulation, the phosphorylation patterns of cells treated in the morning displayed an overall weaker phosphorylation response (patient #23 to #36). While the treatment of cells with ascites from patient #37 to #45 displayed an overall stronger response. This could indicate that something is different in these two "series of samples". Therefore, we decided to stimulate OVCAR-8 cells in a backwards order, starting with patient #45 and finishing with patient #23.

OVCAR-8 cells have a different set of genetic aberrations than SKOV-3 cells, and we wanted to examine the phosphorylation pattern after treatment with multiple patient samples. The fluorescent cell barcoding failed in the last experiment, therefore these data are absent in this thesis.

As described in the last section we treated OVCAR-8 cells in a backwards order to see how this affected phosphorylation response of proteins after stimulation. Studying the results in the heatmap, the overall phosphorylation was strongest in S-6 ribosomal protein. MAPKAPK-2, MEK1, AKT and STAT3 shows somewhat moderate phosphorylation response in OVCAR-8 cells after treatments with multiple patient samples, but no distinct pattern was revealed.

The overall weakest phosphorylation response after treatment of cells with all the patient samples is observed in patient #35 after 20 minutes stimulation. A Patient with non-malignant ascites (#36) induced an overall weak phosphorylation of the exanimated proteins after 20 minutes stimulation; however this could also have been caused by a third variable.

Comparing ascites-induced STAT-3 phosphorylation within SKOV-3 cells and OVCAR-8 cells it appears that the correlations between the experiments performed with SKOV-3 cells are better than between the experiments performed on OVCAR-8 cells. The reason for this might be that the phosphorylation is weaker when OVCAR-8 cells are treated with ascites and that the margin of error is thereby lower.

Ascites from patients #44 and #45 detached during treatment of OVCAR-8 cells, data on these samples are therefore not available. SKOV-3 cells did not detach during treatment with patient sample #44 and #45. Since adherent cell lines are treated when cells are attached to a plastic surface by proteins in membrane, this suggests that mutations in OVCAR-8 cells affect the proteins on the plasma membrane under treatment which leads to detachment. In addition there has to be something that diversifies these samples from the other patient samples, since only these two patients samples detach. It can also be a third variable that affects the cells leading to the detachment from the plastic surface.

The heatmap of ascites-induced phosphorylation with 18 patient samples on OVCAR-8 cells (Figure 34), presents a clear difference in cells that were treated with patient samples early in the morning compared to cells that were treated with patient samples early afternoon.

As mentioned earlier, we treated OVCAR-8 cells with patient samples in a backwards order. In SKOV-3 cells the phosphorylation intensity was stronger for samples treated early afternoon, and in OVCAR-8 cells the intensity was strongest in cells treated early in the morning. This may signify that there are two different populations of patient samples with different phosphorylation pattern.

These differences might be explained by a longer storage time (4-5 hours) before they were barcoded and permeabilizated. However we see this as highly unlikely due to the well-known and established nature of the method. An additional possibility is the time difference that the cells are in contact with the FCS free medium, for example a lower basal phosphorylation level in samples treated early afternoon. However, there can also be a third variable interfering.

11 CONCLUSION

In this thesis we wanted to find ovarian cancer cell lines that were suitable for our experimental setup, characterize intracellular network in ovarian cancer cell lines when treated with ascites from multiple patients, and investigate how dominant IL-6 was in phosphorylation of STAT-3 and if it affected other proteins. Conclusions based on the results are as follows:

Method establishment

- Ovarian cancer cell lines OVCAR-3, OVCAR-5, OVCAR-8, NCI/ADR-RES and SKOV-3 cells yield satisfactory response in our method setup.
- OVCAR-4 cells were not suitable for our experiments
- 3D barcoding allowed parallel analysis of up to 64 conditions

Studies of IL-6 mediated phosphorylation of proteins, with a focus on STAT-3

- The IL-6R is dominant when it comes to mediation of STAT-3 phosphorylation
- Phosphorylation of other investigated proteins is not significantly affected by blockage of the IL-6R

Ascites-induced phosphorylation patterns in SKOV-3 cells

- Ascites from 20 different patients induced a strong phosphorylation response in both STAT-3 and S-6 ribosomal protein
- STAT-3 phosphorylation exhibited low correlation with the phosphorylation of the other proteins that were investigated
- Ascites from some of the patients induced moderate to strong phosphorylation in STAT-1
- The phosphorylation response of AKT, MAPKAPK-2 and MEK-1 was weak after cells were treated with many of the patient samples
- The patient with non-malignant ascites (#36) induced the weakest overall phosphorylation when treated for 20 minutes

Ascites-induced phosphorylation patterns in OVCAR-8 cells

- Ascites from 18 patients induced a strong phosphorylation in S-6 ribosomal protein
- STAT-3 phosphorylation exhibited low correlation with the phosphorylation of the other proteins that were investigated
- The phosphorylation response of AKT, MAPKAPK-2 and MEK-1 was weak to moderate after cells were treated with many of the patient samples
- An overall weaker phosphorylation response were observed after treatment with 18 patient samples in OVCAR-8 cells, compared to the treatment with the same patient samples in SKOV-3 cells

12 FURTHER WORK

First of all, the method used to characterize intracellular phosphorylation signals in cell lines after treatment with ascites from the patient panel needs to be investigated further. The main focus should be to examine what causes the difference in cells that were stimulated early morning versus early afternoon. Then an assessment should be made regarding the results on SKOV-3 and OVCAR-8, if they can be used or not. Further on, other cell lines should be investigated and results compared.

Short time planes;

- Examine what diversifies samples #44 and #45 from the rest of the patient samples
- Improve the validation analysis, Western blot
- Examine the relationship between STAT-3 and STAT-1 phosphorylation
- The effect of IL-6R blocking should be repeated on SKOV-3, and the effect on other cell lines should be investigated
- Perform component analysis of patient samples, like cytokines, chemokines and growth factors, in patient samples so that they can be compared to the characterisation of intracellular phosphorylation pattern
- Investigate new ascites samples from additional patients
- Examine more than one non-malignant patient sample of ascites
- Investigate the effect of known targeted drugs on one or multiple cell lines.

In a longer prospective, we aim to develop a method for mapping the signalling networks directly in fresh tumour cells that are isolated from ovarian cancer patients. By adding ovarian cancer drugs into the equation we hope to be able to obtain information that would support personalized treatment options in ovarian cancer patients.

13 REFERENCES

1. Wikipedia, t.f.e. *Antibody*. 140415 [cited 2014 16.04]; Available from: http://en.wikipedia.org/wiki/Antibody.
2. *Cancer in Norway 2011*, S. Larønningen, Editor. 2013.
3. Day, W.O.C. *5 Facts everyone should know about ovarian cancer*. [cited 2014 04.03]; Available from: http://ovariancancerday.org/about-ovarian/5-facts-everyone-should-know-about-ovarian-cancer/.
4. Prat, J., *Staging classification for cancer of the ovary, fallopian tube, and peritoneum.* Int J Gynaecol Obstet, 2014. **124**(1): p. 1-5.
5. Institute, N.C. *Stages of ovarian epithelial cancer*. 2013 12.03.2013 [cited 2014 03.03]; Available from: http://www.cancer.gov/cancertopics/pdq/treatment/ovarianepithelial/Patient/page2.
6. Prat, J., *New insights into ovarian cancer pathology.* Ann Oncol, 2012. **23 Suppl 10**: p. x111-7.
7. McCluggage, W.G., *Morphological subtypes of ovarian carcinoma: a review with emphasis on new developments and pathogenesis.* Pathology, 2011. **43**(5): p. 420-32.
8. Nossov, V., et al., *The early detection of ovarian cancer: from traditional methods to proteomics. Can we really do better than serum CA-125?* Am J Obstet Gynecol, 2008. **199**(3): p. 215-23.
9. Fritsche, H.A. and R.C. Bast, *CA 125 in ovarian cancer: advances and controversy.* Clin Chem, 1998. **44**(7): p. 1379-80.
10. Lopez, J., S. Banerjee, and S.B. Kaye, *New developments in the treatment of ovarian cancer--future perspectives.* Ann Oncol, 2013. **24 Suppl 10**: p. x69-x76.
11. Banerjee, S. and S. Kaye, *The role of targeted therapy in ovarian cancer.* Eur J Cancer, 2011. **47 Suppl 3**: p. S116-30.
12. Kipps, E., D.S. Tan, and S.B. Kaye, *Meeting the challenge of ascites in ovarian cancer: new avenues for therapy and research.* Nat Rev Cancer, 2013. **13**(4): p. 273-82.
13. Wikipedia, t.f.e. *Lactate dehydrogenase*. 2014.04.01 [cited 2014 30.04]; Available from: http://en.wikipedia.org/wiki/Lactate_dehydrogenase.
14. Yap, T.A., C.P. Carden, and S.B. Kaye, *Beyond chemotherapy: targeted therapies in ovarian cancer.* Nat Rev Cancer, 2009. **9**(3): p. 167-81.
15. Harvey Lodish, A.B., S Lawrence Zipursky, Paul Matsudaira, David Baltimore, and James Darnell., *Molecular Cell Biology, 4th edition*. 2000: W. H. Freeman.
16. Kumar, J. and A.C. Ward, *Role of the interleukin 6 receptor family in epithelial ovarian cancer and its clinical implications.* Biochim Biophys Acta, 2014. **1845**(2): p. 117-125.
17. Matte, I., et al., *Profiling of cytokines in human epithelial ovarian cancer ascites.* Am J Cancer Res, 2012. **2**(5): p. 566-80.
18. Mills, G.B. and W.H. Moolenaar, *The emerging role of lysophosphatidic acid in cancer.* Nat Rev Cancer, 2003. **3**(8): p. 582-91.
19. Hooper, D.C. *EGFR interactions, roles and cancer therapy options by Dr. Claudine Hooper (KCL)*. [cited 2014 28.04]; Available from: http://www.abcam.com/index.html?pageconfig=resource&rid=10723.
20. Lane, D., et al., *Osteoprotegerin (OPG) activates integrin, focal adhesion kinase (FAK), and Akt signaling in ovarian cancer cells to attenuate TRAIL-induced apoptosis.* J Ovarian Res, 2013. **6**(1): p. 82.
21. Nadzeya Goncharenko-Khaider, D.L., Isabelle Matte, Claudine Rancourt and Alain Piche *"Ovarian Cancer - A Clinical and Translational Update* 2013, INTECH - open science, open minds.
22. Klasa-Mazurkiewicz, D., et al., *Clinical significance of VEGFR-2 and VEGFR-3 expression in ovarian cancer patients.* Pol J Pathol, 2011. **62**(1): p. 31-40.

23. Ahmed, N. and K.L. Stenvers, *Getting to Know Ovarian Cancer Ascites: Opportunities for Targeted Therapy-Based Translational Research.* Front Oncol, 2013. **3**: p. 256.
24. Lorenzi, P.L., et al., *DNA fingerprinting of the NCI-60 cell line panel.* Mol Cancer Ther, 2009. **8**(4): p. 713-24.
25. Abaan, O.D., et al., *The exomes of the NCI-60 panel: a genomic resource for cancer biology and systems pharmacology.* Cancer Res, 2013. **73**(14): p. 4372-82.
26. Project, C.C.L. *Catalogue of somatic mutations in cancer*. [cited 2014 18.03]; Available from: http://cancer.sanger.ac.uk/cell_lines/browse/tissue#sn=ovary&ss=all&hn=all&sh=all&in=t&src=tissue.
27. (NCBI), N.C.f.B.I. *TP53 tumor protein p53 [Homo sapiens (human)]* [cited 2014 18.03]; Available from: http://www.ncbi.nlm.nih.gov/gene/.
28. (NCBI), N.C.f.B.I. *KRAS Kirsten rat sarcoma viral oncogene homolog [Homo sapiens (human)]* [cited 2014 18.03]; Available from: http://www.ncbi.nlm.nih.gov/gene/.
29. Rogne, M. and K. Tasken, *Cell signalling analyses in the functional genomics era.* N Biotechnol, 2013. **30**(3): p. 333-8.
30. Biosciences, B., *BD FACSCanto II Flow Cytometer Reference Manual*. 2006.
31. Biosciences, B., *BD LSRFortessa Cell Analyzer User`s Guide*. 2010.
32. Biosciences, B., *An Introduction to Compensation for Multicolor Assays on Digital Flow Cytometers*. 2009.
33. Lea, T., *Immunologi og immunologiske teknikker*. 3 ed. 2006: Fagbokforlaget.
34. eBiosciene, A. *Immunohistochemistry & Immunocytochemistry*. [cited 2014 18.03]; Available from: http://www.ebioscience.com/knowledge-center/application/ihc/direct-conjugate-advantage.htm.
35. Krutzik, P.O. and G.P. Nolan, *Intracellular phospho-protein staining techniques for flow cytometry: monitoring single cell signaling events.* Cytometry A, 2003. **55**(2): p. 61-70.
36. Mahmood, T. and P.C. Yang, *Western blot: technique, theory, and trouble shooting.* N Am J Med Sci, 2012. **4**(9): p. 429-34.
37. Leinco Technologies, I. *General Western blot protocol* [cited 2014 16.04]; Available from: http://www.leinco.com/general_wb.

14 APPENDIX I

14.1 OVCAR-5

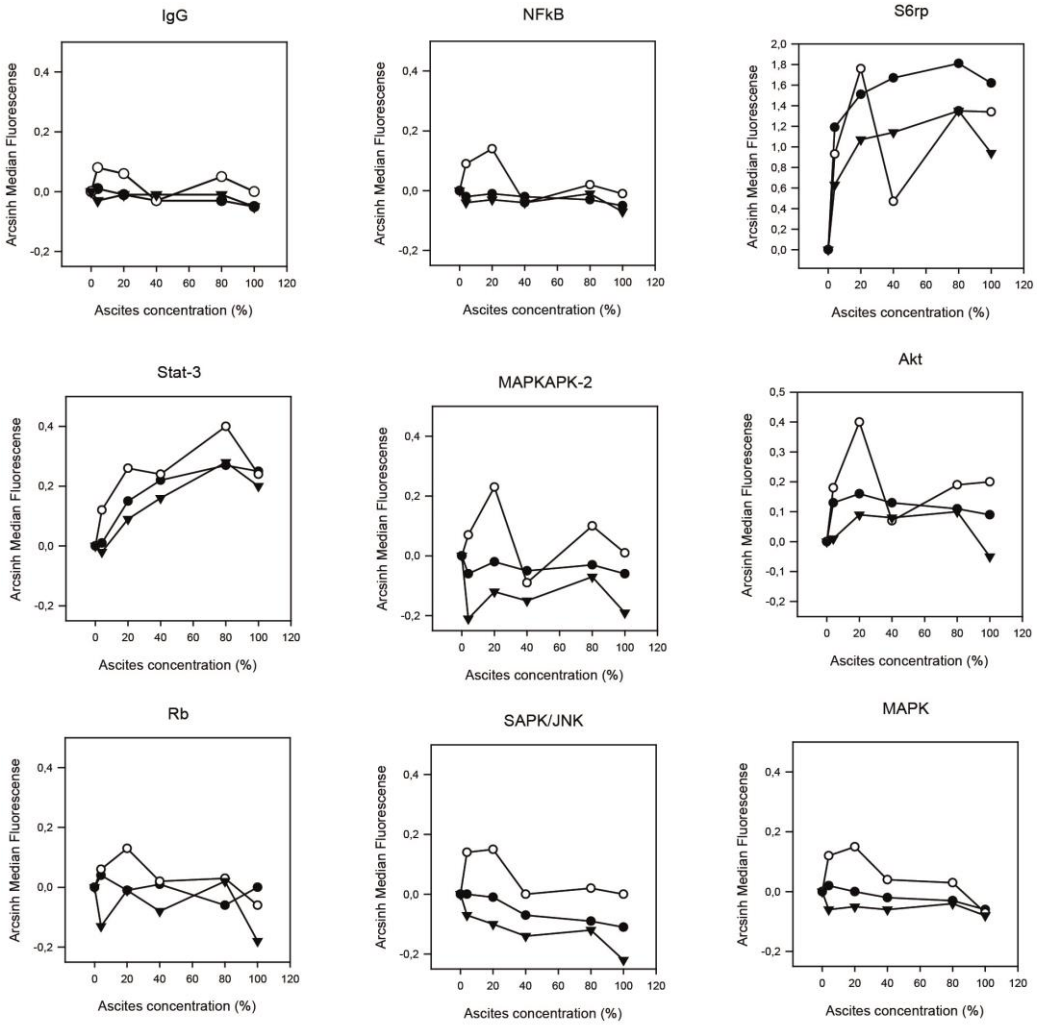

Figure 36 OVCAR-5 treated for 30 minutes with different concentrations of ascites. *Cells were treated for 30 minutes with ascites concentrations; 0%, 4%, 20%, 40%, 80% and 100%. Ascites from patient #40 was used and samples were analysed by phosphoflow cytometry. Result displayed as line diagrams of three experiments.*

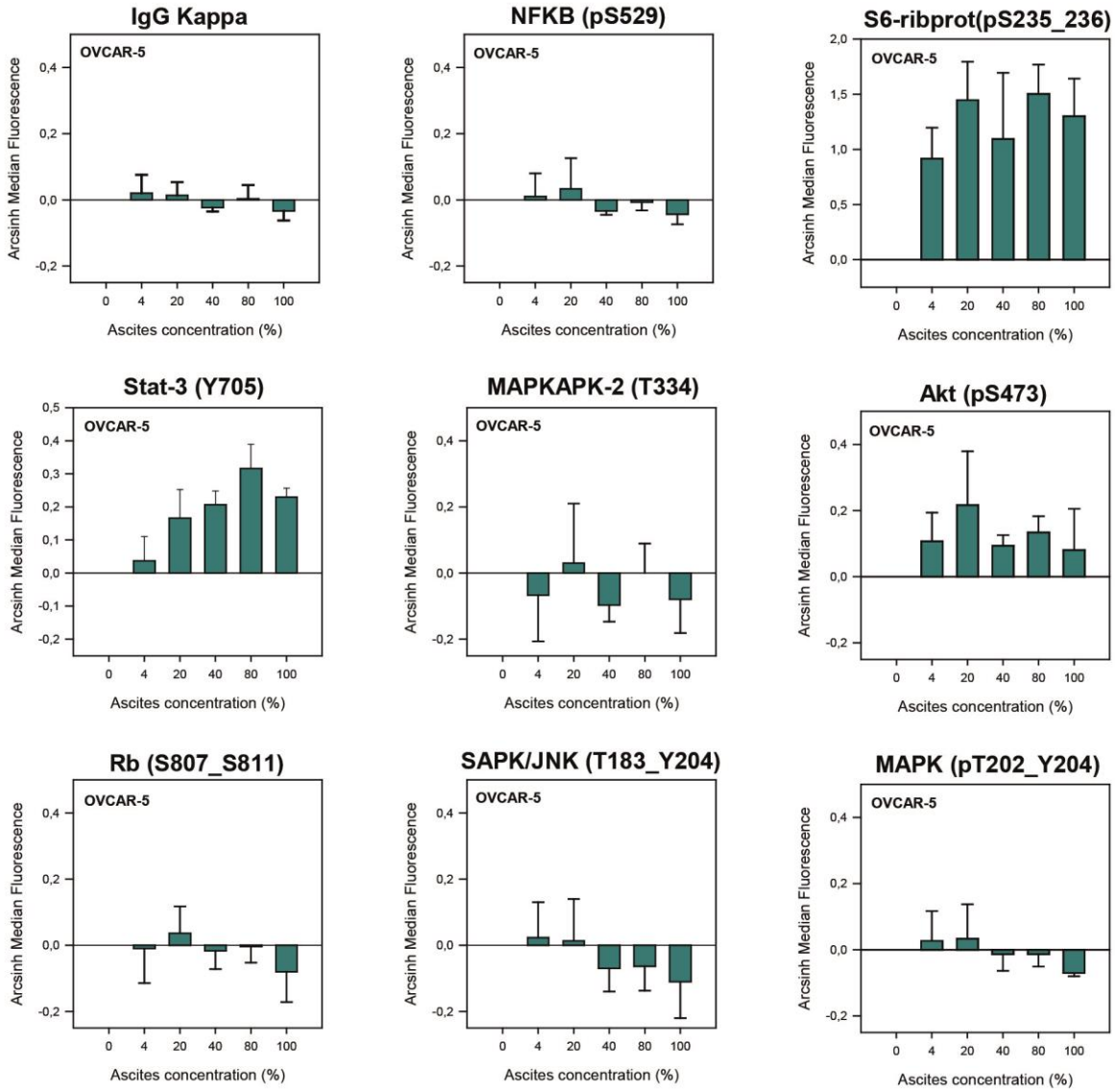

Figure 37 OVCAR-5 treated for 30 minutes with different concentrations of ascites. *Cells were treated for 30 minutes with ascites concentrations; 0%, 4%, 20%, 40%, 80% and 100%. Ascites from patient #40 was used and samples were analysed by phosphoflow cytometry. Results are displayed as bar diagrams with the average of three experiments with standard deviation.*

14.2 OVCAR-8

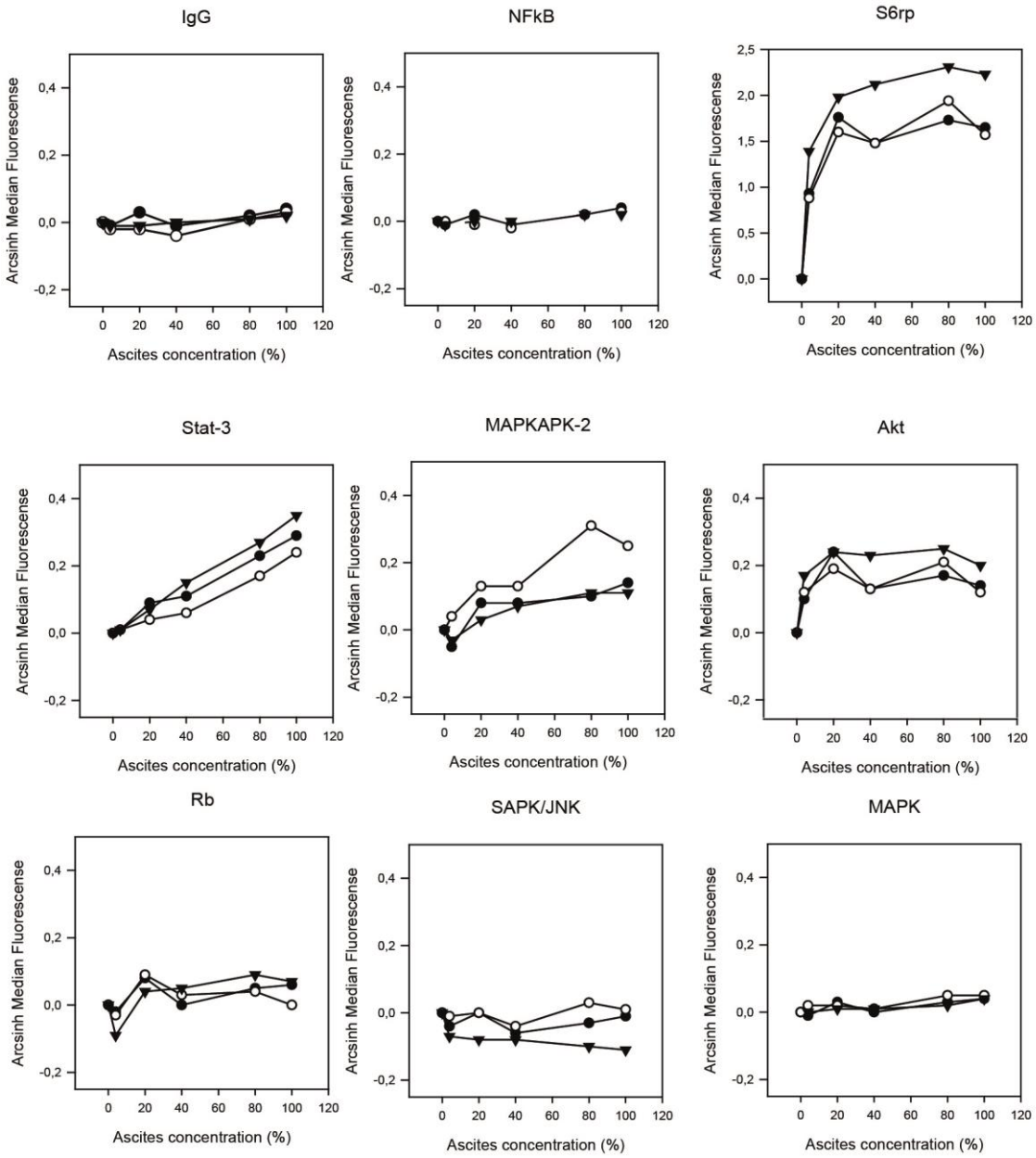

Figure 38 OVCAR-8 treated for 30 minutes with different concentrations of ascites. *Cells were treated for 30 minutes with ascites concentrations; 0%, 4%, 20%, 40%, 80% and 100%. Ascites from patient #40 was used and samples were analysed by phosphoflow cytometry. Result displayed as line diagrams of three experiments.*

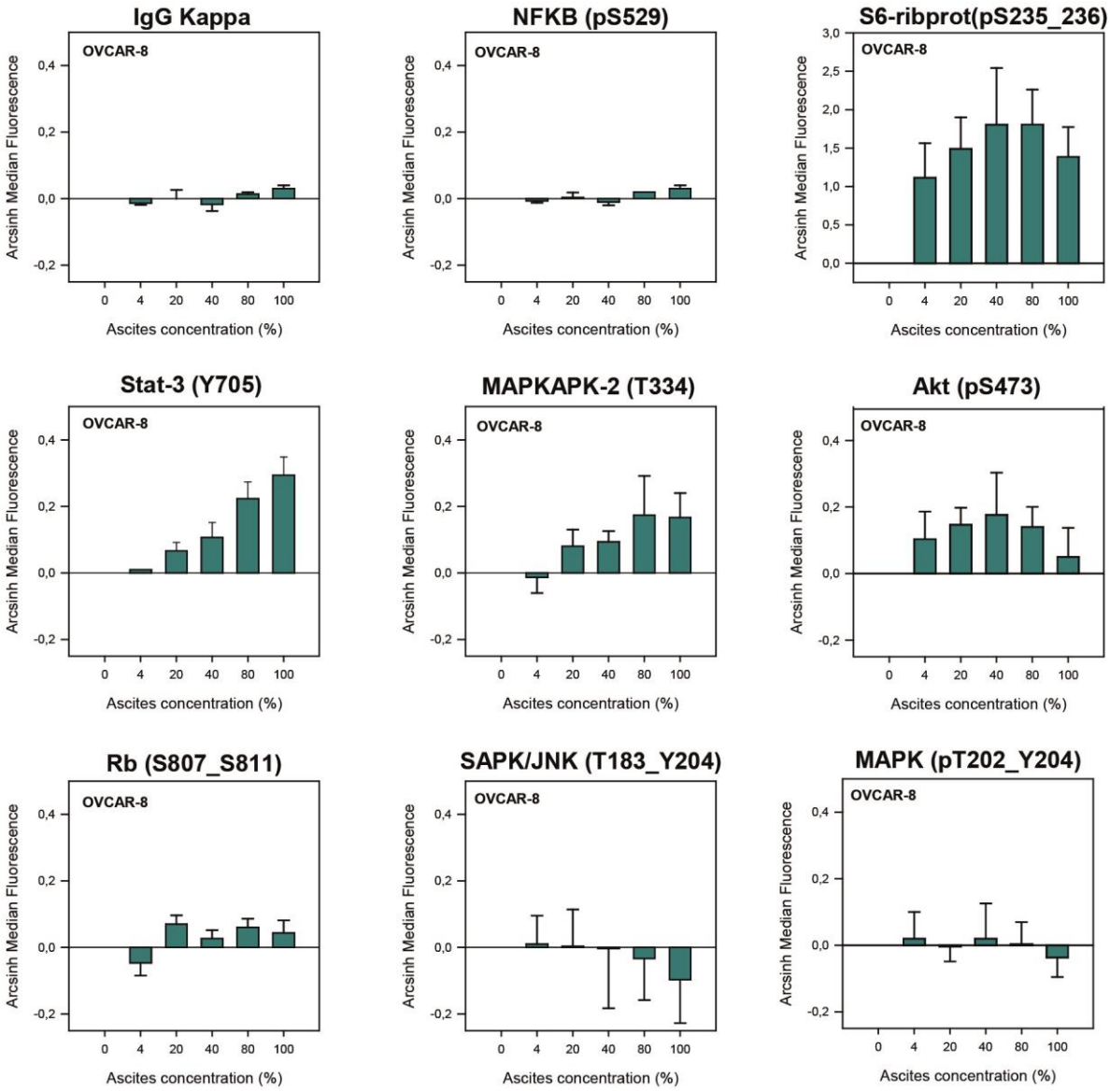

Figure 39 OVCAR-8 treated for 30 minutes with different concentrations of ascites. *Cells were treated for 30 minutes with ascites concentrations; 0%, 4%, 20%, 40%, 80% and 100%. Ascites from patient #40 was used and samples were analysed by phosphoflow cytometry. Results are displayed as bar diagrams with the average of three experiments with standard deviation.*

14.3 NCI/ADR-RES

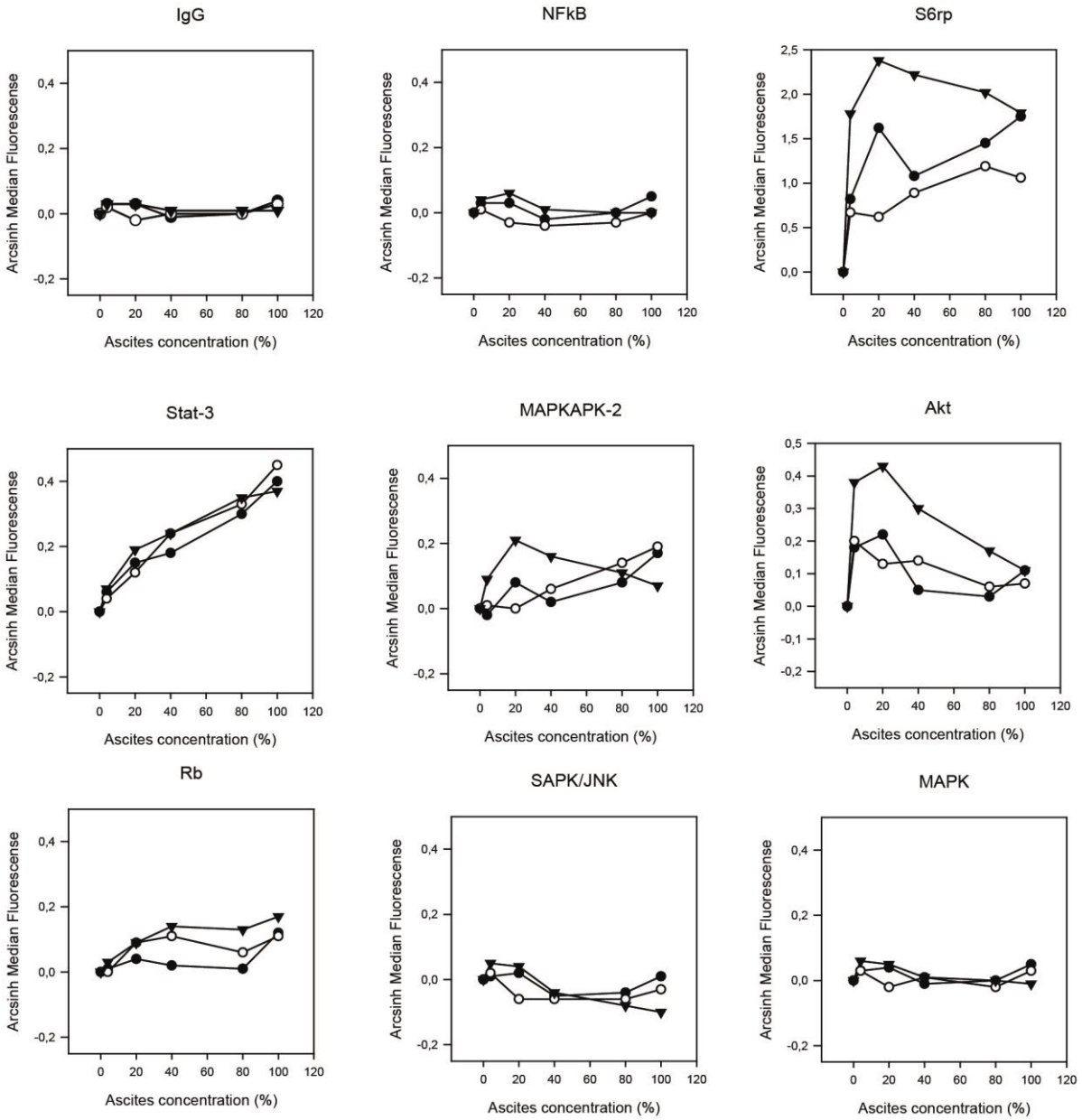

Figure 40 NCI/ADR-RES treated for 30 minutes with different concentrations of ascites. *Cells were treated for 30 minutes with ascites concentrations; 0%, 4%, 20%, 40%, 80% and 100%. Ascites from patient #40 was used and samples were analysed by phosphoflow cytometry. Result displayed as line diagrams of three experiments.*

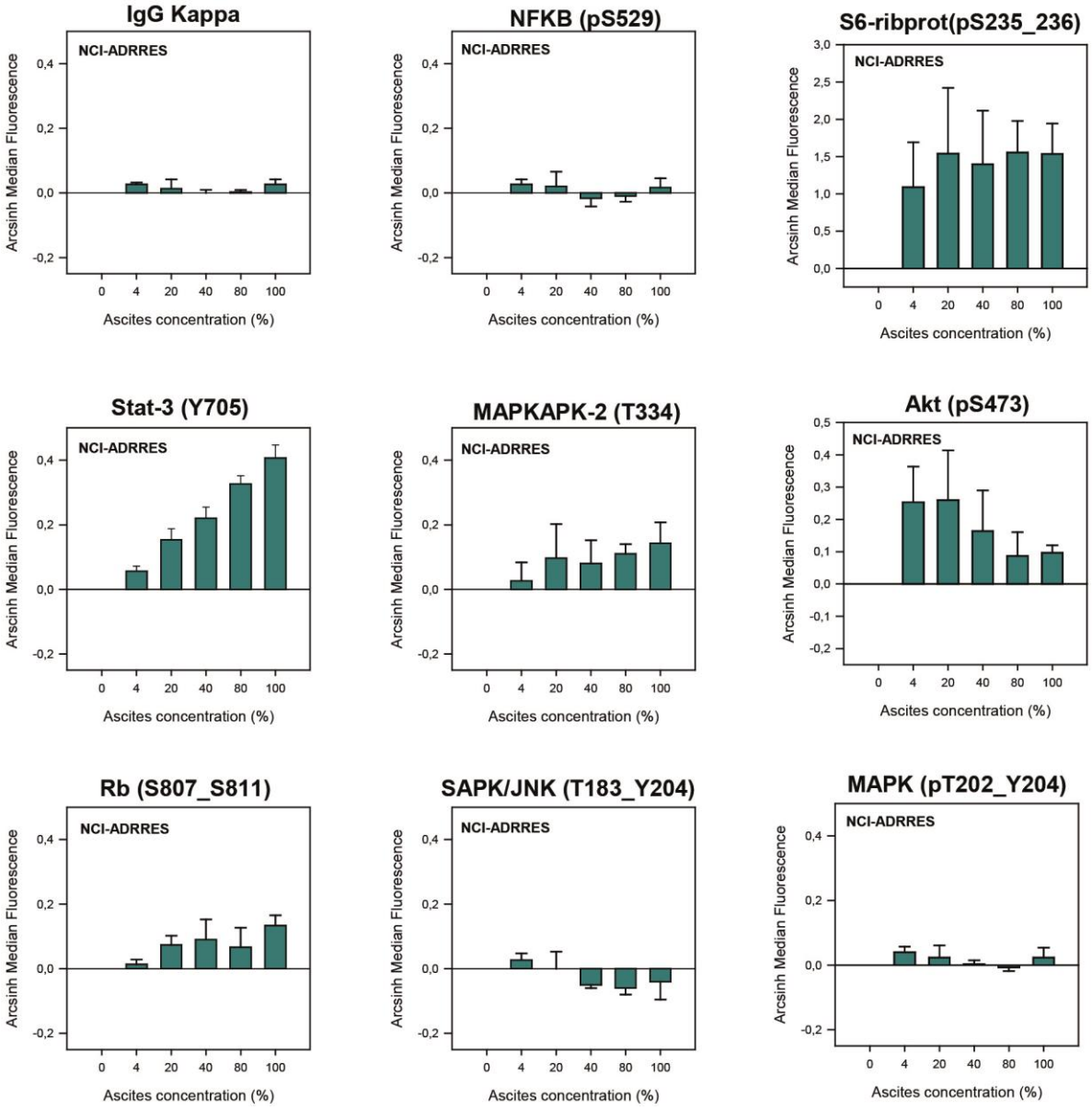

Figure 41 NCI/ADR-RES treated for 30 minutes with different concentrations of ascites. *Cells were treated for 30 minutes with ascites concentrations; 0%, 4%, 20%, 40%, 80% and 100%. Ascites from patient #40 was used and samples were analysed by phosphoflow cytometry. Results are displayed as bar diagrams with the average of three experiments with standard deviation.*

15 APPENDIX II

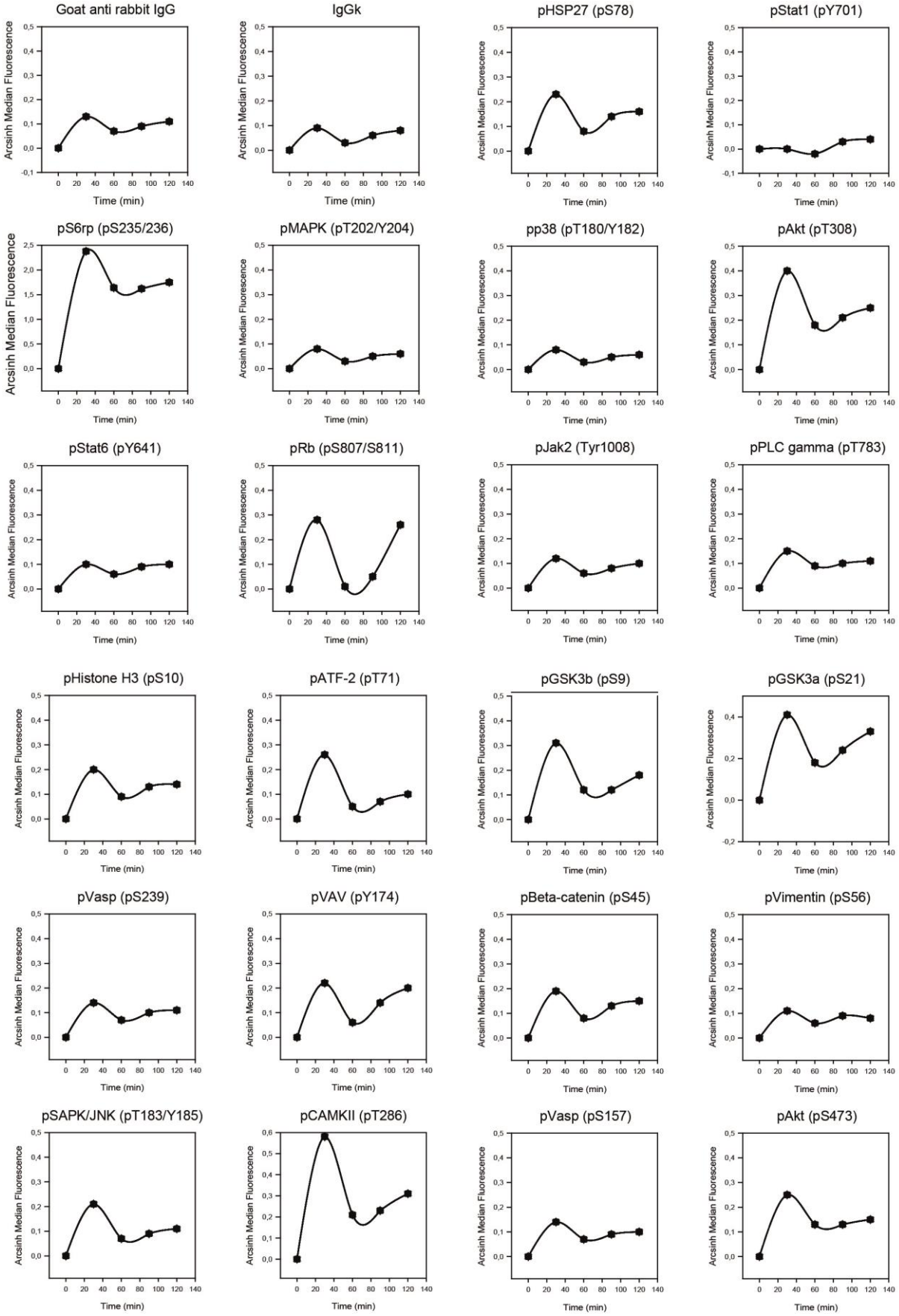

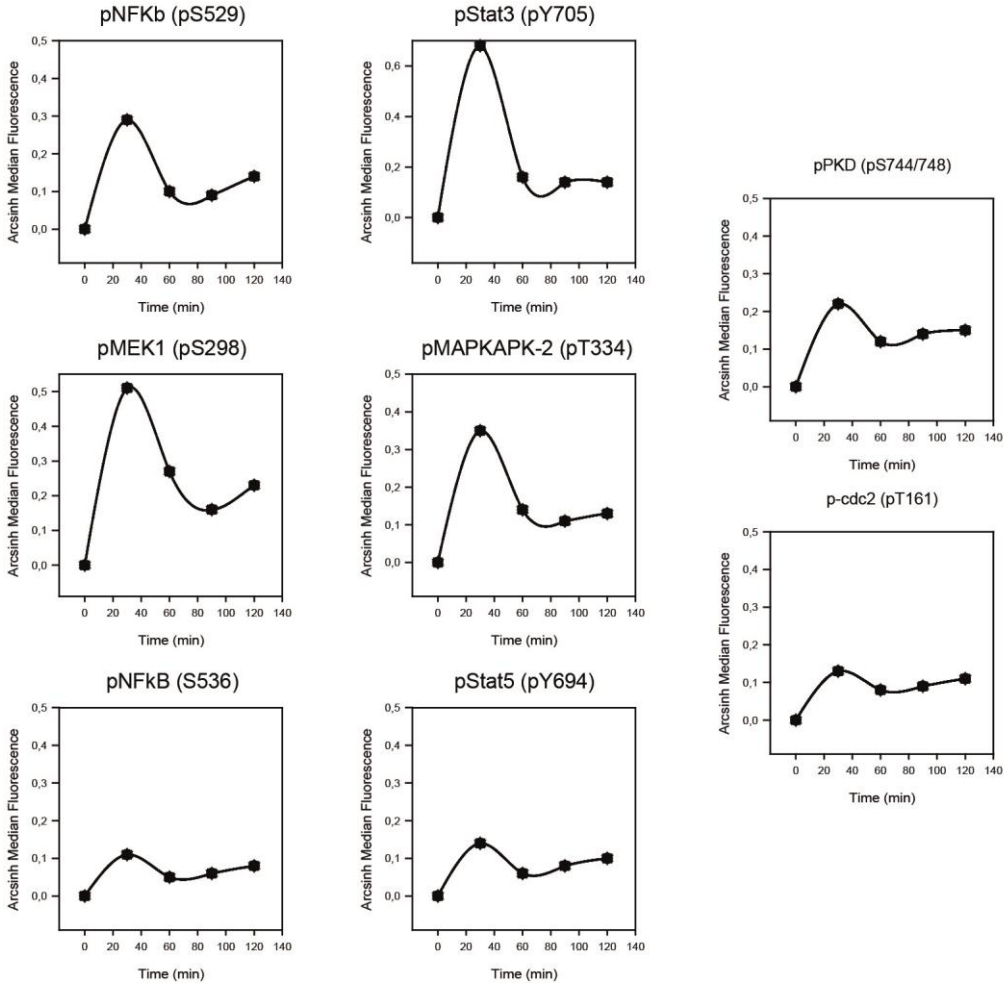

Figure 42 Phosphorylation signal of intracellular proteins at different time points after SKOV-3 cells were treated with ascites. *Treatment was performed at five different time periods (0, 30, 60, 90 and 120 minutes) with SKOV-3 cells. Cells were treated with 50 % ascites from patient #40 and analysed by phosphoflow cytometry.*

16 APPENDIX III

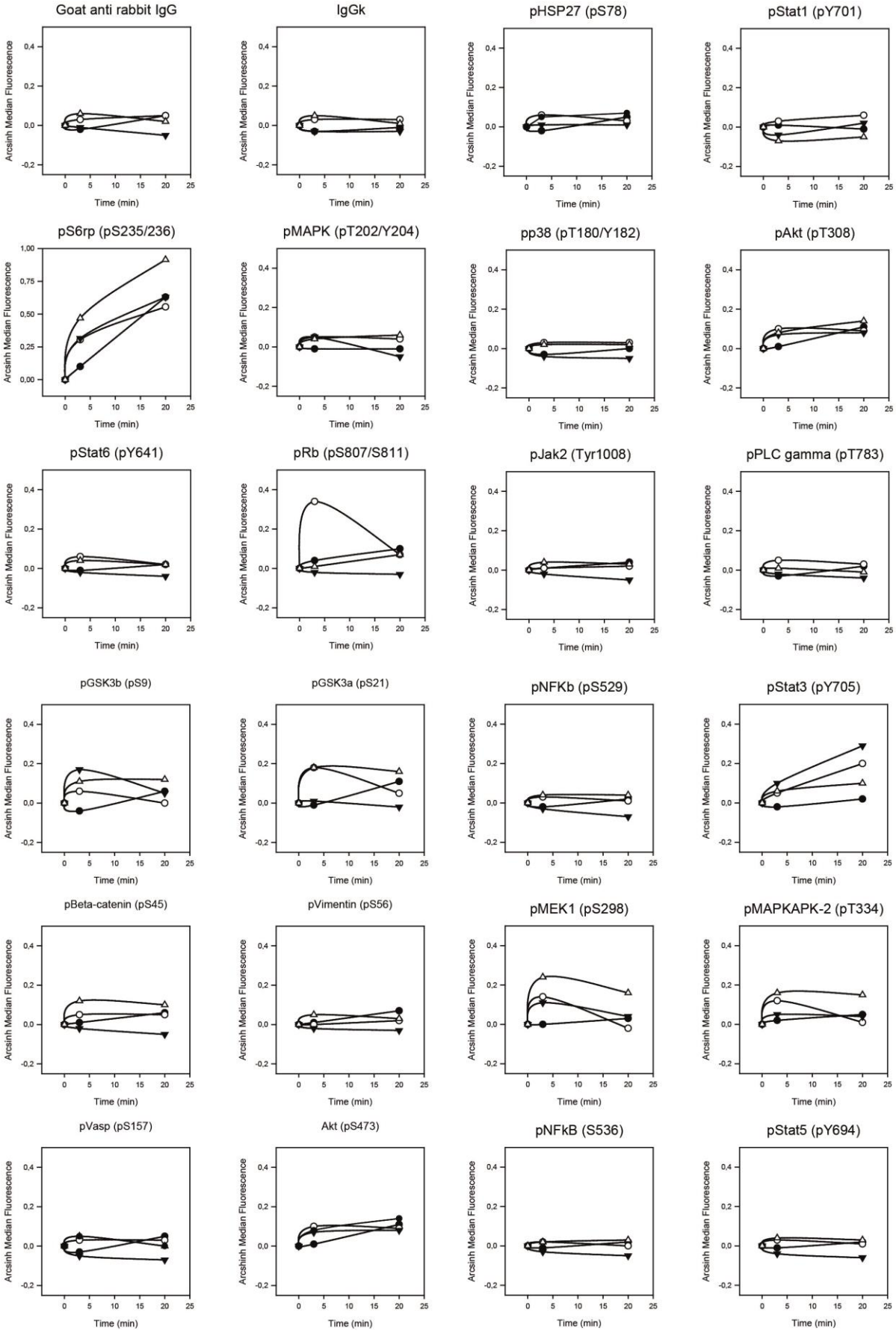

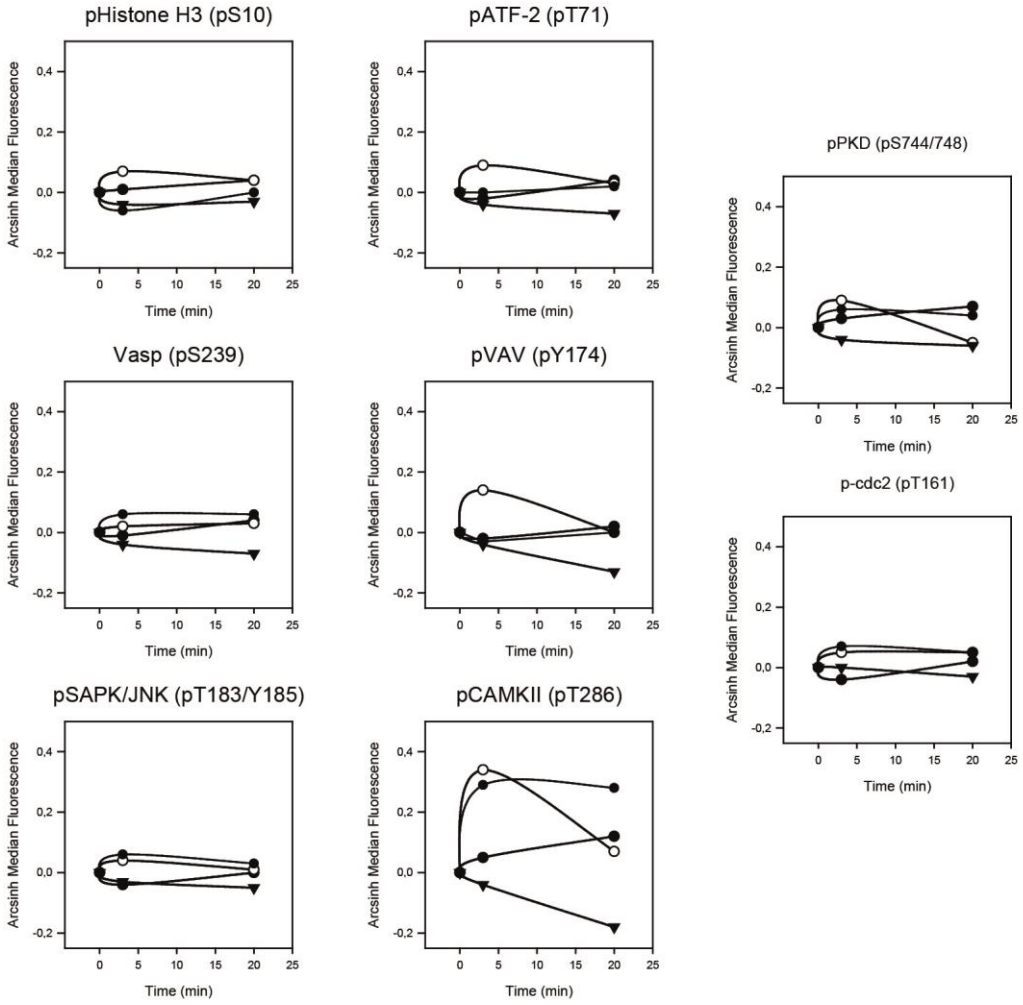

Figure 43 Phosphorylation signals of intracellular proteins in NCI/ADR-RES cells when treated with ascites from patient #35. *Treatment with 50 % ascites from patient #35 on NCI/ADR-RES with three time courses; 0, 3 and 20 minutes. Illustration displays intracellular proteins investigated with values from all four experiments. Samples were analysed by phosphoflow cytometry and calculated in Cytobank with arcsinh ratio of medians, and they were normalized to the first row (untreated cells).*

17 APPENDIX IV

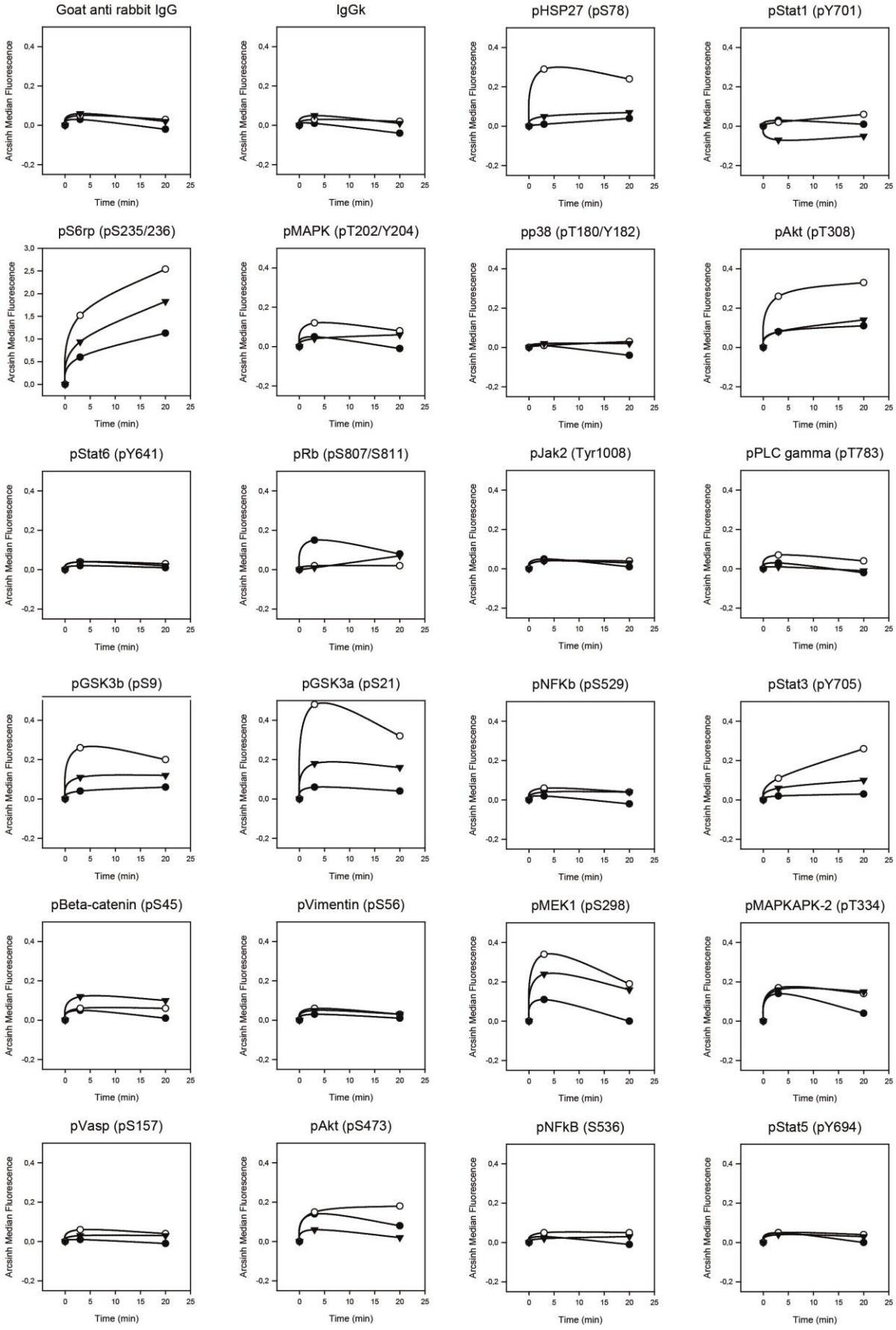

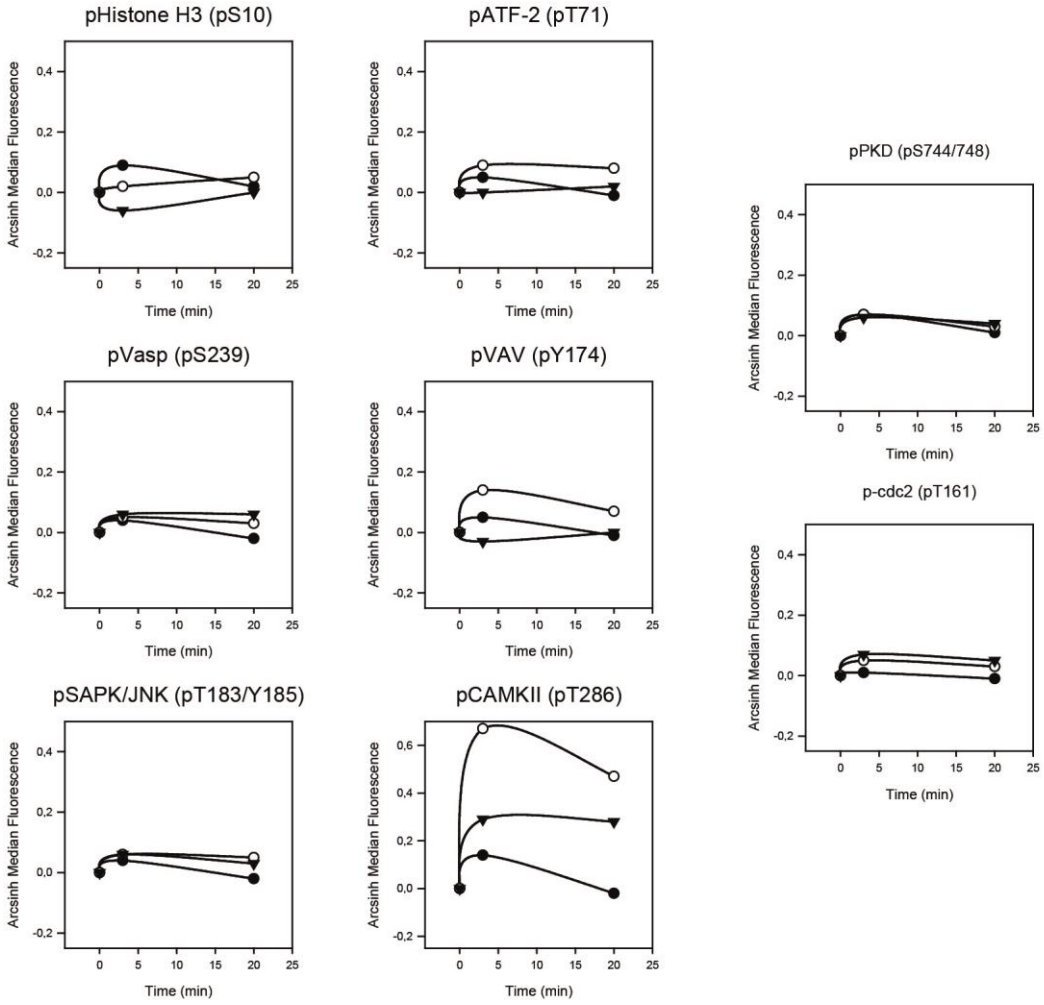

Figure 44 Phosphorylation signals of intracellular proteins in NCI/ADR-RES cells when treated with ascites from patient #40. *Treatment with 50 % ascites from patient #40 of NCI/ADR-RES with three time courses; 0, 3 and 20 minutes. Illustration displays intracellular proteins investigated with values from all three experiments. Samples were analysed by phosphoflow cytometry and calculated in Cytobank with arcsinh ratio of medians, and they were normalized to the first row (untreated cells).*

18 APPENDIX V

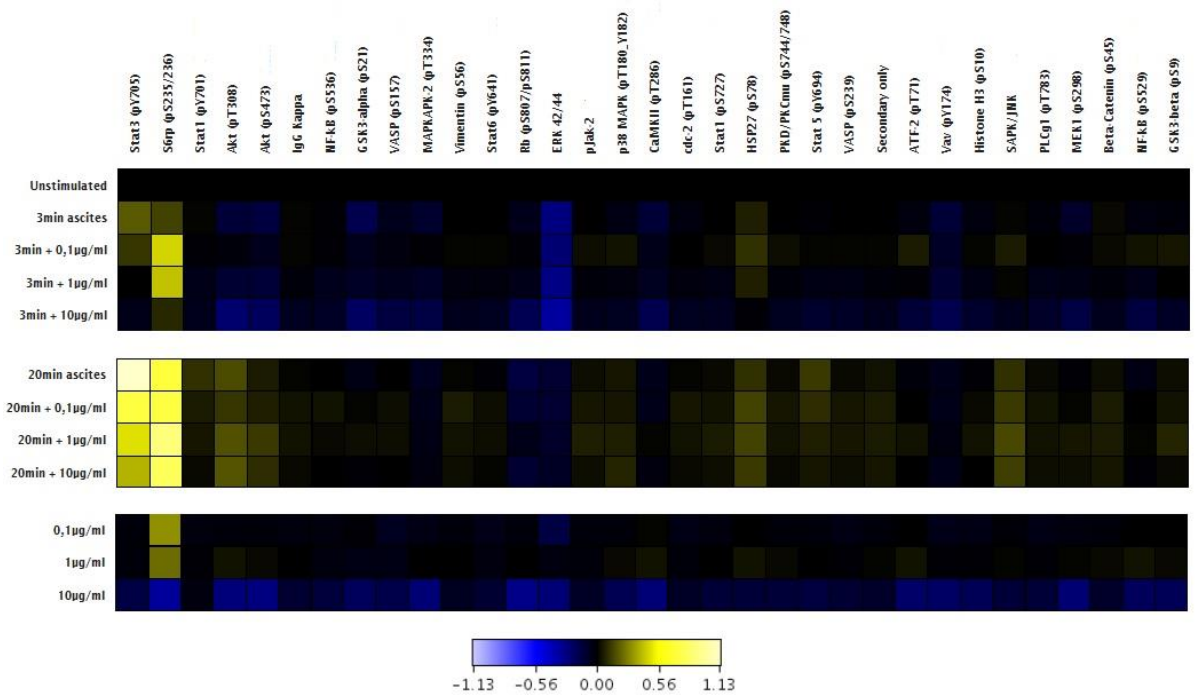

Figure 45 Ascites-induced phosphorylation patterns of investigated proteins after blocking the IL-6R in SKOV-3 cells. *SKOV-3 cells were treated with different conditions for 3 and 20 minutes with ascites from patient #40. Conditions; untreated, 50% ascites only, 50 % ascites with addition of different concentration of IL-6R blocking antibody; 0,1 µg/, 1,0 µg/mL and 10 µg/mL and different concentration of IL-6R blocking antibody; 0,1 µg/, 1,0 µg/mL and 10 µg/mL WITHOUT addition of ascites. Samples was analysed by phosphoflow and are results are displayed in a heatmap.*

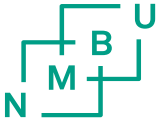

Norwegian University
of Life Sciences

Postboks 5003
NO-1432 Ås, Norway
+47 67 23 00 00
www.nmbu.no